Radial-Growth Response of Mountain Hemlock (*Tsuga mertensiana*) Trees to Climate Variations Along a Longitudinal Transect, Northwestern British Columbia, Canada.

by

Kelly-Anne Penrose
B.Sc.Env., University of Guelph, 2003

A Thesis Submitted in Partial Fulfillment of the Requirements for the Degree of

Master of Science

in the Department of Geography

Radial-Growth Response of
Mountain Hemlock (*Tsuga mertensiana*) Trees
to Climate Variations Along a Longitudinal Transect,
Northwestern British Columbia, Canada.

by

Kelly-Anne Penrose
B.Sc.Env., University of Guelph, 2003

Supervisory Committee

Dr. Dan J. Smith, Supervisor
(Department of Geography)

Dr. Stanton E. Tuller, Departmental Member
(Department of Geography)

Dr. Trudy Kavanagh, Departmental Member
(Department of Geography)

Dr. Ze'ev Gedalof, Outside Member
(University of Guelph, Department of Geography)

Supervisory Committee

Dr. Dan J. Smith, Supervisor
(Department of Geography)

Dr. Stanton E. Tuller, Departmental Member
(Department of Geography)

Dr. Trudy Kavanagh, Departmental Member
(Department of Geography)

Dr. Ze'ev Gedalof, Outside Member
(University of Guelph, Department of Geography)

ABSTRACT

This research was initiated to develop an understanding of the differential radial-growth response of mature mountain hemlock (*Tsuga mertensiana*) trees located along a line of latitude in northwestern British Columbia. Increment core samples were collected from mountain hemlock stands located at five high-elevation sites between the Queen Charlotte Islands and Smithers. Tree ring-width index chronologies were compared to historical precipitation and air temperature data from four climate stations, as well as the El Niño Southern Oscillation and the Pacific Decadal Oscillation. No two mountain hemlock stands had the same growth response to monthly air temperature and precipitation, indicating that the trees are responding to site-specific limiting factors. The response to El Niño Southern Oscillation events was consistent along the transect, while the response to Pacific Decadal Oscillation phase changes was greatest at coastal sites and decreased towards the interior.

Table of Contents

List of Figures

List of Tables

Acknowledgments and Dedication

The adventure that has been my thesis is similar to the experience of traversing a glacier with Dan (both terrifying and exciting!) and has left me with a sense of triumph as I now stand on the other side. I want to thank Dan Smith, my supervisor, for his guidance during each and every step of this thesis, and each shaky step I ever took on the ice! As a supervisor Dan has both challenged and supported me. As a fearless backcountry leader he introduced me to a world of glaciers, grizzlies, mountain peaks, and valleys; a world that can't help but change who you are, and a world that is never far from my thoughts and dreams.

Dr. Stan Tuller was incredibly thorough while editing every version of this thesis and generously offered his time and expertise. I cannot imagine the number of hours and the effort that he has invested in my work, and I want to thank him for making this a better thesis. Dr. Trudy Kavanagh always pushed me to go beyond climate and tree-rings, and look at the life of a mountain hemlock tree. I want to thank her for this advice and for working hard to support me, as well as my work. I also want to thank Dr. Ze'ev Gedalof, my external examiner, who offered helpful suggestions during my defense that have improved the quality of this thesis.

My fieldwork and analysis could not have been completed without the help of UVTRL lab mates. Sarah Laxton was my first guide to UVTRL backcountry living and lab survival. She has become a dear friend and I would not hesitate to be her "5'2" Bear Protector" again! Scott Jackson first helped by teaching me how to core trees and quickly became a friend I could always talk to. Dave Lewis offered advice and guidance both in the lab and the field, and he is probably the reason that I'm now addicted to dark

chocolate! I want to thank Andrea Kenward for being a never-ending source of support, encouragement and smiles. Non-official UVTRL member Michi Main and I have shared adventures, laughter, tears and everything in between during the last two and a half years. She will always be a dear friend and I'll never forget how much she has helped me. More UVTRL lab mates, past and present, are too many to mention but they know who they are and I want to thank them all for making this a wonderful experience.

A big "thank you" to my amazing support network of friends and family from BC (go Q-Tips!) and Ontario. I want to thank Julie for knowing and loving who I was, who I am and who I'm becoming. Thank-you for always being by my side and providing my life with some much needed drama and excitement! I want to thank Ashley for his encouragement and love. He helped me thru the day-to-day frustrations of this thesis with patience and understanding. Every day I consider myself lucky to have him in my life, and luckier still, knowing that he believes in me as much as I believe in him.

Finally, this thesis is dedicated to my sister Pip, and my parents, Don and Sharon. It was their love, support and encouragement that got me to this point, and to every other great moment in my life. They are beautiful and wonderful people who inspire me daily, and I am proud to call them my family. I love you!

Chapter 1 - Introduction

Anticipating and planning for ecosystem response to future climates is an essential component of contemporary forest management (Sinclair and Smith, 1999; Lindenmayer *et al.*, 2000). Bioclimate modeling provides a first approximation of the impact of climate change on forest ecosystems and, if used with due caution and consideration for the limitations, can be a valuable tool for resource management planning (Pearson and Dawson, 2003; Hamann and Wang, 2006). Bioclimate models have limitations, however, due to the large spatial scale of their application (Wilmking and Juday, 2005; Barrio *et al.*, 2006) and varied species response to changing climates (Driscoll, *et al.*, 2005; Wilmking and Juday, 2005). For instance, individuals of a moisture-dependent plant species can live in damp areas but may not have the same physiological response to moisture as individuals living in extremely wet flooded areas. These obstacles to bioclimate modeling highlight the importance of developing a full understanding of the relationship between climate and the growth of a species.

A valuable research tool for determining the varied response of different species to regional climate variations is to use transects (Bowman *et al.*, 2005; McCain, 2005; Botes *et al.*, 2006). This approach is particularly valuable in coastal mountain settings where topography and proximity to the ocean combine to result in environmental variability over relatively short distances. Notable in this regard, dendroclimatic studies have used transects to document regionally-varied climate / radial-growth responses (Hofgaard *et al.*, 1999; Gedalof and Smith, 2001a; Linderholm *et al.*, 2003; Wilmking and Juday, 2005).

The research presented in this thesis was undertaken in response to the need for developing a clearer understanding of climate variability and climate / radial-growth relationships of mountain hemlock trees (*Tsuga mertensiana* (Bong.) Carr.) (MH) in northwestern British Columbia (BC). The intent was to document how these climate / radial-growth relationships vary at sites located along a longitudinal transect series extending from the Queen Charlotte Islands to Smithers, BC. The study focuses on MH trees as previous researchers have shown their radial-growth is strongly related to air temperature, precipitation and snow pack depth (Brubaker, 1980; Graumlich and Brubaker, 1986; Woodward *et al.*, 1994; Gedalof and Smith, 2001a; Peterson and Peterson, 2001; Laroque and Smith, 2003).

In this thesis the following research questions are addressed:

1. What is the temporal and spatial climate variability across the study transect?
2. What is the climate / radial-growth response of MH trees at each study location and how does it change from coastal to interior sites?
3. What is the relationship between annual ring-width of MH trees and climate oscillations, such as the El Niño Southern Oscillation and the Pacific Decadal Oscillation, and how does this relationship change from coastal to interior sites?

Answers to these questions are sought by:

1. Collecting tree cores from high elevation MH stands along a longitudinal transect from the Queen Charlotte Islands to Smithers, BC.
2. Consolidating and analyzing meteorological data from meteorological stations located along the study transect.
3. Determining the relationship between air temperature, precipitation, and tree ring-width.
4. Determining the relationship between climate oscillations and tree ring-width.
5. Comparing coastal and interior tree-ring site chronologies and climate / radial-growth responses.

Following this chapter, Chapter 2 provides a description of the geography of the study transect. Chapter 3 examines the spatial and temporal variability of climate across the transect. Chapter 4 describes the development of the five MH chronologies. Chapter 5 provides an interpretation of the possible climate / radial-growth response of MH ring-width growth to air temperature, precipitation and snow pack depth. Chapter 6 examines radial-growth response of MH trees to the El Niño Southern Oscillation and the Pacific Decadal Oscillation. Finally, Chapter 7 summarizes the findings of this research.

Chapter 2 - Study Area

The research described within this thesis was completed within a small region of northwestern BC. The region spans several biogeoclimatic zones and is characterized by a distinctive west-to-east ecosystem structure (BC Ministry of Forests, 2001). These variations arise due to the orographic influence of the northwest to southeast trending Coast Mountain ranges that directly impact upon the role played by ocean and continental air masses within the region (Koeppe, 1931). Arising from this interplay of climate and topography, forest types in the region range from those dependent upon hypermaritime conditions to those adapted to dry interior conditions (BC Ministry of Forests, 2001). This chapter provides a general description of the physical setting along the study transect, and concludes by focusing on the high elevation climates and vegetation that characterize the mountain sites where sampling was undertaken.

2.1 Location

The research was conducted along a 350 km long transect bisecting the Coast Mountains in northwestern BC (Figures 2.1 and 2.2). Approximately paralleling the 54° N line of latitude, the transect extends eastward from the Queen Charlotte Islands at 132°19' W longitude to terminate at 127°48' W longitude at a site located within the Bulkley Range on the eastern slopes of the Hazelton Mountains (Figures 2.1 and 2.2).

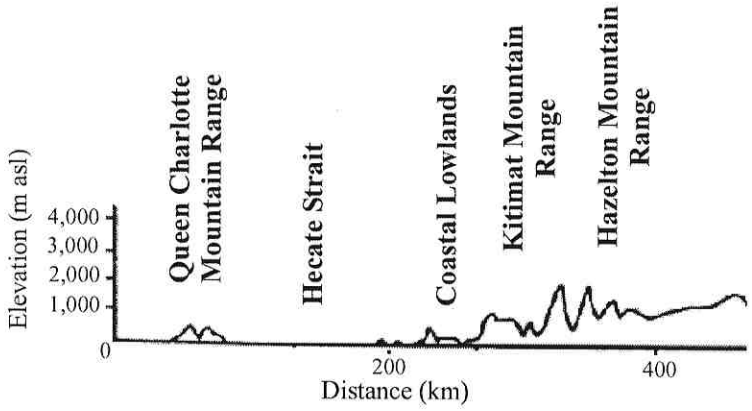

Figure 2.1 Schematic illustration of vertical relief along the study transect (adapted from Kendrew and Kerr, 1955:1).

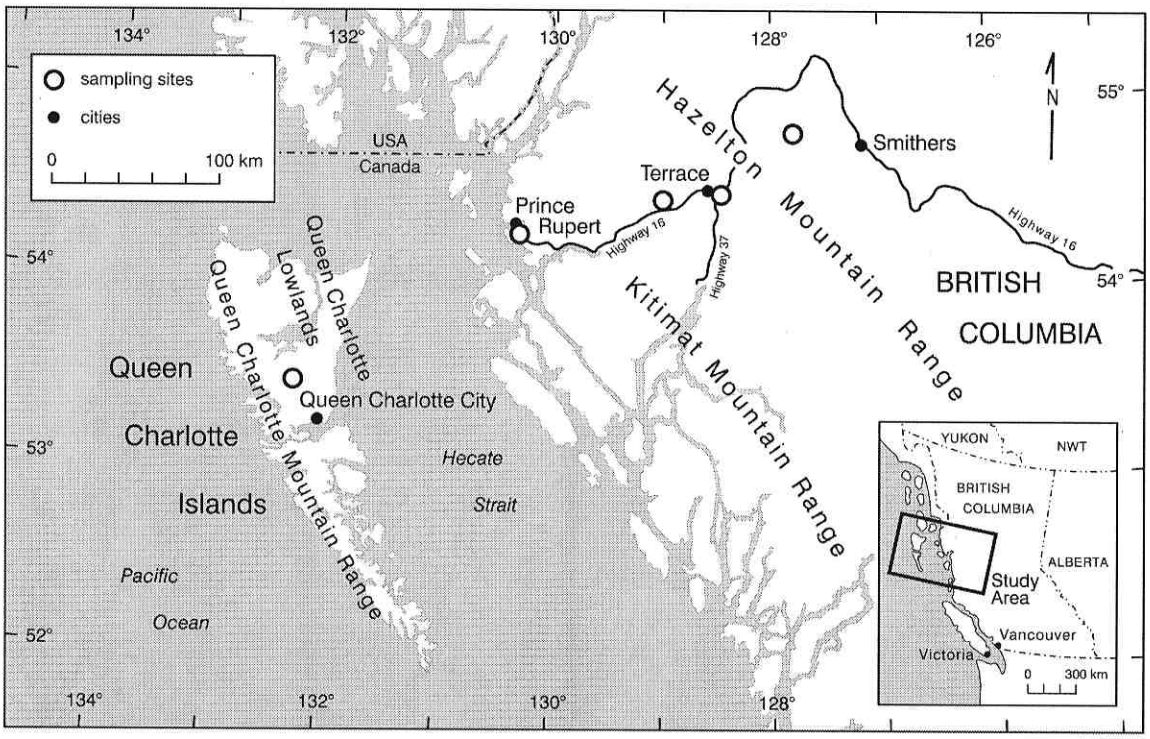

Figure 2.2 Location of mountain hemlock sampling sites along a longitudinal transect in northwestern BC.

2.2 Physiography

This west-east transect begins on the Queen Charlotte Islands at a site located between the northwest edge of the Queen Charlotte Island Mountain Range and the Queen Charlotte Lowlands (Figures 2.1 and 2.2). Eastward across Hecate Strait, the transect resumes in the vicinity of the city of Prince Rupert located at 40 m asl in the coastal lowlands of mainland BC (Figures 2.1 and 2.2). The transect then crosses over the Kitimat Range to reach maximum elevations of 2400 m asl in the vicinity of the city of Terrace, BC (Figures 2.1 and 2.2). East of the Kitimat Ranges, the transect bisects 1800 m asl high peaks in the Nass Range of the Hazelton Mountains before passing through 2100 m asl mountain summits in the Bulkley Range (Figures 2.1 and 2.2). The transect ends near the city of Smithers, BC at 1800 m asl (Figures 2.1 and 2.2).

2.3 Mountain Climate

The transect begins at a high elevation site located in a Marine Temperate Climate (Cfb) region of the Queen Charlotte Islands (Köppen, 1936) (Appendix A). As the transect bisects Prince Rupert and the Coast Mountains it crosses through several elevation-dependent regions varying from Continental Subarctic (Dfc), to Warm Summer Continental (Dfb), to Tundra Climate (ET) and Ice Cap (EF) climates (Appendix A) (Table 2.1).

Table 2.1 Köppen classification regions and characteristics encountered along the longitudinal transect from the Queen Charlotte Islands to Smithers, BC.

Climate Regions	Characteristics
Marine Temperate Climate Cfb	- Temperate/mesothermal climate - significant precipitation in all seasons - warmest month average temperature <22°C, >10°C - mean temperature of coldest month >-3°C, <18°C
Continental Subarctic Climate Dfc	- Continental/microthermal climate - significant precipitation in all seasons - warmest month average temperature <22°C, >10°C - mean temperature of coldest month <-3°C
Warm Summer Continental Climate Dfb	- Continental/microthermal climate - significant precipitation in all seasons - warmest month average temperature <22°C, >10°C - mean temperature of coldest month <-3°C
Tundra Climate ET	- Polar climate - warmest month has an average temperature between 0°C and 10°C
Ice Cap Climate EF	- Polar climate - all twelve months have average temperature below 0°C

The variability of mountain climates along the study transect arises due to three major driving forces: (1) the proximity to the Pacific Ocean; (2) the topography (specifically elevation) of each area; and (3) weather fronts and systems. The following is a summary of the effects these three factors have on the climate regimes along the transect; beginning at the western edge, in areas dominated by island and coastal climates, and then continuing eastward to transition to areas dominated by interior continental climate.

2.3.1 Island and Coastal Climates

Maritime Polar air masses travel across the North Pacific Ocean and bring moist air to the windward slopes of the Queen Charlotte Islands Insular Ranges and the Coast Mountains (Aguado and Burt, 2004). The Coast Mountain system extends along the entire west coast of BC and forms a 160 km wide barrier between the Pacific Ocean air masses and those of the BC interior. Orographic effects release abundant moisture on the windward side of the mountains and result in notable rain shadow effects on the lee side (Tuller, 2001). Similar orographic processes characterize the precipitation climates of the Queen Charlotte Islands, but mountains on the island are smaller and their influence is less significant (Bostock, 1970).

In the winter, the abundant moisture that falls as a result of orographic effects is paired with the influence of the warm ocean temperature relative to the cool land temperature, which results in mild and wet conditions. January air temperatures average 3.4°C in low elevation areas on the Queen Charlotte Islands and the coastal lowlands (Tuller, 2001). Higher elevation coastal sites are significantly cooler which results in the accumulation of deep snow packs during the winter months (Kendrew and Kerr, 1955). Cold Polar air masses from the interior can sweep down through the Coast Mountain valleys and reach coastal areas, resulting in a sudden decrease in air temperature (Koeppe, 1931).

During the winter months, most of the precipitation that falls along the coast region results from mid-latitude cyclonic storms generated along the frontal zone between warm air masses from the south and cool air masses from the north. The positions of the Aleutian Low, a low pressure system located south of the Aleutian

Islands in the North Pacific, and the ridge of high pressure over western Canada favour the flow of warm humid air, bringing mid-latitude cyclonic storms to the Alaskan and Pacific northwest coasts of North America. These storms usually reach maximum intensity in the area of the Aleutian Low, most prominent in January with a mean pressure below 1002 mb (Koeppe, 1931).

In the late spring and summer, the Aleutian Low migrates northward and is replaced by a weak high pressure system along the west coast of BC, which results in a pronounced dry period during the months of July and August (Kendrew and Kerr, 1955). Winds are predominantly westerly and northerly and bring a cooling effect from the ocean to the land (Koeppe, 1931), which results in average July air temperature below 17°C (Tuller, 2001).

2.3.2 Interior Climate

East of the Coast Mountains, the rain shadow effects in the Hazelton Mountains results in cold, snowy winters, warm and dry summers, and seasonal air temperature variations that are much larger than in coastal areas (Kendrew and Kerr, 1955). During the fall and winter months, a continental high pressure system persists over northern BC (Kendrew and Kerr, 1955). This anticyclone is an extension of the polar high pressure system that brings cold and dry conditions to the BC interior during the winter months, with January air temperatures averaging −1.2°C in the valley areas (Tuller, 2001). During the winter months, the interior of BC also experiences the effects of mid-latitude cyclonic storms that bring precipitation from the west, but to a lesser degree than on the coast. The track and intensity of these storms varies over time as they are influenced by the position of the Aleutian Low and the ridge of high pressure over western Canada.

The storms are diminished as they move from west to east over the mountains, which reduces the available precipitation and limits snow accumulation at the eastern edge of the study transect (Tuller, 2001).

In the spring and summer months, the continental high pressure system is replaced by a weakly developed thermal low pressure system (Koeppe, 1931). Summers are warm and dry, with July air temperatures averaging 16.8°C in the valleys (Tuller, 2001). Since the interior of BC experiences a rain shadow effect and mid-latitude cyclonic storms are much less frequent, the spring and summer precipitation is mostly convectional; warm air over the land creates unstable conditions, which results in convectional storms and precipitation (Tuller, 2001).

2.4 Vegetation

The interplay of physiography and climate has a direct effect on the forest structure of northwestern BC. According to the Biogeoclimatic Ecosystem Classification (BEC) developed for the BC Ministry of Forests, the study transect passes through four of the fourteen BEC zones (BC Ministry of Forests, 2001) (Appendix B). The Coastal Western Hemlock zone stretches from the Queen Charlotte islands to 50 km inland from Prince Rupert. Common dominant tree species include western hemlock (*Tsuga heterophylla*), western redcedar (*Thuja plicata*), Sitka Spruce (*Picea sitchensis*), yellow cedar (*Chamaecyparis nootkatensis*), Douglas-fir (*Pseudotsuga menziesii*) and Pacific silver fir (*Abies amabilis*). Approximately 35 km east of Prince Rupert, the dominant forest vegetation transgresses to the Mountain Hemlock zone in mid to high elevation (approximately 400 m asl) areas. This zone is dominated by MH, Pacific silver fir, and yellow cedar trees at high elevations, whereas western redcedar, western hemlock, Sitka

spruce, Douglas-fir and western white pine (*Pinus monticola*) trees characterize lower elevation forests. As the climate shifts to more continental conditions on the leeward side of the Coast Mountains and Hazelton Mountains, the Mountain Hemlock zone also includes subalpine fir trees (*Abies lasiocarpa*) at high elevations. The eastern limit of the study transect is an area of transition between the continental Mountain Hemlock zone and the Engelmann Spruce/Subalpine Fir zone, where common tree species include subalpine fir, Engelmann spruce (*Picea engelmannii*) and lodgepole pine (*Pinus contorta*). Along the entire transect, in areas above treeline, there is the Alpine Tundra zone, where common plant species include mountain heathers *(Phyllodoce spp. and Cassiope spp.*), numerous species of sedges and the occasional tree groups in krummholtz form.

Chapter 3 - Spatial and Temporal Climate Variability

3.1 Introduction

The Environmental Protection Division of the BC Ministry of Environment (MOE) released a report in 2002 titled "Indicators of Climate Change for BC, 2002" (EPD, 2002). Over the period from 1895 to 1995, the northeast Pacific coast and the northern Coast Mountains regions were shown to have experienced an average increase in annual air temperature of 0.6°C. The largest seasonal air temperature increases were recorded during the winter months, with an average increase of 1.9°C over the period of instrumental record. The MOE report also notes that the west coast of BC has experienced a 2% increase in total precipitation, with most of the change due to increased fall precipitation in many areas.

The MOE report describes historical climate changes that have potentially influenced the long-term radial-growth of MH trees in this region. In addition, although there are only 350 km between the most distant climate stations used in this study, large variations in local climates arise due to variables such as topography, elevation, aspect, and proximity to the Pacific Ocean. This chapter first reviews the principal ocean-atmospheric teleconnections influencing the climate of this region (El Niño Southern Oscillation and the Pacific Decadal Oscillation), and then uses local climate data to describe the spatio-temporal variability of climate along the transect for the period of available instrumental data.

3.1.1 El Niño Southern Oscillation and the Pacific Decadal Oscillation Influences on climate in Northwestern BC

El Niño Southern Oscillation (ENSO)

Tropical trade winds normally move warm equatorial water toward the western Pacific Ocean resulting in an upwelling of cool water in the eastern Pacific Ocean. The warm water in the western Pacific Ocean leads to higher air temperatures, lower surface air pressure, an increase in convectional precipitation and a regional sea level that is 0.5 m higher than that found in the eastern Pacific (Aguado and Burt, 2004).

An El Niño event develops when the trade winds weaken or reverse, causing warm equatorial water to flow eastward (also partly due to the higher sea levels in the western Pacific) resulting in above average sea surface temperature (SST) anomalies along the tropical eastern Pacific Ocean coast and in the central Pacific (Aguado and Burt, 2004). A La Niña event is the opposite of El Niño, and creates a below-average SST anomaly along the coast. The Southern Oscillation refers to an oscillation in air pressure between the eastern and western low-latitude Pacific Ocean due to the sea surface temperature changes and variations between uplift and downward-moving air. Because of the link between El Niño/La Niña (EN) and the Southern Oscillation (SO), these events are referred to as ENSO events.

For the purpose of this thesis, ENSO events will be described by the Niño 3.4 definition: above/below average (using 1971-2000 normals) sea surface temperatures in the equatorial Pacific Ocean (in the region between 120°W-170°W and 5°N – 5°S) greater than or equal to 0.5°C for three months or more (Trenberth, 1997b). An El Niño event often brings a mild, wet winter to the area along the longitudinal transect examined

in this study, while a La Niña event often brings low air temperatures and deep snow packs (Environment Canada, 2003). The average length of either an El Niño or La Niña phase is 8 to 15 months and can occur every 3 to 7 years (Hare and Mantua, 2000).

Several records of ENSO events exist; the following list of ENSO events is based on a consensus between records provided by The Western Region Climate Center, Climate Diagnostics Center, and the Climate Prediction Center (GGWS, 2004). The strongest El Niño events since 1950 occurred in 1972/73, 1982/83, 1991/92, and 1997/98; the strongest La Niña events since 1950 occurred in 1955/56, 1973/74, 1975/76, and 1988/89 (these events were all identified as the "strongest" since 1950 and are not listed in any order of strength relative to each other) (GGWS, 2004).

Pacific Decadal Oscillation (PDO)

The PDO refers to SST anomalies in the northern and eastern Pacific Ocean (Mantua *et al.*, 1997). Anomalously cool SST in the north Pacific Ocean and warm SST in the eastern Pacific Ocean characterize a warm (positive) phase of the PDO (Mantua *et al.*, 1997). A cool (negative) phase is the result of the opposite temperature gradient – anomalously warm temperatures in the North Pacific Ocean and cool temperatures along the coast of Pacific Canada. A positive PDO is associated with an eastward-shifted and more intense Aleutian Low which, when accompanied by a ridge of high pressure over western Canada, favours the southwest flow of relatively warm, humid air and alters the storm track position (Trenberth and Hurrell, 1994).

A positive PDO is associated with mild winters in the area surrounding the study transect (Mantua *et al.*, 1997). There is some discrepancy in the literature regarding the effects of the PDO on precipitation regimes of the area surrounding the longitudinal

transect identified in the this study, mostly due to a lack of small-scale regional studies. Cayan and Peterson (1989) observed less streamflow from the Skeena River during positive PDO regimes, indicating a reduction in precipitation. Hartmann and Wendler (2005) however, observed increased precipitation in southeast Alaska (northwest of the study area) and in northwestern BC. Mantua *et al.* (1997) comment on the high pressure system limiting the precipitation in BC during positive PDO regimes.

PDO regime shifts in the 20th century occurred in 1924 (- to +), 1946 (+ to -) and 1976 (- to +) (Minobe and Mantua, 1999; Gedalof and Smith, 2001b). Possible similar regime shifts have been identified back to 1600 AD (Wiles *et al.*, 1998; Kadonaga *et al.*, 1999; Minobe and Mantua, 1999; Gedalof and Smith, 2001b; Mantua and Hare, 2002; Jacoby *et al.*, 2004) and more are suspected to have occurred before this time (D'Arrigo *et al.*, 2001).

Biondi *et al.* (2001) identified possible PDO regime shifts, from 1661 to 2001, within a network of tree-ring chronologies collected in southern California and Baja California. They reported a post-1900 shift to longer periods between events, but a higher frequency of strong events. Although they hypothesized these changes may be due to greenhouse warming, Shen *et al.* (2006) proposed that the Gleissberg cycle (70-100 year) of variability in solar irradiance may offer an explanation for the 75-115 year low frequency PDO shifts.

If an El Niño event occurs during a PDO positive phase, there is an enhanced northern Hemisphere association including increased SST along the eastern Pacific coast and a deepening and eastward shift of the Aleutian Low. The PDO modulates ENSO teleconnections affecting North America since El Niño (La Niña) events tend to be strong

and stable during positive (negative) PDO phases (Gershunov and Barnett, 1998; Bonsal *et al.*, 2001). Kadonaga *et al.* (1999) found that El Niño events were more frequent and stronger post-1925 (positive PDO) but returned to pre-1924 (negative PDO) frequency in 1947. These results correspond with the recognized PDO regime shifts, further emphasizing the links between El Niño events and the PDO. However, it is important to note that this relationship is not perfect; there can be El Niño and La Niña events during both positive and negative PDO regimes (Hare and Mantua, 2000).

3.2 Methods

Climate data from four long-term climate stations included within Environment Canada's Adjusted Historical Canadian Climate Data set were used in this analysis: 1) Sandspit A (SS); 2) Prince Rupert A (PR); Terrace A (TR); and Smithers A (SM) (Figure 3.1; Table 3.1). These climate stations were selected because they are the most proximate to the sampling sites shown in Chapter 2 (Figure 2.2). The climate data set provides monthly precipitation totals, monthly mean daily maximum and minimum air temperatures and monthly mean air temperature. Note that maximum and minimum air temperatures in the following discussion refer to the mean daily maximum and mean daily minimum and not the lowest and highest air temperatures recorded in the relevant period.

All the station data were adjusted to address data gaps or station inhomogeneity resulting from location changes and urbanization. Missing values were estimated using a methodology developed by Vincent (1998) in which the climate series were tested for relative homogeneity in relation to neighbouring stations (AHCCD, 2005). Any inhomogeneities were identified and, wherever possible, regression analysis was used to

adjust monthly data with the use of highly correlated neighbouring stations (AHCCD, 2005). Data from the Prince Rupert A station were statistically adjusted (Vincent, 1998; Vincent and Gullett, 1999) to account for station relocations in 1914 and 1962 (Lucie Vincent, Environment Canada, personal correspondence).

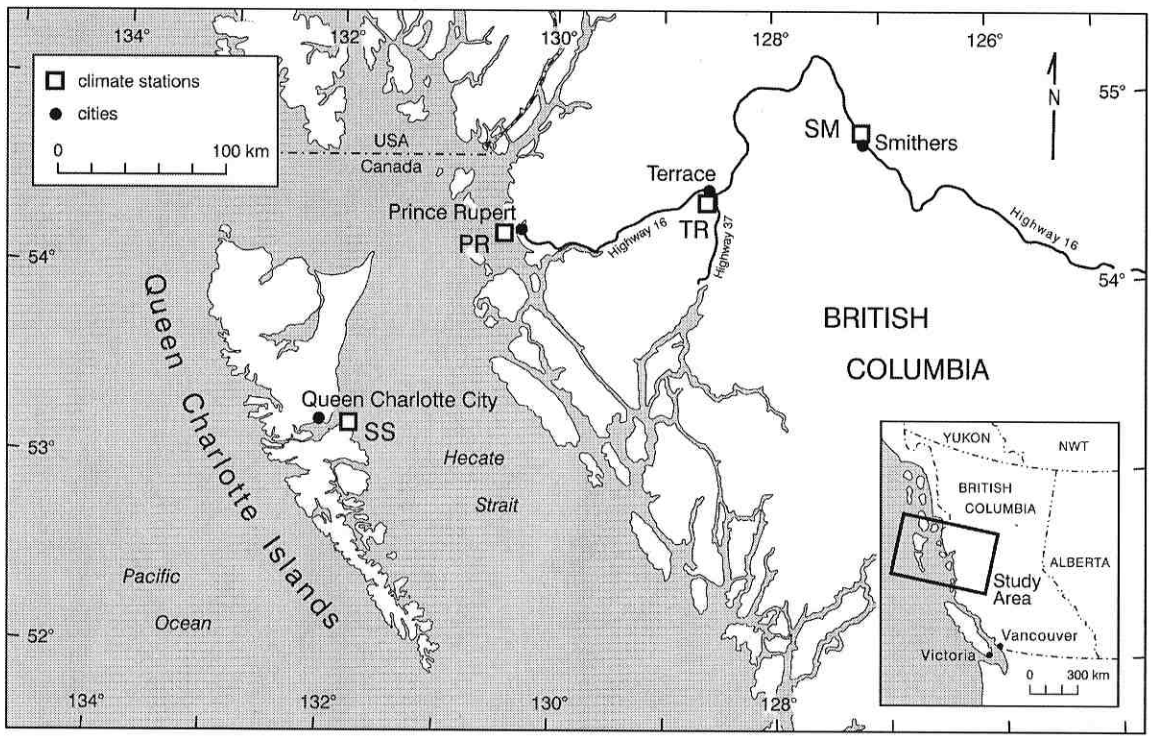

Figure 3.1 Location of the four Environment Canada climate stations used along a longitudinal transect in northwestern BC. Station acronyms are given (SS: Sandspit A, PR: Prince Rupert A, TR: Terrace A, SM: Smithers A).

Table 3.1 Location and duration of four Environment Canada climate stations used along a longitudinal transect in northwestern BC.

Station and ID#	Latitude	Longitude	Elevation (m asl)	Years of data
Sandspit A (SS) 1057050	53°15'N	131°49'W	6	1948-2002
Prince Rupert A (PR) 1066481	54°18'N	130°27'W	35	1908-2002
Terrace A (TR) 1068130	54°28'N	128°35'W	217	1954-2004
Smithers A (SM) 1077500	54°49'N	127°11'W	522	1938-2003

* Data from Environment Canada's Adjusted Historical Canadian Climate Data Set. From http://www.cccma.bc.ec.gc.ca/hccd/ [accessed September 20, 2005]

The monthly climate data were compiled into seasonal groupings:

- Winter - December of the previous year, January and February
- Spring – March, April, May
- Summer – June, July, August
- Fall – September, October, November.

In the case of air temperature (max, min and mean), the monthly data from each grouping (winter, spring, fall, summer) were averaged to provide a seasonal value. In the case of the precipitation data, the annual monthly records within each seasonal grouping were totalled. All months were used to calculate the annual averages/totals.

Linear regression techniques were used to identify trends within the annual and seasonal air temperature (max, min and mean) and precipitation data sets. This method is widely used and provides a meaningful way to observe general trends in climate data (Moore and McCabe, 1999). In this instance, the slope values of the trend lines were used to determine the change in °C and mm of precipitation per year, and were multiplied by the number of years of record to determine the trend in air temperature and precipitation over time. The slopes of the air temperature and precipitation trends were

plotted to determine if they were normally distributed, and t-tests were performed to determine if the trends were significantly different from zero (95% confidence level).

Cumulative departure from the mean was calculated for mean annual air temperature and total annual precipitation to produce graphical representations of the yearly trends at each site. For total annual precipitation, cumulative departure from the mean was calculated following (Karanka, 1986):

$$y_i = 100*\sum((x_i / x_{mean}) - 1)$$

where y_i is the cumulative percent departure from the mean to year i of the record, x_i is the total precipitation for year i, and x_{mean} is the mean annual total precipitation for the entire record. Since there is no absolute 0 for air temperature in degrees °C, the cumulative departure from the mean is calculated using the following formula:

$$y_i = \sum(x_i - x_{mean})$$

where y_i is the cumulative departure from the mean to year i of the record, x_i is the average annual air temperature (°C) for year i, and x_{mean} is the mean annual air temperature for the entire record. A zero slope would indicate a time of average conditions; a positive slope would indicate a time of above-average conditions; and a negative slope would indicate a time of below-average conditions (Karanka, 1986).

3.3 Results

3.3.1 Air Temperature

Table 3.2 summarizes the mean seasonal air temperature at each of the climate stations (from 1957 to 2002). The TR station experiences the highest mean summer air temperatures (15.4°C), while the PR station records the lowest (12.5°C). During the winter season the lowest mean air temperature is found at the SM station (-7.1°C), while

the highest winter air temperature occurs at the SS station (3.5°C), contributing to the warmest annual mean air temperature (8.3°C). The SM station exhibits the largest range in seasonal mean air temperatures (21.1°C), followed by the TR station (18.3°C), the PR station (10.6°C) and finally the SS station (10.1°C).

Table 3.2 Mean seasonal and annual air temperatures at four Environment Canada climate stations along a longitudinal transect in northwestern BC (1957 – 2002).

	Winter (°C)	**Spring (°C)**	**Summer (°C)**	**Fall (°C)**	**Annual (°C)**	**Seasonal Range [Summer to Winter] (°C)**
Sandspit (SS)	3.5	6.6	13.6	9.3	8.3	10.1
Prince Rupert (PR)	1.9	6.0	12.5	7.8	7.1	10.6
Terrace (TR)	-2.9	6.1	15.4	6.4	6.3	18.3
Smithers (SM)	-7.1	4.4	14.0	4.1	3.8	21.1

3.3.2 Precipitation

Table 3.3 shows the total seasonal and annual precipitation at each of the stations (from 1957-2002). Of the four stations, Prince Rupert receives the highest total annual precipitation (2654.7 mm) and has the greatest seasonal range (353.8 mm). SM receives the lowest total annual precipitation (586.2 mm) and also has the lowest seasonal range (12.0 mm). At all stations, the majority of precipitation occurs in the fall and winter seasons.

Table 3.3 Total seasonal and annual precipitation at four Environment Canada climate stations along a longitudinal transect in northwestern BC (1957 – 2002).

	Winter (mm)	Spring (mm)	Summer (mm)	Fall (mm)	Annual (mm)	Seasonal Range [Summer to Winter] (mm)
Sandspit (SS)	492.6	278.0	171.8	483.9	1427.4	320.8
Prince Rupert (PR)	775.2	527.9	421.4	933.8	2654.7	353.8
Terrace (TR)	477.9	203.7	166.2	480.4	1322.3	311.7
Smithers (SM)	160.0	91.0	148.0	190.5	586.2	12.0

3.3.3 Temporal Trends

Table 3.4 shows the slope of the trendlines for seasonal and annual mean daily maximum, minimum and mean air temperatures, and total precipitation[1] for each climate station over all the years of available data. All the variables have kurtosis and skewness values under ± 2.0, indicating they are normally distributed (Table 3.6). A one-sample t-test was performed to test whether trend slopes for each climate variable (maximum, mean, minimum air temperature and total precipitation) were significantly different from zero, at a 95% confidence level (Table 3.5). The significance level of each climate variable was below 0.05, indicating they had statistically significant slopes.

Air temperature and precipitation data from all stations had a positive slope (increase in either air temperature or precipitation over the years of record) for seasonal values with the following exceptions: SS - fall precipitation; PR – summer and fall

1 See Appendix C for graphs of seasonal and annual air temperature (max, mean and min) and precipitation trends.

maximum air temperature, winter and spring precipitation; TR – winter precipitation; SM – fall maximum and mean air temperature (Table 3.4). While there does seem to be a warming trend for all seasons at all stations, the greatest air temperature increases seem to be occurring in the winter season. The greatest increase in seasonal maximum and mean air temperature measured by the slope of the linear trend line has been during the winter at the SS station (0.036 °C/yr and 0.034 °C/yr) (Table 3.4). The greatest increase in minimum air temperature has also been during the winter at the SM station (0.038 °C/yr) (Table 3.4). The fall season shows the lowest air temperature increase across all stations.

All four stations demonstrate positive annual air temperature trends. The SS station recorded the greatest increase in annual mean daily maximum air temperature, as indicated by the slope of the linear trend line, (0.021°C/yr), while the TR station recorded the greatest increase in annual mean daily minimum air temperature (0.024 °C/yr) (Table 3.4). The greatest increase in annual mean air temperature is the same for the SS and TR stations (0.019 °C/yr).

There is an increase in annual precipitation across all sites, with the largest increase recorded at the SS station (slope of the trend line is 2.536 mm/yr) (Table 3.4). The SM station recorded the smallest annual increase in precipitation (0.759 mm/yr) followed closely by the TR station (0.940 mm/yr) (Table 3.4). The largest seasonal increase is seen at the PR station in the fall (2.414 mm/yr) (Table 3.4). The SS station has experienced a substantial increase in winter precipitation (1.883 mm/yr), while the remaining three stations experienced either a decrease in winter precipitation or a very

small increase (Table 3.4). An interesting note is that the increase in winter precipitation at the SS station follows a decrease in fall precipitation (-0.479 mm/yr) (Table 3.4).

The four climate stations examined in this study exhibit significant trends in air temperature and precipitation. The data from each climate station indicates an average increase in annual mean air temperature of 0.015°C/yr. The largest seasonal mean air temperature increase occurred in the winter (0.036 °C/yr). Annual minimum temperatures increased more (0.080°C/yr) than annual maximum temperatures (0.010°C/yr). Annual total precipitation has increased at all the stations, with the greatest seasonal increase occurring in the fall (when averaged across all stations).

Table 3.4 Slopes of seasonal and annual trend lines for max, min and mean annual and seasonal air temperatures and total precipitation from four Environment Canada climate stations along a longitudinal transect in northwestern BC.

		Annual	Winter	Spring	Summer	Fall
Sandspit	Max °C/yr	0.021	0.036	0.021	0.015	0.012
	Mean °C/yr	0.019	0.034	0.021	0.012	0.010
	Min °C/yr	0.018	0.032	0.022	0.009	0.008
	Precip mm/yr	2.536	1.883	0.946	0.244	*-0.479*
Prince Rupert	Max °C/yr	0.004	0.013	0.004	*-0.001*	*-0.002*
	Mean °C/yr	0.009	0.016	0.009	0.007	0.004
	Min °C/yr	0.015	0.019	0.013	0.015	0.010
	Precip mm/yr	2.402	*-0.557*	*-0.055*	0.742	2.414
Terrace	Max °C/yr	0.014	0.002	0.015	0.028	0.003
	Mean °C/yr	0.019	0.033	0.019	0.011	0.005
	Min °C/yr	0.024	0.037	0.023	0.020	0.007
	Precip mm/yr	0.940	*-0.296*	0.629	0.522	0.062
Smithers	Max °C/yr	0.001	0.012	0.005	0.001	*-0.009*
	Mean °C/yr	0.012	0.025	0.012	0.012	*-0.002*
	Min °C/yr	0.022	0.038	0.019	0.023	0.006
	Precip mm/yr	0.759	0.034	0.097	0.100	0.273

Table 3.5 Results of t-test for trend slopes of seasonal and annual maximum, mean, and minimum air temperatures and total precipitation from four Environment Canada climate stations along a longitudinal transect in northwestern BC.

Climate Variables	t – test statistic	Degrees of Freedom	Significance (2-tailed)	Mean Difference from 0	95% Confidence Interval of the Difference	
					Lower	*Upper*
Maximum Temp	3.871	19	0.001	0.0095	0.0044	0.0147
Mean Temp	7.013	19	0.000	0.0143	0.0100	0.0186
Minimum Temp	9.141	19	0.000	0.0191	0.0147	0.0234
Total Precip.	3.099	19	0.006	0.6598	0.2142	1.105

Table 3.6 Descriptive statistics of air temperature and precipitation trend lines from four Environment Canada climate stations along a longitudinal transect in northwestern BC.

	Maximum Temperature	Mean Temperature	Minimum Temperature	Total Precipitation
Mean	0.0095	0.0143	0.0191	0.6598
Median	0.00820	0.0118	0.0192	0.3975
Mode	0.0007	0.0118	0.0229	-0.5565
Std. Deviation	0.0110	0.0091	0.0093	0.9522
Skewness	0.673	0.708	0.577	0.928
Kurtosis	0.282	0.393	-0.087	-0.128

Table 3.7 Total change in seasonal and annual max, min and mean air temperature and total precipitation determined from the linear trend line.

		Years	Annual	Years	Winter	Spring	Summer	Fall
Sandspit	Max °C	1948-2002	1.13	1949-2002	1.92	1.13	0.80	0.66
	Mean °C		1.06		1.84	1.15	0.64	0.54
	Min °C		1.00		1.75	1.18	0.46	0.42
	Ppt mm	1949-2003	139.49	1950-2003	101.66	51.07	13.18	*-25.86*
Prince Rupert	Max °C	1908-2002	0.35	1909-2002	1.18	0.38	*-0.08*	*-0.22*
	Mean °C		0.86		1.50	0.81	0.67	0.38
	Min °C		1.40		1.82	1.25	1.41	0.96
	Ppt mm	1911-2002	220.97	1912-2002	*-50.64*	*-5.01*	67.55	219.65
Terrace	Max °C	1956-2004	0.67	1957-2004	0.09	0.70	1.34	0.12
	Mean °C		0.94		1.58	0.89	0.54	0.23
	Min °C		1.20		1.79	1.10	0.97	0.33
	Ppt mm	1954-2004	47.95	1955-2004	*-14.79*	31.43	26.10	3.10
Smithers	Max °C	1938-2003	0.05	1939-2003	0.75	0.32	0.05	*-0.59*
	Mean °C		0.76		1.61	0.78	0.77	*-0.10*
	Min °C		1.47		2.48	1.24	1.49	0.40
	Ppt mm	1942-2003	47.08	1943-2003	2.06	5.90	6.12	16.65

Common to all stations is a trend of below-average mean air temperatures from 1963 through 1976, followed by a period of little change until 1979 (with the exception of the PR station) and then a trend of above-average mean air temperatures until present (Figure 3.2). The PR and SM stations, which have the longest records, also show a trend of below-average mean air temperatures around 1946 to 1957 (Figure 3.2). The PR station, having the longest record, shows changes from above- to below-average mean air temperature in 1915 and 1932 and changes from below to above-average mean air temperatures in 1912 and 1922 that are not comparable to trends at any of the other sites. There does not appear to be a common pattern in annual total precipitation among all stations; each station shows site-specific precipitation patterns of normal, below- and above-average mean precipitation (Figure 3.3).

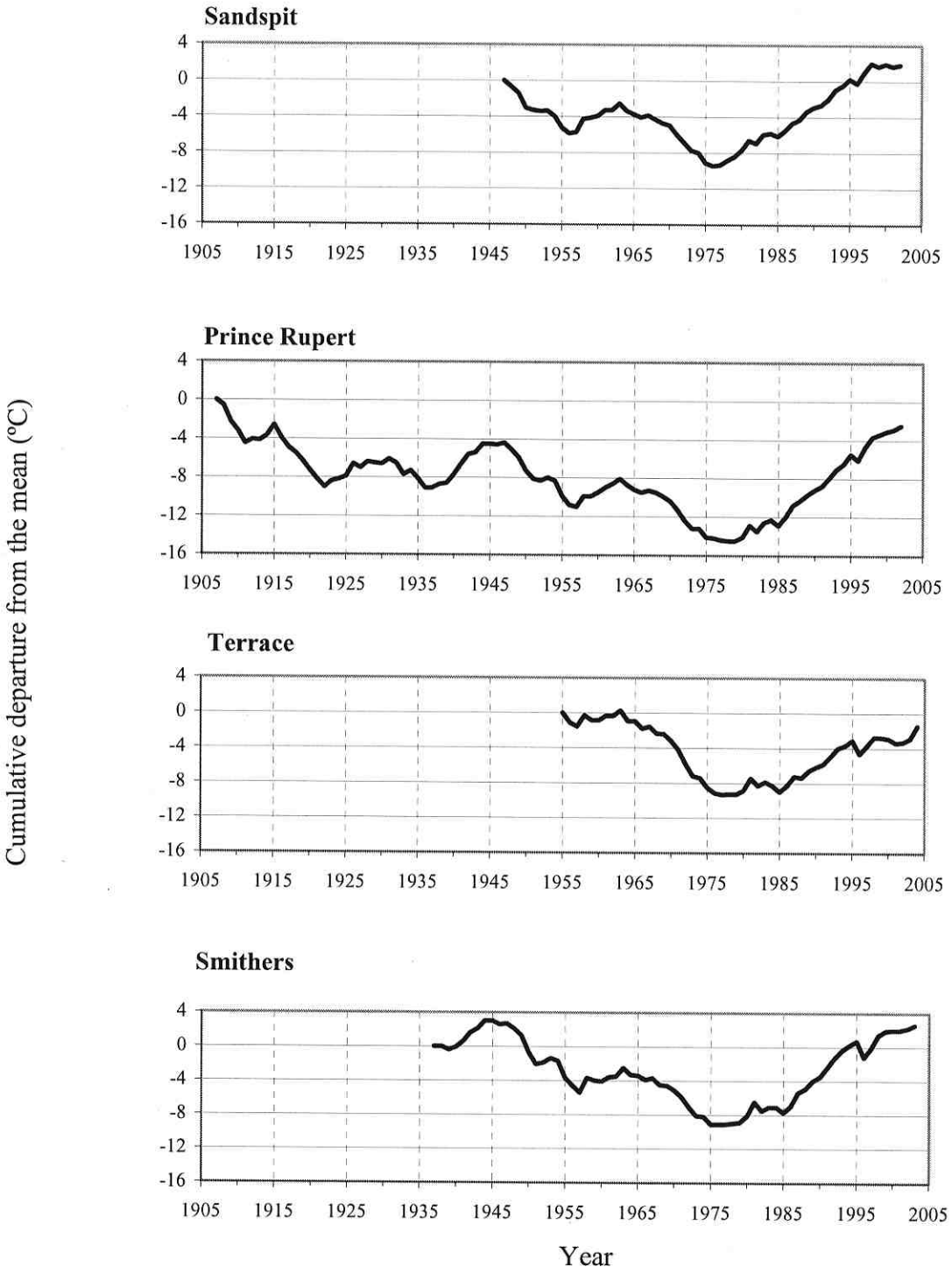

Figure 3.2 Annual average air temperature cumulative departure from the mean for four Environment Canada climate stations along a longitudinal transect in northwestern BC.

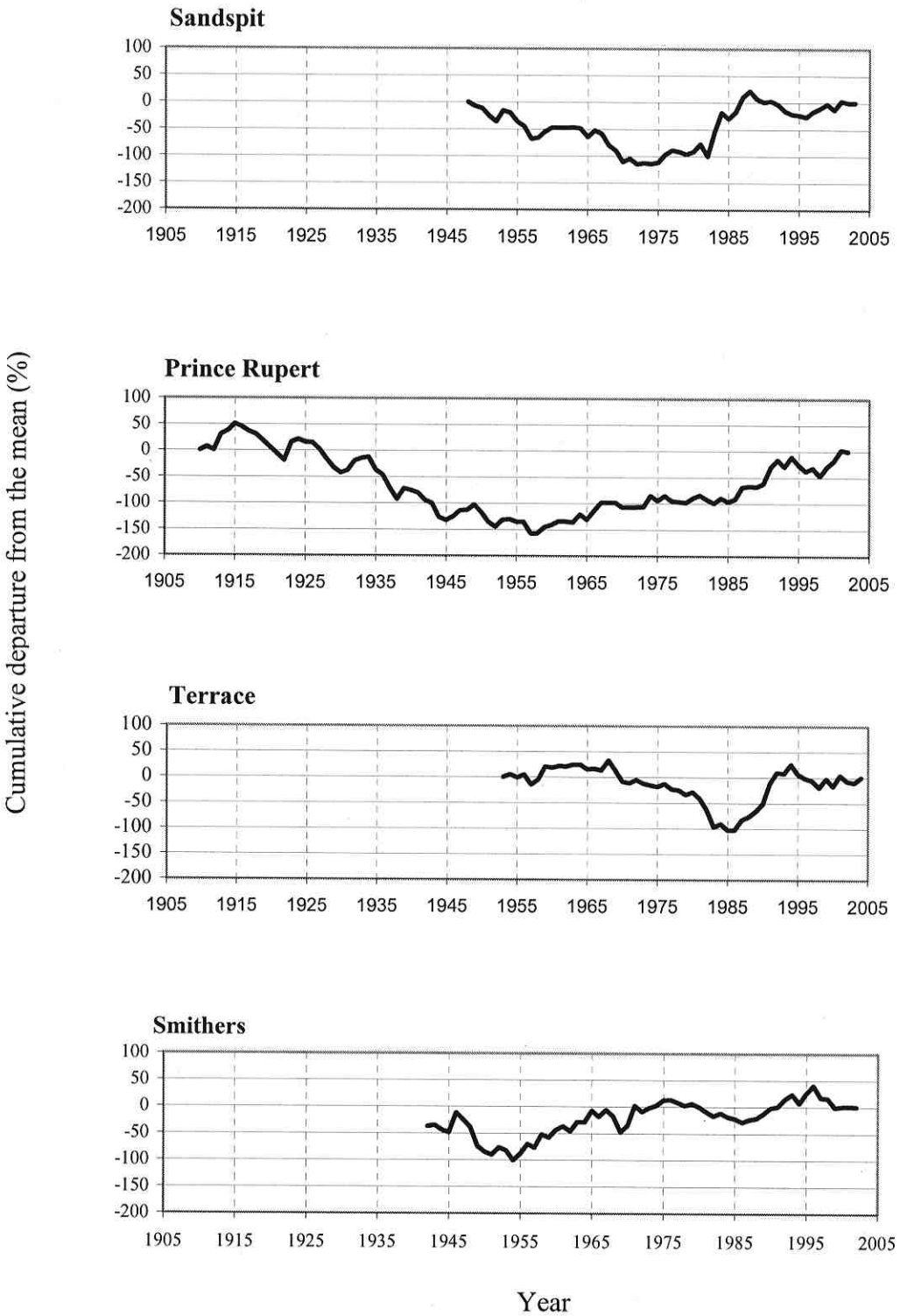

Figure 3.3 Annual total precipitation cumulative departure from the mean for four Environment Canada climate stations along a longitudinal transect in northwestern BC.

3.4 Discussion

3.4.1 Evidence of Climate Oscillations Effects Across the Transect

The four study climate station records all show evidence of ENSO effects. This point is emphasized in Figure 3.2 where significant departures from the mean annual air temperature are shown to correspond to dates assigned to some El Niño and La Niña events by GGWS (2004). There is a clear change from below- to above-average mean air temperatures in 1982/83 and 1997/98 possibly due to the effects of El Niño events (Figure 3.2). The La Niña event of 1974 - 1976 (GGWS, 2004) is also seen in a period of below-average mean air temperature in each of the stations cumulative departure from the mean (Figure 3.2). Therefore, though not all El Niño or La Niña events cited by GGWS (2004) appear in the records of the four climate stations, there is some evidence to suggest the possibility that ENSO is affecting the climate across the study transect in at least a few instances. The lack of evidence of all ENSO events could be because some events are more subtle than others and may only appear in higher resolution data. It is also possible that natural climate variability, caused by the location of pressure systems, advection of air masses and storm tracks, have countered the effects of an ENSO event.

The records of the four climate stations along the study transect show evidence of PDO regime shifts that correspond in time to those reported by Minobe and Mantua (1999) and Gedalof and Smith (2001b) (Figure 3.2). The PR station, having the longest record does show the 1924 shift (Figure 3.2). The two longest records (PR and SM) both show a shift from a trend of above average annual air temperatures to a trend of below average air temperatures around 1946 (Figure 3.2). The PR station shows a similar shift closer to 1948 and there is an apparent lag (Figure 3.2). The 1977 shift is evident in the

QCI station, while the PR, TR and SM stations all show a PDO-like shift by 1980, possibly a lag effect from the documented 1977 shift (Figure 3.2). The lag effects can be explained by the fact that the PDO regime shifts are identified by SST anomalies in the northern and eastern Pacific Ocean, and it follows that the resulting atmospheric conditions, affected by or affecting the SST anomalies, may not appear in the same year. There is sufficient evidence to suggest that the PDO affects the air temperature across the study transect from the mid 1940s to the end of the record.

3.5 Summary

Due to physiography, proximity to the Pacific Ocean, pressure systems and climate oscillations the transect from the Queen Charlotte Islands to Smithers BC, is an area of spatial and temporal climate variability. The climate across the study transect, transitions from a mild and wet climate to a dry climate exhibiting more extreme air temperatures.

The largest range in seasonal mean air temperatures was found at the Smithers station, followed by the Terrace station, the Prince Rupert station and finally the Queen Charlotte Islands station. The station receiving the highest annual precipitation is Prince Rupert, while the annually driest site is in Smithers. All annual air temperature trends are positive and while there does seem to be a warming trend for all seasons at all of the stations, the greater air temperature increases seem to be occurring in the winter seasons. There is an increase in annual precipitation across all sites with the largest increase seen at the Sandspit station on the Queen Charlotte Islands. There is also some evidence of the possible influence of the Pacific Decadal Oscillation and the El Niño/La Niña events at each of the sites in the instrumental air temperature records.

Chapter 4 - Mountain Hemlock Ring-width Chronologies

4.1 Introduction

The study of dendroclimatology relies upon identifying a tree species that is sensitive to changes in climate. Previous research has established that MH is a useful species for dendroclimate studies in northwestern BC. The following chapter introduces the distribution and habitat of MH trees and reviews the prior use of this species in dendroclimate research. A description of the sampling sites, field methods, analytic methods and results of the study chronologies will be given.

4.1.1 MH Distribution and Habitat

MH is a conifer that is found in Pacific North America at locations as far north as 61° N latitude along the Alaskan coastline to as far south as the crest of the Sierra Nevada in California at 37° N latitude (Figure 4.1). In the Coast Mountains of northwestern BC, MH trees are found at elevations from sea level to 1800 m asl, in areas characterized by a cool, wet climate with deep snow packs. This distribution is evidence of the robust nature of this tree species and its ability to withstand harsh growing conditions in areas of heavy snow-loading (Arno and Hammerly, 1977).

Mature MH trees range in height from 15 m to 46 m and can live to 990+ years (Laroque, 1995). The diameter of older trees range from 30 cm to 150 cm (Means, 1990). In a study conducted in the Cascade Mountains of central Oregon, it was found that MH trees are the most susceptible species in the area to laminated root rot (*Phellinus weiri*); a disease that eventually shortens the life of the tree (Means, 1990). Other common diseases affecting MH trees include various types of heart rots (*Heterobasidion*

annosum, Phellinus pini, Fomitopsis pinicola, Phaeolus schweinitzii, Echinodontium tinctorum), needle diseases and snow mold (*Herpotrichia nigra*) (Means, 1990).

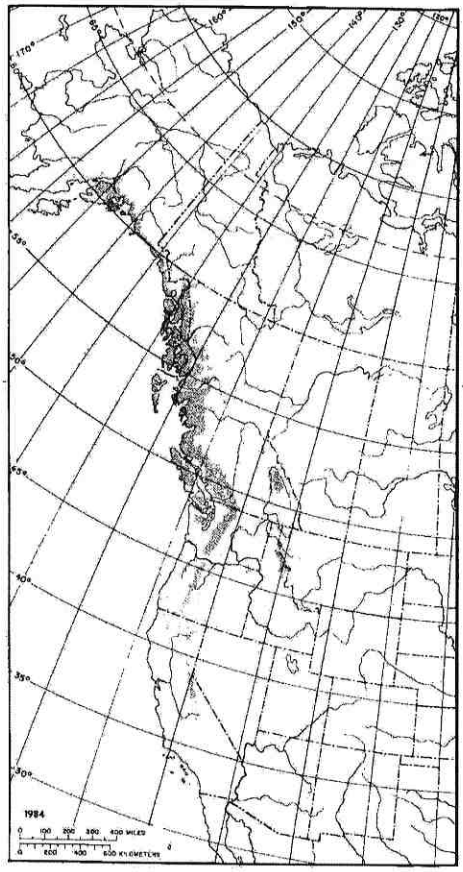

Figure 4.1 The native range of MH shown in shaded areas (from Means, 1990: 623).

MH trees are found on various types of parent material including volcanic, sedimentary, metamorphic, and glacial sediments (Means, 1990). They can grow on immature to mature acidic soils (pH 3.4 to 5.0) (Means, 1990). In BC, mature soils found under stands of MH trees typically have a 13 to 28 cm thick forest floor[2] with a root mor or mycelial root mor humus layer (Means, 1990).

[2]Forest floor is fresh and decomposing organic litter which forms the surface layer of a soil under forest vegetation.

Typically the understory of MH forests (mixed and pure) in coastal BC is dominated by deciduous shrubs such as Cascades azalea (*Rhododendron albiflorum*), Alaska huckleberry (*Vaccinium alaskaense*), rustyleaf menziesia (*Menziesia ferruginea*), ovalleaf huckleberry (*Vaccinium ovalifolium*), and several mosses. MH trees are considered tolerant of shade and forms of competition. Common tree associates are western hemlock and western redcedar (at lower elevations throughout the zone); Douglas-fir and western white pine (at lower elevations in the south); Sitka spruce (at lower elevations in the north); lodgepole pine (on very dry sites); subalpine fir (near timberline and leeward of high elevations in the Coast Mountains); whitebark pine (*Pinus albicaulis*) (near timberline); and Pacific silver fir (middle to upper elevations of moist mountain ranges) (Arno and Hammerly, 1977; Means, 1990).

4.1.2 MH Dendroclimatology

MH trees have been widely used in dendroclimate studies due to their sensitivity to monthly mean air temperature, monthly total precipitation and spring snow pack depth (Brubaker, 1980; Graumlich and Brubaker, 1986; Woodward *et al.*, 1994; Gedalof and Smith, 2001a; Peterson and Peterson, 2001; Laroque and Smith, 2003). Laroque and Smith (2003) found that of five high-elevation conifers species on Vancouver Island, MH was the tree species most responsive to climate, which makes it a useful species for climate reconstruction.

The science of dendroclimatology is based on the assumption that the annual ring-width pattern of a tree reflects yearly changes in climate (Cook, 1990). The total annual ring-width increment is, however, a factor of a number of variables playing a role in the aggregate growth of an individual tree-ring (Cook, 1990):

$$R_t = A_t + C_t + *D1_t + *D2_t + E_t$$

A_t - age related growth trend due to normal physiological aging processes
C_t - climate that occurred during that year
$D1_t$ - occurrence of disturbance factors *within* the forest stand (for example, a blow down of trees)
$D2_t$ - the occurrence of disturbance factors from *outside* the forest stand (for example, an insect outbreak that defoliates the trees, causing growth reduction)
E_t - random (error) processes not accounted for by these other processes.
* - either a "0" for absence or "1" for presence of the disturbance signal

If the non-climatic parameters associated with these variables can be removed or accounted for, a relationship between climate and the radial-growth of trees can be defined. Alternatively, when climate variables act as the sole factors limiting radial-growth, a climate / radial-growth response can be defined to describe the annual ring-width increment (Schweingruber, 1989). Using this relationship between climate and tree growth, an annual tree-ring increment record can provide a proxy indicator of climatic conditions (Fritts, 1976).

The radial-growth of MH trees is influenced by limiting factors[3] and, since there can be several climatic limiting factors at high elevations (Kramer and Kozlowski, 1960), MH trees from high elevation sites are ideal candidates for extracting proxy climate signals. MH trees found at low to mid-elevation sites face fewer limiting factors and have not been considered as living in ideal locations for dendroclimate research (Fritts, 1976; Gedalof and Smith, 2001a). Because of this, several studies have focused on the high elevation MH sites. There is, however, some evidence that low-elevation stands are more climatically sensitive than previously thought (Holman and Peterson, 2006). Table

[3] Limiting factor is an environmental factor that limits the growth, abundance, or distribution of an organism in an ecosystem.

4.1 summarises the research examining the climate / radial-growth relationship of MH trees.

Table 4.1 Summary of major research studies investigating the climate / radial-growth relationship of mountain hemlock trees in western North America.

Source	Positive Relationship	Negative Relationship	Location
Peterson and Peterson (2001)	-growth-year summer temp (Washington/N. Oregon) - previous summer precipitation (S.Oregon)	- spring snow pack depth (at high elevation and mid range sites in Washington/ N.Oregon) - spring snow pack depth (S.Oregon) -previous summer temperatures (S.Oregon)	Latitudinal and elevational range of the Pacific Northwest
Gedalof and Smith (2001a)	- summer temp	-previous summer temp -winter snow pack	Latitudinal transect from California to southern Alaska
Smith and Laroque (1998)	- July temp	-snowfall of previous winter	Strathcona Park, Vancouver Island
Woodward et al. (1994)	-cool, wet weather in July and August (Oregon) -precipitation in July and August (Washington)		Cascade Mtns. (Washington/ Oregon)
Graumlich and Brubaker (1986)	-summer temp (July to Sept)	-spring snow pack depth (March)	Cascade Mtns. (Washington)
Brubaker (1980)	-rainfall (spring-summer)	-summer temperature -winter precipitation	Olympic Mtns. (Washington), Cascade Mtns. (Washington/ Oregon), Rocky Mtns. (Washington/Idaho), Blue Mtns. (Oregon)

4.2 Methods

4.2.1 Site Selection

Sample sites were selected based upon their location and the condition of the stand. High elevation stands were preferentially selected because moisture and/or temperature stresses limit radial-growth at those sites (Fritts, 1976). Attention was given to ensuring that disturbances such as fires, avalanche, rock falls, debris flows, and clear

cutting were not playing a role in the stand dynamics. The stands selected for sampling ideally showed little or minimal evidence of bore/crown damage or heart rot. Only pure or MH-dominated stands with mature trees were selected for sampling to reduce the degree of any ring-width growth variability resulting from the effects of interspecific competition (Schweingruber *et al.*, 1989).

4.2.2 Site Descriptions

Queen Charlotte Islands (QCI)

The Queen Charlotte Islands site is located 50 km northwest of Queen Charlotte City, on a steep upper slope (60%) (53°28'00" N 132°19'04" W, elevation: 781 m asl, south-southeast facing slope) (Figure 4.2; Table 4.2). The site occupied most aspects, although south-southeast was the most prominent. The overstory was composed of MH, while the herb layer was *Smilacina racemosa* (false Solomon's seal), *Polytrichum junipernium* (juniper haircap moss) and *Pleurozium schreberi* (red-stemmed feathermoss).

Mount Hayes (MtHY)

The Mount Hayes site is located approximately 3 km south of Prince Rupert, on a wet 30% slope 30 m below the crest of Mount Hayes (54°17'03" N 130°18'48" W, elevation: 665 m asl, east facing slope) (Figure 4.2; Table 4.2). The overstory is dominated by a mix of MH, subalpine fir and western hemlock. The understory is grassy and contains seedlings, saplings and some false azalea (*Menziesia ferruginea).*

Exstew River (ER)

The Exstew River site is located approximately 35 km west of Terrace, on a mossy 60% slope approximately 100 m below the local treeline (54°28'31" N

129°07'01" W, elevation: 875 m asl, southeast facing slope) (Figure 4.2; Table 4.2). This site is a MH tree dominated stand (with approximately 10% subalpine fir) found approximately 20 m (in distance, not elevation) upslope from a western hemlock/MH mixed stand. The steep slope of this site caused several trees to grow curved upwards with a J-shaped base.

Copper Mountain (CM)

The Copper Mountain site is located approximately 12 km east of Terrace, on a 50% slope, 50 m below the local MH parkland situated on the crest of Copper Mountain (54°30'19" N 128°27'49" W, elevation: 887 m asl, west facing slope) (Figure 4.2; Table 4.2). This is a MH tree dominated stand. Approximately 50% of the trees exhibited signs of heart rot. The understory was composed of seedlings, saplings, lady fern (*Athyrium filix-femina*), thimble berry (*Rubus parviflorus*), mountain ash (*Sorbus sitchensis*) and black huckleberry (*Vaccinium membranaceum*).

Cable Spur (CS)

The Cable Spur site is located approximately 40 km west of Smithers on a mossy 20% slope (54°49'43" N 127°48'11" W, elevation: 1090 m asl, south facing slope) (Figure 4.2; Table 4.2). This site is a MH tree dominated stand. The mature trees are all growing straight due to the slight slope at this site, and show little sign of disturbance.

Table 4.2 Summary of mountain hemlock tree-ring chronology sampling site locations, slope characteristics and distance from nearest climate station.

Site	Latitude	Longitude	Slope Aspect	Slope Angle	Elevation (asl)	Distance to Nearest Climate Station
QCI	53°28'00"N	132°19'04"W	SSE	60%	781m	32 km
MtHY	54°17'03"N	130°18'48"W	E	30%	665m	20 km
ER	54°28'31"N	129°07'01"W	SE	60%	875m	105 km to PR 35 km to TR
CM	54°30'19"N	128°27'49"W	W	50%	887m	20 km
CS	54°49'43"N	127°48'11"W	S	20%	1090m	32 km

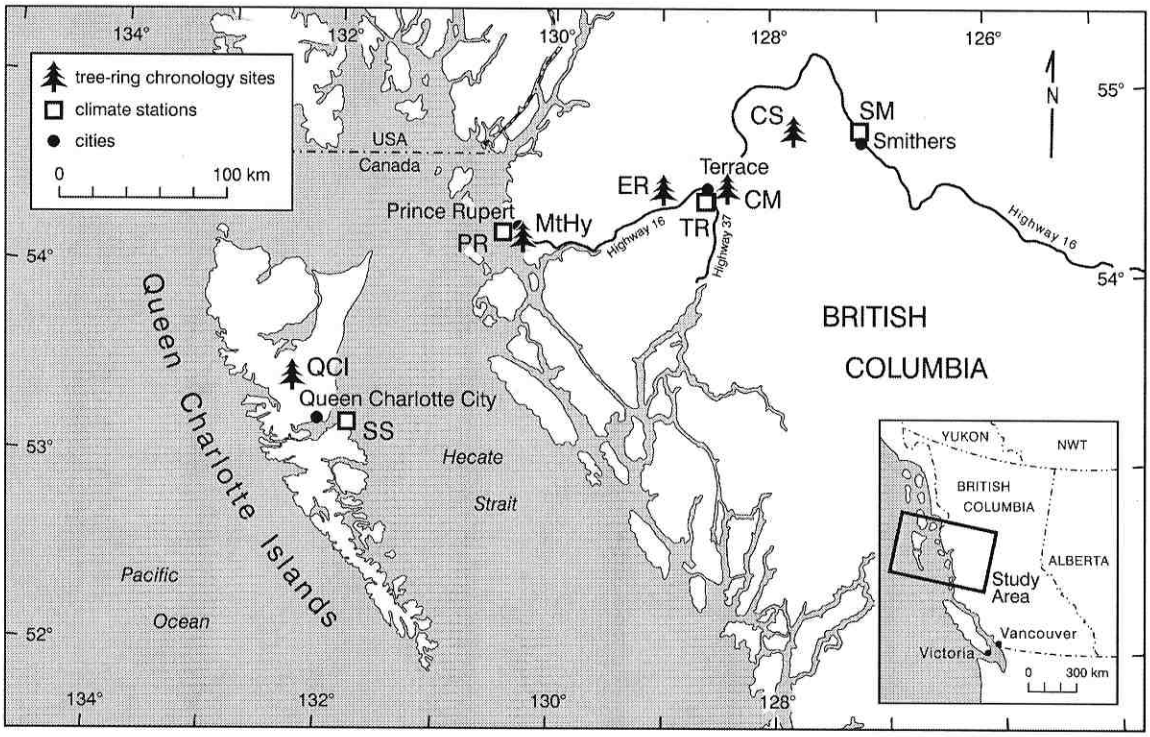

Figure 4.2 Location of mountain hemlock tree ring-width chronology sites and climate stations along a longitudinal transect in northwestern BC.

4.2.3 Field Methods

At each study site a minimum of 20 mature MH trees were selected for sampling following standard techniques (Stokes and Smiley, 1968). Two cores, at 90° to each other, were extracted at breast height from each tree with the use of an 18" increment borer. The cores were inserted into dry plastic straws that were taped shut at both ends and labelled.

4.2.4 Lab Methods

The tree cores were returned to the University of Victoria Tree-Ring Laboratory and left to air dry. Once dry, the cores were mounted in slotted wood blocks using furniture glue. Following drying, the cores were sanded flat with progressively finer sand paper and then polished with 600 grit paper.

Each core was scanned with an Epson Expression 10000XL scanner using the WinDENDRO ™ (version 4.1.2, 1994) image analysis system. The total ring-width of each annual ring was measured to the nearest 0.01 mm. Master tree-ring chronologies for each site were compiled using the COFECHA program (Version 2.04P). Each site chronology was crossdated[4] and quality checked to ensure that a minimum series intercorrelation[5] of 0.30 was achieved. The master chronologies from all sites were then standardized using the program ARSTAN (version 6.05P). The process of standardizing removes non-climatic age-related growth trends and provides a dimensionless ring-width index for each chronology (Cook *et al.*, 1989). A double-detrending method was employed using a negative exponential curve or linear regression and a 128 year cubic-smoothing spline with a 50% frequency cutoff.

---

[4] Crossdating is a way to ensure that each tree-ring core is assigned the correct year of growth.
[5] Intercorrelation is a measure of correlation between cores.

4.2.5 Chronology Correlation

To establish the level of commonality among the chronologies, a Pearson's r test of correlation was performed on the standard index output file to show which chronologies exhibited similar growth patterns. The statistical analysis software package SPSS (version 10) was used to construct the correlation matrix.

4.3 Results

4.3.1 MH Chronologies

Table 4.3 summarizes the length of each chronology, the number of cores used and the series intercorrelation value (r value). Not all of the cores collected at the study sites were used; although it is in the best interest of tree-ring research to incorporate as many tree-ring samples into each master chronology as possible. During the process of crossdating some individual cores did not crossdate well and were omitted from the master chronology.

Table 4.3 Description of mountain hemlock master tree-ring width chronologies along a longitudinal transect in northwestern BC.

Site	Number of Cores Collected	Number of usable Cores	Chronology Dates	Chronology Length	Series Intercorrelation
QCI	40	16	1611-2002	392	0.550
MtHY	52	20	1556-2004	449	0.619
ER	50	30	1576-2004	429	0.610
CM	48	41	1642-2004	359	0.682
CS	40	33	1616-2004	389	0.621

The QCI chronology exhibits an approximate 50-year cycle, showing repeating periods of below- and above-average ring-width growth (Figures 4.3 and 4.4). This growth cycle is not found in the other four chronologies (Figure 4.4). In the QCI

chronology, the most recent shift from below- to above-average ring-width growth was in 1984 and continued to the final year of the chronology (2002) (Figure 4.4). Notably wide tree-rings were produced in the years: 1652, 1713, 1777, 1792, 1840, 1902, 1942 (Figure 4.3; Table 4.4). Notably narrow tree-rings were produced in the years: 1619, 1704, 1706, 1810, 1876, 1910, 1954, 1973, 1974 (Figure 4.3; Table 4.4).

The most recent growth trend fluctuation in the MtHY chronology was initiated in 1957 when there was a shift to a trend of increasing annual radial-growth that was sustained until 1985 (Figure 4.4). After 1985 the average annual radial-growth declined until 1997. Following several years of reduced annual radial-growth rates, radial-growth increased from 2001 to 2004 (Figure 4.3). Notably wide annual rings were produced in the years: 1565, 1578, 1583, 1610, 1632, 1683, 1763, 1765, 1816, 1860, 1892, 1980 (Figure 4.3; Table 4.4). Notably narrow tree-rings were produced in the years: 1560, 1572, 1596, 1618, 1706, 1810, 1849, 1876, 1887, 1949, 1960 (Figure 4.3; Table 4.4).

The ER chronology is the most complacent chronology investigated; it shows the least amount of deviation from the average annual ring-width in the past 200 years (Figure 4.4). The most recent changes in the ER chronology occurred in 1978 when there was a shift to a trend of increasing growth until 1987 (Figure 4.4). From 1987, the annual radial-growth resumed a decreasing trend until 1997, followed by an increasing trend in annual radial-growth from 2001 to 2004 (Figure 4.3). Notably wide tree-rings were produced in the years: 1591, 1600, 1608, 1610, 1702, 1704, 1710, 1722, 1777, 1918, 1965 (Figure 4.3; Table 4.4). Notably narrow tree-rings were produced in the years: 1585, 1596, 1603, 1614, 1676, 1698, 1744, 1746, 1974, 1976 (Figure 4.3; Table 4.4).

The most recent changes in the CM chronology occurred in 1979 when there was a shift to a trend of increasing annual radial-growth until 1984 (this occurs after a period of consistent below-normal growth from 1952 to 1979) (Figure 4.4). After 1984 the annual radial-growth decreases until 1995, followed by another shift to increasing annual radial-growth from 2001 to 2004 (Figures 4.3 and 4.4). Notably wide tree-rings were produced in the years: 1647, 1661, 1674, 1721, 1804, 1905, 1918, 1938, 1941, 1980, 2004 (Figure 4.3; Table 4.4). Notably narrow tree-rings were produced in the years: 1655, 1664, 1676, 1697, 1744, 1866, 1956 (Figure 4.3; Table 4.4).

The most recent changes in the CS chronology occurred in 1966 when there was a shift to a decreasing annual radial-growth trend until 1979 (Figure 4.4). From 1979, the annual radial-growth resumed an increasing trend until 1994, followed by a short decreasing trend until 1997 and then an increasing trend in growth from 2001 to 2004 (Figure 4.3). Notably wide tree-rings were produced in the years: 1659, 1673, 1686, 1690, 1747, 1763, 1848, 1905, 1941, 1966, 1994 (Figure 4.3; Table 4.4). Notably narrow tree-rings were produced in the years: 1699, 1718, 1735, 1815, 1880, 1896, 1956, 1974, 1976 (Figure 4.3; Table 4.4).

Table 4.4 Years of notably wide and narrow tree-rings in MH ring-width chronologies from the five sample sites in northwestern BC.

Site	Years of Notably Wide Tree-Rings	Years of Notably Narrow Tree-Rings
QCI	1652, 1713, 1777, 1792, 1840, 1902, 1942	1619, 1704, 1706, 1810, 1876, 1910, 1954, 1973, 1974
MtHY	1565, 1578, 1583, 1610, 1632, 1683, 1763, 1765, 1816, 1860, 1892, 1980	1560, 1572, 1596, 1618, 1706, 1810, 1849, 1876, 1887, 1949, 1960
ER	1591, 1600, 1608, 1610, 1702, 1704, 1710, 1722, 1777, 1918, 1965	1585, 1596, 1603, 1614, 1676, 1698, 1744, 1746, 1974, 1976
CM	1647, 1661, 1674, 1721, 1804, 1905, 1918, 1938, 1941, 1980, 2004	1655, 1664, 1676, 1697, 1744, 1866, 1956
CS	1659, 1673, 1686, 1690, 1747, 1763, 1848, 1905, 1941, 1966, 1994	1699, 1718, 1735, 1815, 1880, 1896, 1956, 1974, 1976

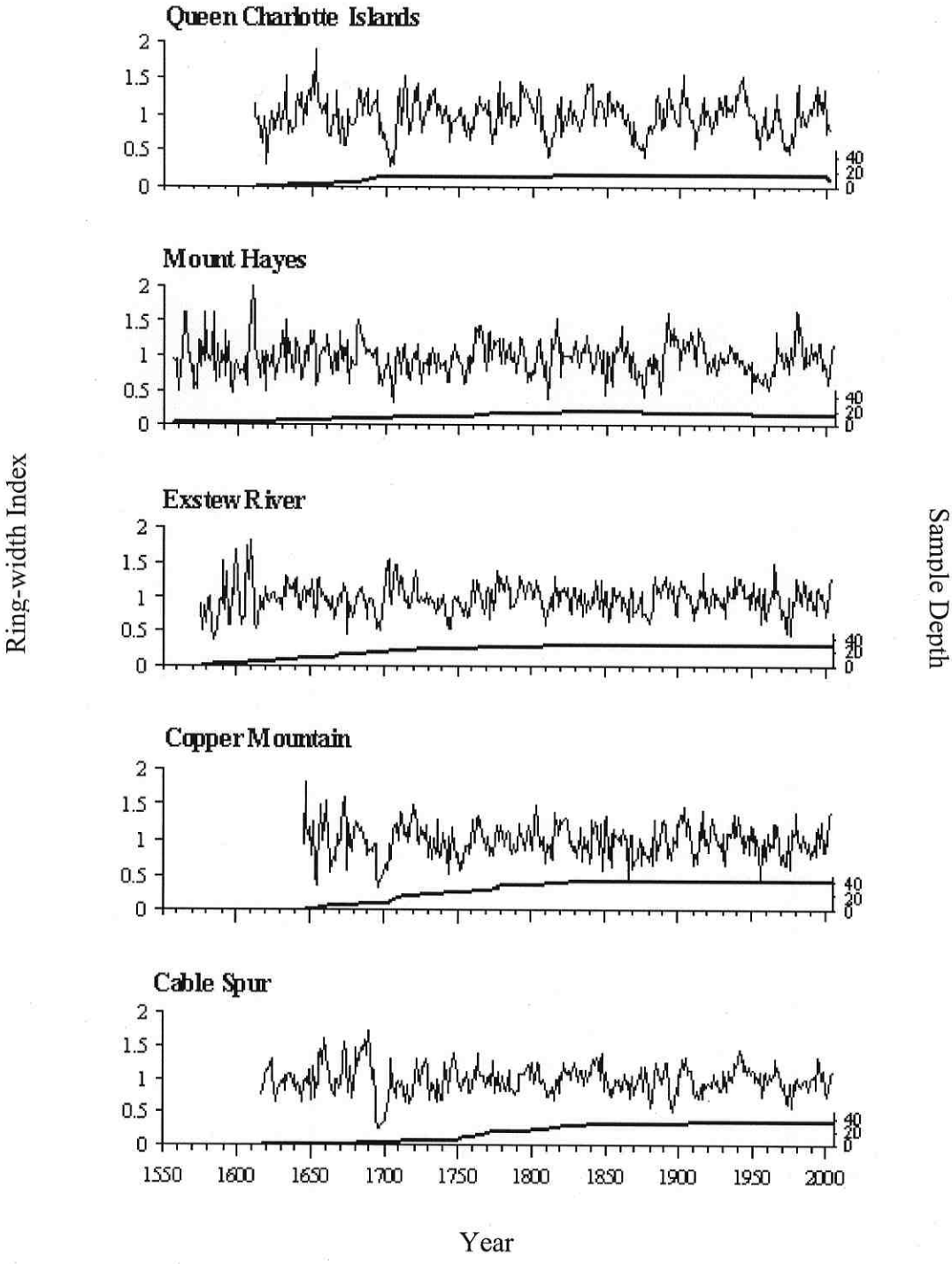

Figure 4.3 Standardized mountain hemlock master tree-ring chronologies and sample depth (# of individual cores included) from five study sites along a longitudinal transect in northwestern BC.

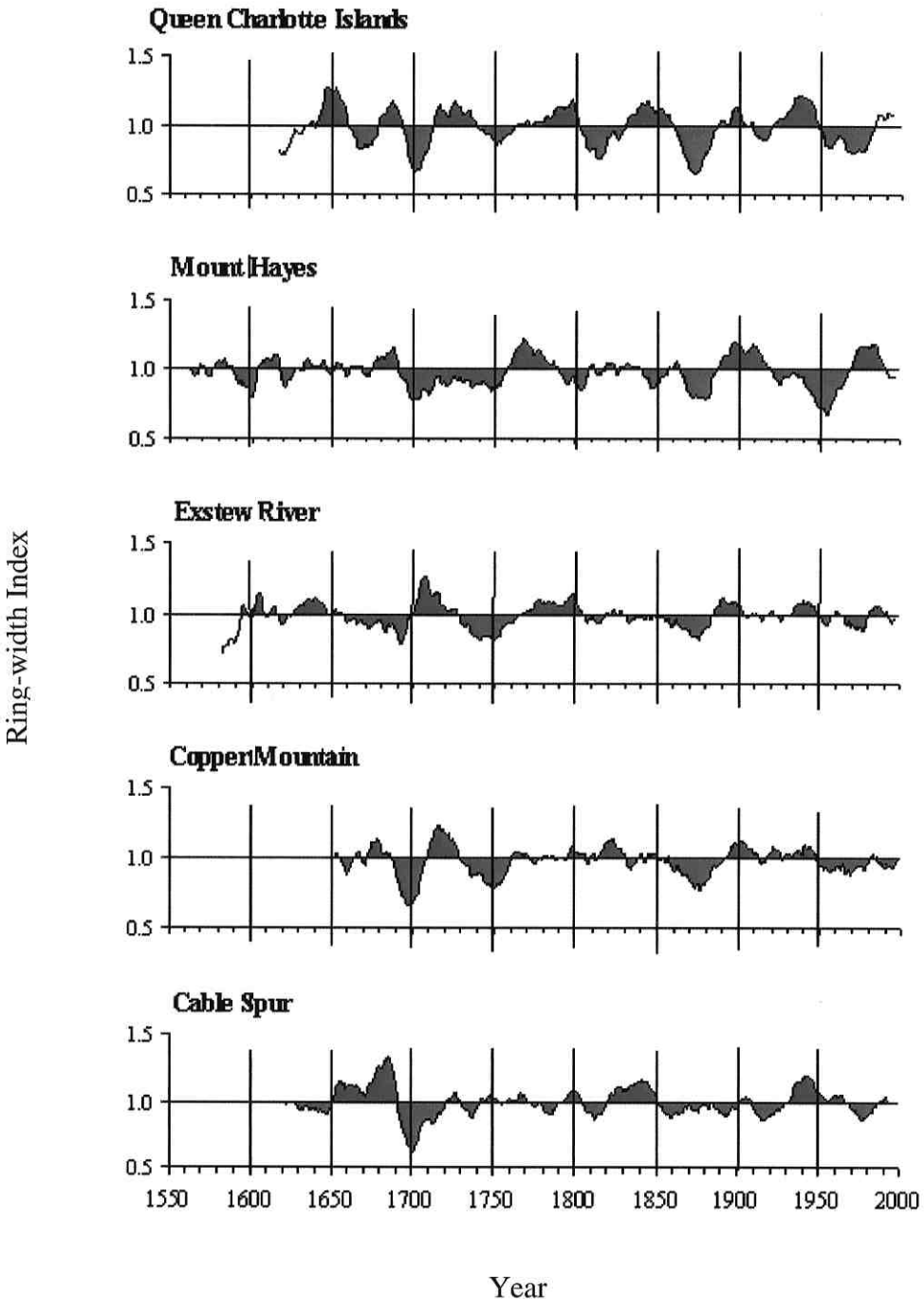

Figure 4.4 Fifteen-year running mean of standardized master tree-ring chronologies from five study sites along a longitudinal transect in northwestern BC. Periods of above-average radial-growth are coloured red, and periods of below-average growth are coloured blue.

4.3.2 Chronology Correlation

The Pearson's r test shows that all five chronologies are significantly correlated at the 0.01 level (99% significance) (Table 4.5). The correlation coefficients, however, do vary in strength. The strongest correlation is between the Exstew River and Copper Mountain sites (r = 0.602). The second strongest is between Copper Mountain and Cable Spur sites (r = 0.526). The weakest correlation is between Cable Spur and Mount Hayes (r = 0.241).

Table 4.5 Mountain hemlock tree-ring chronology correlations from the five sample sites in northwestern BC (1642-2002).

	Statistics	QCI	MtHY	ER	CM	CS
Queen Charlotte Islands (QCI)	r*	1.000	0.393	0.365	0.411	0.314
	sig. value#	-	0.000	0.000	0.000	0.000
Mount Hayes (MtHY)	r	0.393	1.000	0.429	0.469	0.241
	sig. value	0.000	-	0.000	0.000	0.000
Exstew River (ER)	r	0.365	0.429	1.000	0.602	0.398
	sig. value	0.000	0.000	-	0.000	0.000
Copper Mountain (CM)	r	0.411	0.469	0.602	1.000	0.526
	sig. value	0.000	0.000	0.000	-	0.000
Cable Spur (CS)	r	0.314	0.241	0.398	0.526	1.000
	sig. value	0.000	0.000	0.000	0.000	-

*r – Pearson's product moment correlation coefficient
#sig. value – significance value

4.4 Discussion

4.4.1 Chronology Correlation

The five chronologies developed for this investigation were constructed from MH trees located within mature undisturbed high elevation stands. These common site characteristics helped to ensure that commonalities among sites were most likely due to region-wide climate forcing mechanisms (Briffa, 2000). Although other variables, such as slope, bedrock geology and soil type could also contribute to commonalities between

sites (Schweingruber, 1989), these variables cannot be accounted for within the scope of this study.

The strongest site correlations exist between sites located in close proximity to one another (Table 4.4). ER and CM are found within 40 kms of each other, and CM and CS are separated by 60 kms. The inherent similarity in growth trends between the three sites is assumed to be a growth response to the regional climate. Similar to the findings of Gedalof and Smith (2001a), Pearson's correlation coefficients provide a robust tool for identifying regional growth zones. The CM chronology shows high correlations with MtHY , ER and CS chronologies, but the MtHY and ER chronologies do not correlate well with CS. Thus, the site east of the CM site could be considered a regional zone of growth patterns separate from the sites west of the CM site, with an undistinguished area of transition surrounding the CM site (Figure 4.5).

Despite the proximity between the two sites, the QCI chronology is not strongly correlated with the MtHY chronology. This observation is most likely due to orographic effects; the QCI site is on the lee of the Queen Charlotte Mountain Range, while the MtHY site is on the windward side of the Coast Mountains. The correlation results can be interpreted to suggest that the area surrounding the QCI site could be identified as one regional zone of growth patterns (Figure 4.5).

The results of the correlation analysis among the five chronologies indicates a common growth pattern across the transect; however, high correlations between select sites suggests the existence of three regional zones of growth patterns: (a) the Queen Charlotte Islands, (b) from Mount Hayes to Copper Mountain, and (c) from Copper

Mountain to Cable Spur; with an undistinguished area of transition surrounding Copper Mountain (Figure 4.5).

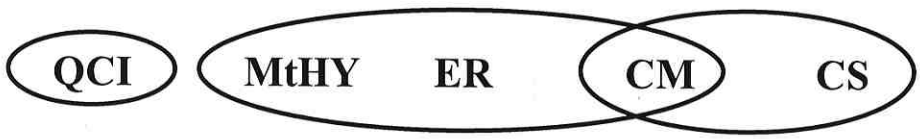

Figure 4.5 Schematic illustration of regional zones of growth patterns along the study transect based on Pearson's chronology correlation results.

4.4.2 Differences and Similarities Across the Transect

The correlation matrix offers a general overview of which sites show common growth patterns. A visual examination of the actual chronologies, however, suggests that the site-to-site growth trends are more complex as there does not seem to be any clear or consistent pattern either within each chronology or between chronologies.

Each master chronology exhibits periods of higher and lower than average growth of varying amplitudes, but no chronology shows any kind of consistent, predictable pattern. When all chronologies are considered, there is no consistent pattern of similarities and differences among them; however, by breaking the chronologies into time periods and comparing them to each other, some interesting observations can be made. For example, the period around 1870-1900 is an interval when all the chronologies record a period of below-average ring-width (Figure 4.4). In contrast to this, during the interval 1690-1730 when all the chronologies show a period of below-average ring-width, the ER chronology demonstrates a period of above-average ring-width (Figure 4.4). Furthermore, during some time periods there is no correlation across the transect, for example 1830-1860 (Figure 4.4).

The causal factor responsible for the inconsistent relationships between the chronologies is difficult to distinguish. The time periods when there is no similarity in growth across the transect could indicate that, during that time, the trees are responding to site-specific conditions. A time period when sites show opposing growth (meaning a time period when some chronologies show above-average growth while others show below average growth) across the transect could indicate that regional climate forcing factors may be at work. For example, around 1950 the above-average growth indices in the CS chronology contrast with the below average growth indices in all the other chronologies. The variable influence of coastal and interior climate systems could explain this response. The CS chronology is from the most eastern site and is less affected by coastal climate forcing mechanisms, which are affecting all the other sites during that time period. This explanation, however, does not account for the time periods, such as the one around 1700, where the chronology in the middle of the transect (ER) is the one exhibiting a growth pattern different than the other chronologies. There is no clear explanation for why at times the chronologies seem to all have similar growth trends, and at other times there are no similarities.

4.5 Summary

MH trees are a valuable species for dendroclimate studies due to their sensitivity to monthly mean temperature, monthly total precipitation and spring snow pack depth. Five high elevation MH stands were sampled along a longitudinal transect from the Queen Charlotte Islands to Smithers, in northwestern BC. A ring-width chronology was built from each of the high elevation MH stands, tested for correlation and compared to each other. A correlation matrix was used to identify three regional zones of growth

patterns: (a) the Queen Charlotte Islands, (b) from Mount Hayes to Copper Mountain, and (c) from Copper Mountain to Cable Spur; with an undistinguished area of transition surrounding Copper Mountain; however, when comparing specific time periods across the transect inconsistent results were found. At times the chronologies exhibited similar growth patterns, while at others, no similarities were observed across the transect or select chronologies were similar to each other. The conflicting responses point to either inconsistencies in climate, and/or inconsistencies in the growth response to climate across the transect, and/or the influence of other local factors that influence growth.

Chapter 5 – Climate / Radial-growth Response of MH Trees

5.1 Introduction

Climate change is expected to impact the radial-growth behaviour of MH trees over the long-term. This physiological susceptibility to climate-induced changes in tree growth provides an opportunity to develop a spatial understanding of how MH productivity varies across an air temperature/precipitation gradient. The purpose of this chapter is to describe the climate / radial-growth relationships of MH trees found along a longitudinal transect extending from coastal to interior BC. The chapter begins with a review of MH physiology and then considers the role that climate plays in the radial-growth of MH trees.

5.1.1 The Growth of MH

The length of the growing season for MH trees depends upon the number of frost-free days and varies considerably in length due to the wide geographical distribution of this species (Means, 1990). For example, the growing season ranges from 95 to 148 days in southwestern BC to 49 to 63 days in the central Sierra Nevada of California (Means, 1990).

MH trees generally remain dormant from mid-October to mid-April (Owens, 1984a) (Figure 5.1). Cell division in vegetative buds begins in mid-April, and is followed by the elongation of shoots and leaves, which causes the buds to burst in late June (Owens, 1984a) (Figure 5.1). Reproductive buds can be identified in the late summer and early fall (Means, 1990). Radial-growth begins mid-June and is due to the function of cambium cells, located between the bark and the wood of the tree. Cambium cells give rise to new wood and bark cells, a process largely dependent on the energy

provided by photosynthesis (Kramer and Kozlowski, 1960). By the beginning of August, radial-growth has ceased in MH trees and energy is focused on needle initiation and seed/cone development until mid-October, when the tree moves into a dormant state.

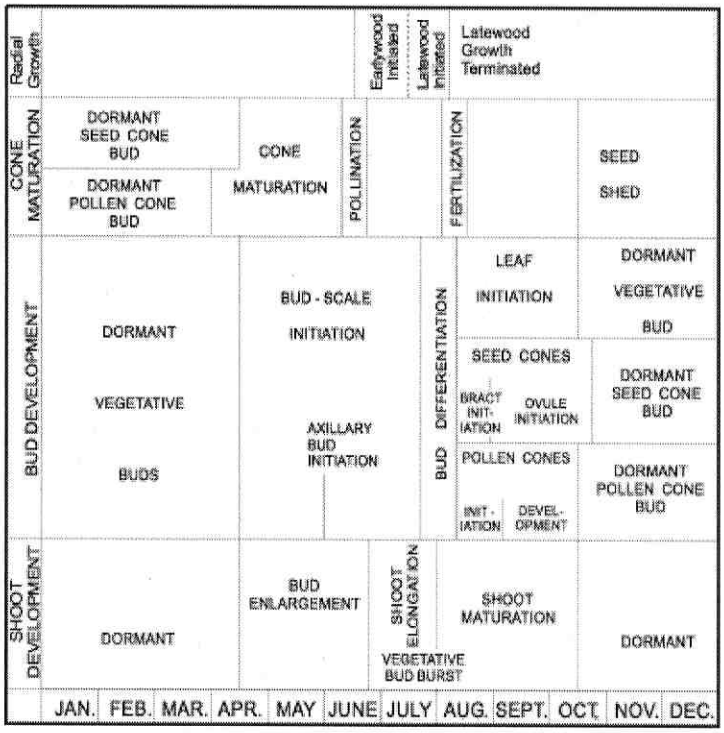

Figure 5.1 The yearly growth cycle of mountain hemlock growing at high elevations in BC (adapted from Owens and Molder, 1975; Owens, 1984a; Owens, 1984b; Owens and Molder, 1984; Gedalof and Smith, 2001a).

5.1.2 Environmental Factors Affecting Radial-Growth

The basic life requirements for MH trees are sufficient light, water, carbon dioxide, mineral nutrients and tolerable air temperatures. A change in any one of these environmental factors or the processes affecting them (such as climate) will affect the radial-growth of the tree. Factors such as competition (inter- and intra-species), air temperature, moisture, soil properties, snow pack can all affect the growth of a tree. For example, a deficiency in nitrogen in the soil will reduce growth since nitrogen is crucial

in the formation of new protoplasm and enzymes (Kramer and Kozlowski, 1960). Furthermore, deficiencies and excessive amounts of phosphorus, potassium, calcium, sulfur, and other mineral elements in the soil will affect the functioning of the tree since they can act as coenzymes (Kramer and Kozlowski, 1960).

For the purpose of this study, attention will be given to the climatic factors that are known to affect the radial-growth of MH trees: air temperature, precipitation and snow pack. The following provides a brief summary of these climatic variables and describes how they affect the radial ring-width growth of MH trees.

Precipitation / Moisture

MH trees do not thrive in dry conditions, as moisture is recognized as a dominant limiting factor (Arno and Hammerly, 1977; Woodward, 1998). Brubaker (1980) found that in the Pacific Northwest, water stress was the primary factor limiting the growth of MH trees. For MH needles to produce the sugars and usable foods needed for cambium development and radial-growth there needs to be an input of water (Kramer and Kozlowski, 1960; Brubaker, 1980; Pielou, 1988). For a plant, water is a raw material in photosynthesis, the transport medium for nutrients from the soil, and is needed for evapotranspiration (the primary cooling mechanism that enables the tree to maintain an equitable temperature). Without adequate moisture available in the soil, the rates of photosynthesis decrease and cell enlargement is compromised, which results in restricted cambial activity (Kramer and Kozlowski, 1960). It follows that moisture conditions in previous years can affect the radial-growth in the following season by leaving the tree with more or less available energy (or reserves) for the next year (Peterson and Peterson, 2001).

Precipitation will not directly affect the radial-growth of a tree, rather it will affect soil moisture, which in turn affects tree growth (as described above). Available soil moisture is also affected by: snowmelt from the preceding winter's snow pack; soil temperature, which influences the availability and rate of movement of water within the soil and tree; soil characteristics (depth, structure, composition); and slope (for runoff and internal drainage toward or away from the tree).

Air Temperature

The internal temperature of the tree will influence the radial-growth because it is linked to physiological processes such as photosynthesis, respiration[6], cell division and elongation, enzymatic activity, chlorophyll synthesis, and transpiration[7] (Kramer and Kozlowski, 1960). Generally, as the plant temperature increases there is a corresponding increase in the rate of photosynthesis, which translates into an increase in radial-growth. This is the case until temperatures get too high, which will stress the tree and result in photosynthesis decline (Kramer and Kozlowski, 1960).

Several dendroclimate studies have examined the relationship between radial ring-width growth and air temperature in MH trees (Woodward *et al.*, 1994; Gedalof and Smith, 2001a; Peterson and Peterson, 2001). Air temperature will not directly affect the growth of a tree; however, it will affect the temperature of the tree and the soil which, in turn, affects tree growth.

High-elevation MH tree ring-widths in the Pacific Northwest have a positive response to high spring and summer air temperatures during the growing season (Gedalof and Smith, 2001a; Peterson and Peterson, 2001); however, Brubaker (1980), found that

---

[6]Respiration is the oxidization of food in living cells which releases energy to the tree
[7] Transpiration is the loss of water by a tree in the form of vapor

the radial-growth of MH trees in the Olympic and Cascade Mountains of Washington State was negatively correlated with summer air temperature. These opposing climate / radial-growth relationships reflect the variable responses due to site-specific limiting factors (due to elevation, microclimate, and habitat) (Fagre *et al.*, 2003), and the impacts of interaction between climate variables. For instance, if MH trees are growing in an area where air temperatures can increase to a critical point there will be an increase in evaporation resulting in less moisture available for the trees' metabolic processes and, therefore, a decrease in radial-growth. The challenge for dendroclimatologists is to account for more than the effect of a single climate variable, and consider the interaction of several other climate variables such as wind speed (as it affects the convective heat flux density), cloud cover, humidity and incoming long wave radiation.

MH trees show a negative growth response (narrow radial-growth rings) to higher summer air temperatures in the year preceding growth (Gedalof and Smith, 2001a; Peterson and Peterson, 2001). This response is most likely due to warmer summer air temperatures being associated with an increase in the production of reproductive buds (Woodward *et al.*, 1994). There is a large energy cost in the following growth season as the reproductive buds mature into cones, leaving less energy for radial-growth and resulting in narrow rings (Woodward *et al.*, 1994).

Snow pack

In a study of MH stands at high elevation sites in Oregon, Peterson and Peterson (2001) found that radial-growth was negatively correlated with spring snow pack depth. Smith and Laroque (1998) also found a negative relationship existed between radial-growth and winter (November and January) precipitation. They suggest that this growth

response is actually a response to long-lasting snow packs that shorten the growing season, which then results in decreased growth and a smaller ring. Several additional studies report similar findings (Woodward *et al.*, 1994; Gedalof and Smith, 2001a; Peterson and Peterson, 2001; Fagre *et al.*, 2003; Laroque and Smith, 2003).

5.1.3 Understanding the Climate / Radial-growth Relationship

Interaction Effect of Climate Variables

Difficulties in interpreting the climate / radial-growth relationship of MH trees are most likely related to an oversimplification of the complex interactions of several climate factors. Some high elevation MH tree studies have assumed that a linear relationship exists between radial-growth and an individual climate parameter (e.g. Arno and Hammerly, 1977; Woodward, *et al.*, 1994; Peterson and Peterson, 2001). Gedalof and Smith (2001a), however, note that these relationships are not always linear. For example, precipitation in combination with air temperature is an important variable influencing the radial-growth of MH trees. When air temperatures are high in the spring there is a positive correlation between March precipitation and radial-growth (Gedalof and Smith, 2001a). If there is a link between high March air temperatures and large March precipitation totals it might fairly be assumed that the majority is falling as rain (Gedalof and Smith, 2001a). If this is the case, these rain-on-snow events likely hasten snowmelt (Moore and McKendry, 1996) and may result in a lengthening of the growing season, allowing for enhanced radial-growth (wider tree-ring). Consequently, a holistic approach must be applied to understand the interactions among the climatic factors and their effect on MH tree growth.

Limiting Factors

Limiting factors on tree growth can vary with site location, which may mean that the radial-growth of trees will also respond differently at each site. Woodward *et al.* (1994) and Peterson and Peterson (2001) report on the results of investigations of MH trees found at comparable sites in high elevation areas of Oregon. Despite the apparent similarity of the sites, their microclimates (air temperature and precipitation) were different enough to cause an opposite growth response to high summer air temperatures. It is, therefore, important to have a clear understanding of how the trees in an individual stand respond to climate in order to understand their climate / radial-growth relationship.

5.2 Methods

An appraisal of the detailed physiology of MH is beyond the scope of this project, as we are lacking detailed stand and micro-climate data (such as soil temperature, soil depth, tree temperature). In this case, air temperature is the most useful proxy for solar radiation, long wave radiation, soil temperature and plant temperature. Precipitation is the best proxy for soil moisture. Several other MH dendroclimate studies have relied on similar air temperature and precipitation data to investigate physiological effects of climate on MH trees (Woodward et al., 1994; Gedalof and Smith, 2001a; Peterson and Peterson, 2001; Laroque and Smith, 2003).

5.2.1 Response Function

The relationship between climate data and the radial ring-width index at each site was determined using the PRECON program - 32 bit version 5.17a (Fritts *et al.*, 1971). PRECON ("PRECONditioning") is a program that computes a statistical relationship between climate and tree-ring growth. In this case, PRECON was used to perform a

response-function analysis between the growth indices of the MH ring-width chronologies discussed in Chapter 4 and the mean monthly air temperature and total monthly precipitation data obtained from the Environment Canada climate stations discussed in Chapter 3.

A response function analysis performed in PRECON provides a multiple regression equation which integrates two sets of data: orthogonalized climate variables (to ensure that the climate variables are independent of each other) and a standardized tree-ring index (Guiot *et al.*, 1982). Bootstrapping was also used because it is a powerful method for evaluating result replicability by creating multiple repetitions of the data sets and then selecting a random sample to compute averaged results (Thompson, 1995). A bootstrapped response function with 200 repetitions and a one-year lag on a period of 16 months beginning in the 5^{th} month of the previous growing season was used in this analysis (Gedalof and Smith, 2001a). The PRECON output for response functions provides R^2 values (explained variance), showing the proportion of the variability in the tree-width index which is accounted for by climate (CL), previous growth (PG) and total (the value of CL and PG combined) (T).

A challenge for dendroclimatology studies is to find reliable climate data from stations proximate to the tree-ring sampling sites; stations located as far away as 32 km could reduce the correlation between climate parameters and ring-width indices (Fritts, 1976). Without a climate station at the sampling site, an error is introduced due to differences in microclimate conditions between the station location and the sampling site. Within the scope of this study there is no way around this problem and, therefore, differences in distances and elevations between climate stations and sampling sites must

be taken into consideration during the interpretation of results. The most proximate station to each sampling site was used for analysis and it is expected that the general regional climate recorded at each climate station will be reflected in the chronologies. The Exstew River chronology site is the only case where a climate station was not proximate to the chronology site, therefore, this chronology was analyzed using climate data from the two nearest stations (PR and TR). Snow pack data were not used in this analysis due to a lack of proximate monitoring sites and/or the instrumental records being too short.

5.3 Results

Figure 5.2 is the PRECON output graphs showing the response function results. The X axis shows the months of the year beginning in May of year^{-1} and following to August of year^{0}, the Y axis shows the regression coefficient value (r). Statistically significant relationships between climate and ring-widths are represented by symbols visible in the legend to the right of each graph. Table 5.1 is a summary of the R^2 values and the statistically significant climate / radial-growth relationships observed in the response function results.

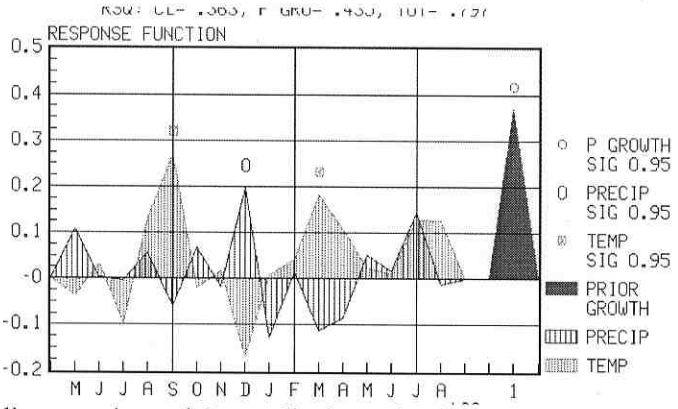

(a) Sandspit climate station and Queen Charlotte Islands MH ring-width index chronology

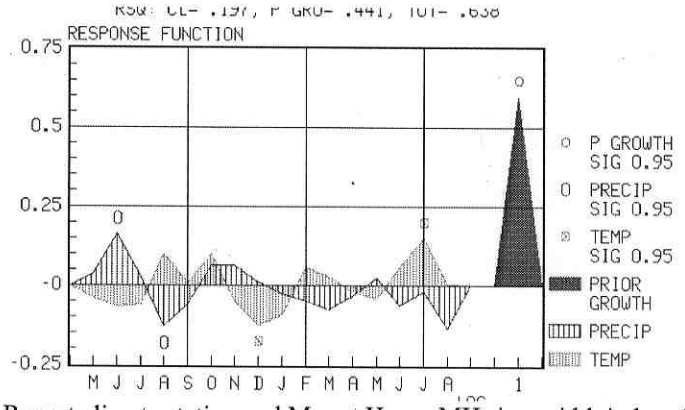

(b) Prince Rupert climate station and Mount Hayes MH ring-width index chronology

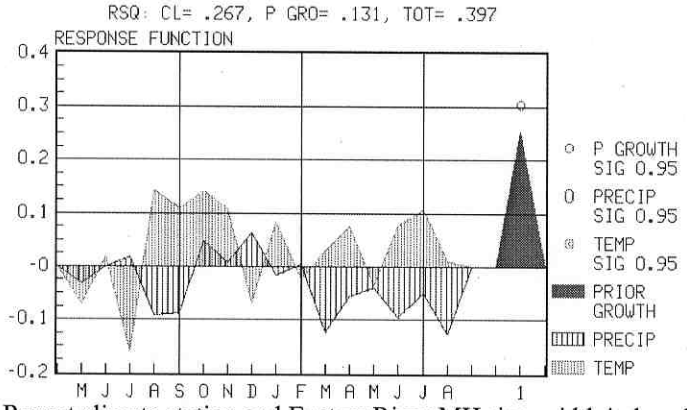

(c) Prince Rupert climate station and Exstew River MH ring-width index chronology

Figure 5.2 Response function graphs representing climate / radial-growth relationship between MH ring-width chronologies, air temperature and precipitation along a longitudinal transect in northwestern BC. X axis shows months of the year beginning in May of year^{-1} and following to August of year^{0}, Y axis shows regression coefficient values (r). [Continue on following page]

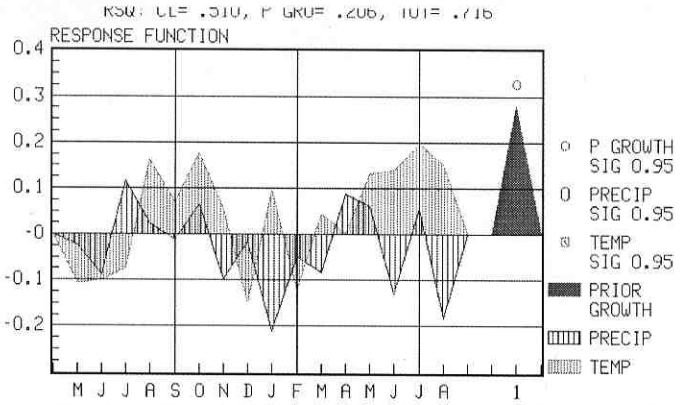

(d) Terrace climate station and Exstew River MH ring-width index chronology

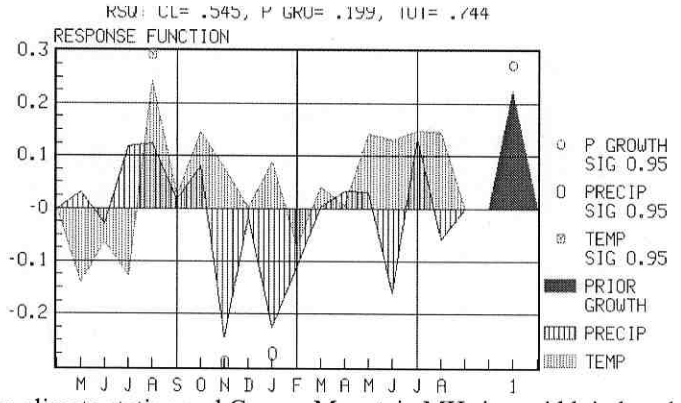

(e) Terrace climate station and Copper Mountain MH ring-width index chronology

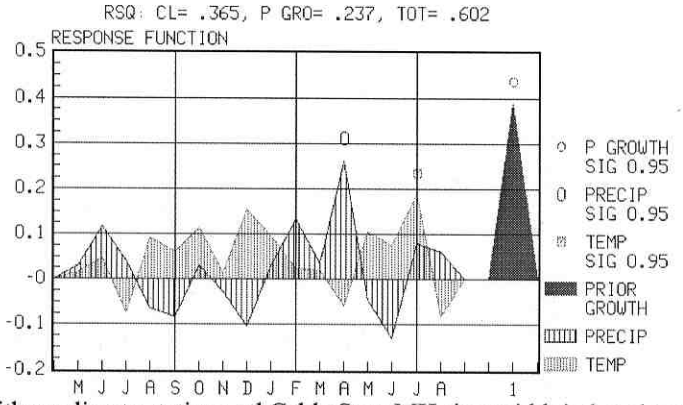

(e) Smithers climate station and Cable Spur MH ring-width index chronology

Figure 5.2 [Continued] Response function graphs representing climate / radial-growth relationship between MH ring-width chronologies, air temperature and precipitation along a longitudinal transect in northwestern BC. X axis shows months of the year beginning in May of year^{-1} and following to August of year^{0}, Y axis shows regression coefficient values (r).

Table 5.1 Climate / radial-growth response functions, at a 95% confidence, between air temperature and precipitation and MH ring-width chronologies along a longitudinal transect in northwestern BC.

Chronology and Climate Station	R^2 Value			Significant Positive Relationship (95%) ($p<0.05$)	Significant Negative Relationship (95%) ($p<0.05$)
	CL[a]	PG[b]	T[c]		
Queen Charlotte Islands and Sandspit station	0.363	0.435	0.797	September temp (P)[d] March temp December precip Previous growth	
Mount Hayes and Prince Rupert station	0.197	0.441	0.638	June precip (P) July temp Previous growth	August precip (P) December temp
Exstew River and Prince Rupert station[e]	0.267	0.131	0.397	Previous growth	
Exstew River and Terrace station	0.510	0.206	0.716	Previous growth	
Copper Mountain and Terrace station	0.545	0.199	0.744	August temp (P) Previous growth	November precip January precip
Cable Spur and Smithers station	0.365	0.237	0.602	April precip July temp Previous growth	

a. **CL** = R^2 value for explained variance due to climate
b. **PG** = R^2 value for explained variance due to prior growth
c. **T** = R^2 value for total explained variance due to climate and previous growth
d. **(P)** indicates relationship with month in previous growth year
e. There are no climate stations located in the ER valley and, therefore, the ER chronology was analyzed with the PR and the TR climate stations. An examination of the R^2 values for climate (explained variance due to climate) for the ER site, shows that the R^2 value is much lower with the PR station (0.267) than with the TR station (0.510). This could indicate that the trees at the ER site are responding to climate conditions more closely related to the conditions in Terrace rather than the ones in Prince Rupert

5.4 Discussion

5.4.1. Prior Growth

At all sites there was a significant positive relationship between the ring-width index and prior growth (Figure 5.2; Table 5.1). If it is assumed that radial-growth in the

previous year reflects overall tree productivity, then it follows that there is an increased potential for carbohydrate storage resulting from an increase in needle production (Ericsson *et al.,* 1980). In the following year, this enhanced storage capacity provides an opportunity for enhanced radial-growth (Lebourgeois, 2000). Since the annual increment of radial-growth is determined by the length of the growing season (Owens, 1984a), it can be assumed that there is also a positive relationship between the length of the previous growing season and current radial-growth.

5.4.2.Spring and Summer Air Temperature

As tree temperature increases there is usually a corresponding increase in physiological processes that translates into an increase in the radial-growth increment (Lebourgeois, 2000; Kramer and Kozlowski, 1960). This observation may provide an explanation for the positive relationship between July air temperature and radial-growth found at the CS and MtHY sites (Figure 5.2; Table 5.1). Similar climate / radial-growth MH relationships have been found in Washington and Northern Oregon (Peterson and Peterson, 2001), Vancouver Island (Smith and Laroque, 1998) and in the Cascade Mountains (Graumlich and Brubaker, 1986).

The QCI and CM were the only sites to exhibit a positive relationship between previous late summer / early fall air temperature and radial-growth (Figure 5.2; Table 5.1). August and September are often excluded as being a part of the growing season because late wood growth is normally terminated after the month of July (Owens, 1984a), but other physiological processes, such as leaf initiation continue until mid-October (Owens, 1984a). A greater air temperature in late summer and early fall could lead to greater plant and soil temperature and enhance needle initiation which leads to an

increase in the overall magnitude of photosynthesis and, in turn, and increase in the amount of available energy for radial-growth in the following growing season.

These results presented above differ from those of Woodward *et al.* (1994) who observed a negative relationship between previous July/August air temperature and radial-growth; the warm summers in the previous year result in increased production of reproductive buds, which mature during the following year, limiting the energy available for radial ring growth resulting in narrow rings. The discrepancy (between Woodward *et al.* (1994) and this study) can be explained by the fact that bud initiation begins at the beginning of the summer growing season (closer to May) and higher than normal late summer and early fall air temperatures are not likely to affect the production of reproductive buds (Owens, 1984b).

The QCI site also exhibits a positive relationship with March air temperature. An increase in March air temperature could contribute to the melting of the existing snow pack, reducing the overall snow pack depth, and/or represent conditions when snow won't be falling. Therefore, the positive relationship between March air temperature and radial-growth at the QCI site could be indicative of the negative relationship between snow pack depth and growing season length.

5.4.3. Growing Season Precipitation

At the MtHY site a positive relationship with previous June precipitation and a negative relationship with previous August precipitation was recorded (Figure 5.2; Table 5.1). A possible explanation for this is that June is the driest month at the PR station (with a mean total monthly precipitation of 118 mm when averaged over the entire length of record) and the trees respond positively to any increase in moisture by increasing their

physiological processes, which then results in more energy available for growth in the following year. Since this site drains poorly and can be very wet, above-average amounts of precipitation in August (which receives an average of 43 mm more than June) can flood the tree roots. This results in decreased productivity, leaving less energy available for radial-growth in the following year. Given this explanation, if summer precipitation is important at the MtHY site, it is unclear as to why there is no climate / radial-growth relationship with current year precipitation.

At the CS site it can be assumed that in the month of April some of the precipitation falls as rain and not snow, even though higher elevations in the area can receive snow until the beginning of June. The positive relationship between April precipitation and radial-growth at the CS site might then be explained by the effect of rain melting snow (Figure 5.2; Table 5.1). An increase in rain will increase snowmelt, leading to a smaller snow pack and ultimately contribute to a longer growing season and more radial-growth (Gedalof and Smith, 2001a).

The rain on snow events contributing to the melting snow pack at the CS site could also be a part of soil moisture recharge. The Smithers climate station data suggests that the CS site is the driest site during the growing season (Table 3.3). It is also the only site to exhibit a relationship with current-year spring precipitation. An increase in April precipitation, falling as rain, could contribute to additional available soil moisture during the growing season. Given this relationship, it could be that spring precipitation regimes increase in importance to MH growth towards interior BC where dry springs and summers are common.

5.4.4. Winter Precipitation

A year of abundant winter precipitation (falling as snow) could decrease the length of a growing season by contributing to a large snow pack. A larger snow pack would take longer to melt in the spring and, thus, shorten the overall length of the MH growing season, resulting in reduced radial ring-width growth (Gedalof and Smith, 2001a). Furthermore, snow has a high albedo, so solar radiation is reflected off the snow and is not available to warm the soil. This is possibly the case at the CM site, where there is a negative relationship between radial-growth and November, and January precipitation (Figure 5.2; Table 5.1).

Unlike the CM site, the QCI site shows a positive relationship between December precipitation and radial-growth (Figure 5.2; Table 5.1). A threshold snow pack depth could explain this. Depths above the threshold shorten the growing season (as explained above) and depths below the threshold contribute to increased soil moisture recharge when the snow melts in the spring. Therefore, the positive relationship between winter precipitation (December) and radial-growth at the QCI site is a reflection of an increase in snow pack contributing to soil moisture recharge and, since moisture availability is a key limiting factor in MH growth, this results in greater radial ring-width growth during the growing season.

5.4.5. December Air Temperature

The MtHY site was the only site to exhibit a negative relationship with average December air temperature (Figure 5.2; Table 5.1). This relationship is interpreted to mean that in years of higher than average December air temperatures the trees at this site experience a decrease in radial-growth in the following growth season. In high elevation

areas around the MtHY site, snow begins to accumulate in November (Weather Network, 2006), so that by December there could be sufficient snow pack to prevent the ground from freezing (Means, 1990). In the case of a mild spell in December, the snow may completely melt leaving the trees exposed to cold temperatures, and roots susceptible to damage caused by freezing. If this impact is severe enough, overall condition of the tree can be compromised, leading to a reduction in radial-growth in the following growth year (Kramer and Kozlowski, 1960).

The rain on snow events contributing to the melting snow pack at the CS site could also be a part of soil moisture recharge. The Smithers climate station data suggests that the CS site is the driest site during the growing season (Table 3.3). It is also the only site to exhibit a relationship with current-year spring precipitation. An increase in April precipitation, falling as rain, could contribute to additional available soil moisture during the growing season. Given this relationship, it could be that spring precipitation regimes increase in importance to MH growth towards interior BC where dry spring and summers are common.

5.5 Summary

An examination of the climate / radial-growth relationships between high elevation MH ring-width chronologies from each of the five sites along the transect showed very site-specific relationships. No two MH stands had the same relationship with monthly air temperature and precipitation data, indicating that the trees are responding to site-specific limiting factors. There were no climate / radial-growth relationship trends evident across the transect; this study only included five sites it is

likely that stronger patterns and trends could be found if additional sites were added, therefore, further investigations are suggested.

Chapter 6 - Dendroclimate Response of Mountain hemlock to the ENSO and the PDO

6.1 Introduction

Climate forecasts derived from coupled (atmosphere-ocean) general circulation models (CGCMs) provide a powerful tool for predicting ecosystem responses to future climates (Chahine and Susskind, 1991; Barnett *et al.*, 1994). In Pacific North America, CGCM outputs suggest that future climate changes will be accompanied by an increase in the variability and intensity of ENSO and PDO events (Salinger, 2005; Shiogama *et al.*, 2005). Although there is no agreement on the degree of change that might be expected, there is consensus that to develop realistic forest management strategies there is a need for a better understanding of the ecological influence of these teleconnections (Lindner *et al.*, 2002; Chapin *et al.*, 2004; Hamann and Wang, 2006).

This chapter examines the regional influence of ENSO and PDO events on high elevation MH ecosystems in northwestern BC. For this study, positive and negative ENSO events and PDO phases were compared to MH ring-width chronologies (discussed in Chapter 4) to determine whether any relationships exist between the ring-width series and the El Niño/La Niña and PDO climate oscillations (Chapter 3).

6.1.1 Climate Indices

A climate index represents a single time-series used to describe the state of a given climate system (IRI, 2006). Climate indices are used to simplify the detailed descriptions of atmospheric and oceanic conditions. Some indices are defined by measurements made in one area that are directly linked to other regions through teleconnections (IRI, 2006).

The Southern Oscillation Index (SOI) defines the atmospheric component of the El Niño Southern Oscillation (ENSO). It is based upon the observed sea level pressure (SLP) difference between Tahiti, French Polynesia and Darwin, Australia (NOAA/CPC, 2004). A negative phase of the SOI is represented by below-normal air pressure at Tahiti and above-normal air pressure at Darwin (Ropelewski and Jones, 1987). A prolonged negative SOI is associated with abnormally warm ocean temperatures in the eastern tropical Pacific and is indicative of an El Niño episode, whereas a prolonged positive SOI is associated with abnormally cold ocean temperatures in the eastern tropical Pacific and is indicative of a La Niña episode (Ropelewski and Jones, 1987).

The Pacific Decadal Oscillation Index (PDI) summarises the PDO and is defined as the leading principal component of the monthly North Pacific sea surface temperature variability poleward of 20°N Lat. (Mantua *et al.*, 1997). The index identifies the positive and negative phases of the PDO (see Chapter Three).

6.2 Methods

Superposed Epoch Analysis (SEA), also referred to as compositing, is a way of grouping many observations of an event into categories and then comparing the means of those categories (Hartmann, 2006). For instance, Mass and Portman (1989) used SEA to examine the effects of volcanic eruptions on climate by grouping land and ocean temperature, surface pressure and precipitation into categories defined by volcanic activity. Similarly, Prager and Hoenig (1989) used SEA to determine the relationship between extreme environmental events (such as El Niño) and recruitment success of chub mackerel.

SEA is used in this study to determine the effects of ENSO and the PDO on the radial-growth of MH trees at each of the five tree-ring study sites. An independent t-test statistic is used to compare the ring-width means during positive and negative phases of ENSO and the PDO at a 95% confidence. A two-tailed t-test was used to test whether there was any significant difference between the mean ring-widths during positive and negative SOI events and PDO phases (H_o2). Two one-tailed t-tests were used to test the following hypotheses (H_o1):

I. ring-width index values during years of positive SOI events are greater than ring-widths index values during years of negative SOI events;

II. ring-width index values during years of positive PDO phases are smaller than ring-width index values during years of negative PDO phases.

As the instrumental SOI record extends only to 1866 (Climate Prediction Centre, 2006), the proxy dendroclimate record of winter SOI constructed by Stahle *et al.* (1998) is used in this SEA. Stahle *et al.* (1998) used tree-ring chronologies from ENSO-sensitive regions in subtropical North America and Indonesia to construct a proxy SOI record from 1706 to 1977 (Brown and Wu, 2005; Taylor and Beaty, 2005; Girardin *et al.*, 2006). For this study, the Allan *et al.* (1996) record will also be used to fill the gap between 1977 and 1996 in the Stahle *et al.* proxy record (see Appendix D). In addition, a record of winter SOI extremes (SOI index > +5.0, < -5.0) derived from the Stahle *et al.* (1998) and Allan *et al.* (1996) proxy record was prepared in order to identify El Niño/La Niña events (see Appendix D). For the purpose of the SEA the actual proxy SOI values were not used, instead the values were simply separated into two groups: positive events and negative events (Appendix D).

Because there are only 3 PDO shifts represented within the instrumental data, the proxy spring PDI presented by Gedalof and Smith (2001b) was selected as representative of possible PDO regime shifts from 1662 to 1998. This proxy record was constructed using MH chronologies located along a latitudinal transect spanning the North American Pacific coast. Identified in this record are 11 possible PDO regime shifts and a lengthy period between 1840 and 1923 when neither a positive nor negative PDO state is indicated (Gedalof and Smith, 2001b) (Appendix E). For the purpose of the SEA the actual proxy PDO values were not used, instead the values were simply separated into three groups: positive events, negative events and undefined events (1840-1923) (Appendix E).

6.3 Results

6.3.1.Superposed Epoch Analysis with Southern Oscillation Index

The t-test results show that a statistically significant difference exists between the mean widths of tree-rings produced in the growing season following positive and negative SOI phases in the QCI ($p = 0.001$) and the CS ($p = 0.025$) chronologies (reject H_o2) (Table 6.1). Furthermore, H_o1 for the QCI and CS chronologies was also rejected which means that, at these sites, ring-widths during years of positive SOI phases are statistically smaller than ring-widths during years of negative SOI phases.

There was no statistically significant difference between mean ring-width values during positive and negative SOI phases in the MtHY ($p = 0.073$), ER ($p = 0.133$) and CM ($p = 0.111$) chronologies (do not reject H_o2 or H_o1). These results suggest that there is no statistical evidence that MH ring-width is affected by the Southern Oscillation at the MtHY, ER and CM sites.

Table 6.1 t-test results for the Stahle *et al.* (1998) / Allan *et al.* (1996) reconstructed SOI index compared to five MH ring-width chronologies along a longitudinal transect in northwestern BC. At a 95% confidence, if the significance value was less than 0.05, the H_o2 was rejected; if it was less than 0.025, the H_o1 was rejected.

Site	Mean Ring-Width Index Value		t-test Sig. Value	95% Confidence Intervals (difference in ring-width values between +/ - SOI)		Reject (R) or Accept (A) H_o?	
	(+) phase	*(-) phase*		*Lower*	*Upper*	*H_o1**	*H_o2**
QCI	0.9327	1.0241	0.001	0.03765	0.1450	R	R
MtHY	0.9461	0.9945	0.073	-0.0046106	0.1013	A	A
ER	0.9676	1.0009	0.133	-0.010200	0.07675	A	A
CM	0.2022	1.0062	0.111	-0.0092964	0.08927	A	A
CS	0.1592	1.0036	0.025	0.005912	0.08857	R	R

The sample size was 177 years of –SOI, 114 years of +SOI
*H_o1 – one-tailed null hypothesis
*H_o2 – two-tailed null hypothesis

6.3.2 Superposed Epoch Analysis with Southern Oscillation Index Extremes

The results of the t-test for SOI extremes identified in the Stahle *et al.* (1998) and Allan *et al.* (1996) records (Table 6.2) show that there are statistically significant differences between mean ring-width values during positive and negative SOI extremes in the QCI ($p = 0.000$), MtHy ($p = 0.010$), CM ($p = 0.024$) and the CS ($p = 0.006$) chronologies (reject Ho2). These findings indicate that the MH ring-widths at these four sites have a statistical relationship with the signal of El Niño/La Niña events; during the growing season after El Niño events these MH trees grow statistically larger tree-rings than they do after La Niña events.

The ER ($p = 0.152$) chronology is the only site that did not show a statistical difference between mean ring-width values during positive and negative SOI extremes (do not reject Ho2). Based on this finding, there is no statistical evidence to suggest that the radial-growth of MH trees at this site is affected by El Niño / La Niña events.

Table 6.2 t-test results for the Stahle *et al.* (1998) / Allan *et al.* (1996) reconstructed SOI index extremes (>+5.0, <-5.0) compared to five MH ring-width chronologies along a longitudinal transect in northwestern BC. At a 95% confidence, if the significance value was less than 0.05, the H_o2 was rejected; if it was less than 0.025, the H_o1 was rejected.

Site	**Mean Ring-Width Index Value**		**t-test Sig. Value**	**95% Confidence Intervals (difference in ring-width values between +/ - SOI extremes)**		**Reject (R) or Accept (A) H_o?**	
	(+) phase	*(-) phase*		*Lower*	*Upper*	*H_o1**	*H_o2**
QCI	0.9347	1.1092	0.000	0.08673	0.2623	R	R
MtHY	0.9294	1.0384	0.010	0.02620	0.1919	R	R
ER	0.9766	1.0313	0.152	-0.020488	0.1299	A	A
CM	0.9613	1.0614	0.024	0.01380	0.1866	R	R
CS	0.9425	1.0549	0.006	0.03269	0.1922	R	R

The sample size was 63 years of –SOI extremes, 32 years of + SOI extremes
*Ho1 – one-tailed null hypothesis
*Ho2 – two-tailed null hypothesis

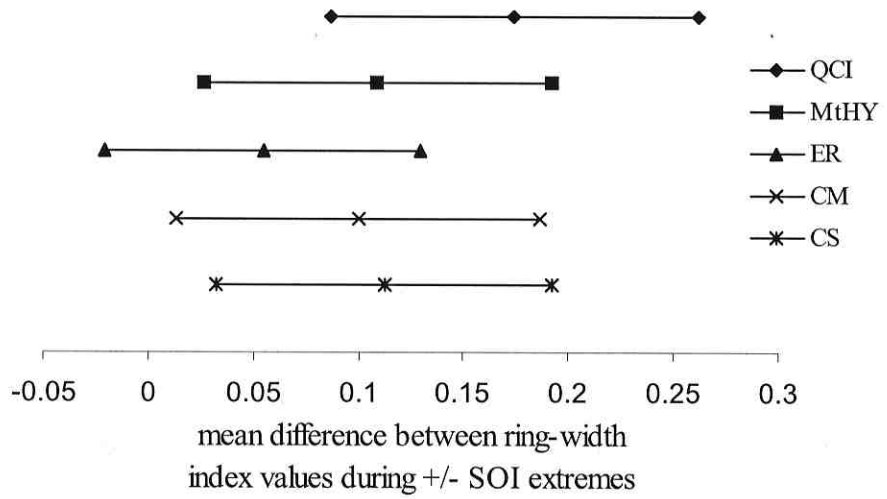

Figure 6.1 Confidence interval (95%) of the difference between mean ring-width index values during positive and negative reconstructed SOI extremes identified in the Stahle *et al.* (1998) / Allan *et al.* (1996) record.

The difference between ring-width index values during positive and negative SOI extremes seems to be greatest at the QCI site and least at the ER (not a statistically significant difference) (Figure 6.1). However, there does not seem to be a clear pattern of mean ring-width differences across the transect.

6.3.3 Superposed Epoch Analysis with Pacific Decadal Oscillation Index

The results of the t-test (Table 6.3) show that there are statistically significant differences in mean ring-width values between positive and negative PDO phases in the QCI ($p = 0.000$), MtHY ($p = 0.000$), ER ($p = 0.012$), CM ($p = 0.000$) and the CS ($p = 0.001$) chronologies (reject Ho2). Furthermore, the one-tailed hypothesis for all sites is also rejected which means that ring-widths are statistically smaller during negative PDO phases than positive phases.

Table 6.3 t-test results for the Gedalof and Smith (2001b) reconstructed PDO index compared to five MH ring-width chronologies along a longitudinal transect in northwestern BC. At a 95% confidence, if the significance value was less than 0.05, the H_o2 was rejected; if it was less than 0.025, the H_o1 was rejected.

Site	**Mean Ring-Width Index Value**		**t-test Sig. Value**	**95% Confidence Intervals (difference in ring-width values between +/ - PDO phases)**		**Reject (R) or Accept (A) H_o?**	
	(+) phase	*(-) phase*		*Lower*	*Upper*	*H_o1**	*H_o2**
QCI	1.0924	0.8401	0.000	0.1976	0.3070	R	R
MtHY	1.0301	0.8856	0.000	0.09235	0.1967	R	R
ER	1.0123	0.9453	0.012	0.01509	0.1190	R	R
CM	1.0300	0.9097	0.000	0.06452	0.1760	R	R
CS	1.0358	0.9462	0.001	0.03511	0.1440	R	R

The sample size was 146 years of + PDO phases, 108 years of – PDO phases
*H_o1 – one tailed null hypothesis
*H_o2 – two tailed null hypothesis

The difference between ring-width index values during positive and negative PDO phases seems to be greatest at the QCI site (0.2523) (Figure 6.2). There seems to be

a pattern of reducing mean differences between ring-width index values between positive and negative phases as you move from west to east. An exception to this pattern is the ER site, which has the lowest mean difference (0.06705) (Figure 6.2).

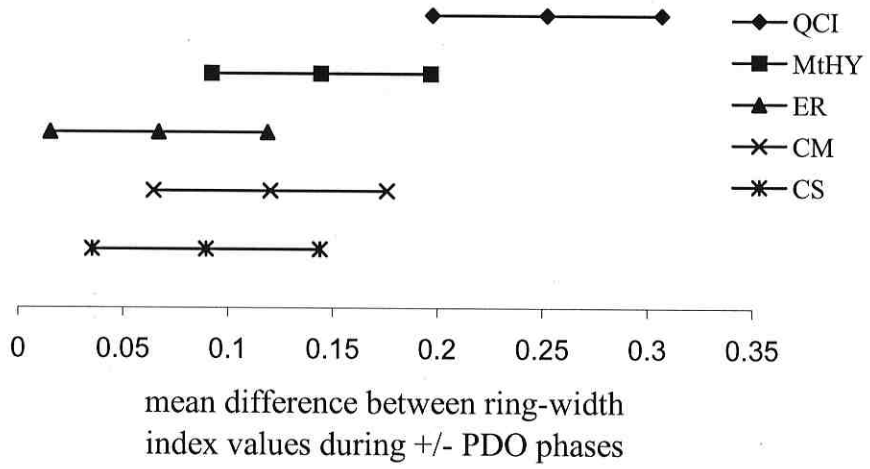

Figure 6.2 Confidence interval (95%) of the difference between mean ring-width index values during positive and negative PDO phases identified in the Gedalof and Smith (2001b) record.

6.4 Discussion

6.4.1 Interpreting the SEA for ENSO Events

The Stahle *et al.* (1998) reconstruction SOI proxy record proved useful for identifying SOI extremes representing El Niño / La Niña events. There was a stronger relationship between the chronologies and SOI extremes than between the chronologies and the SOI proxy record (with the exception of the ER chronology, where no significant difference between ring-widths during El Niño and La Niña events was found). These results suggest that MH trees are responding to extreme events such as El Niño and La

Niña across the transect, but not to the climate changes that accompany the SOI on a yearly basis. The increased variability of the year-to-year SOI effects in the higher latitudes could explain this (Trenberth, 1997a).

The results of the one-tailed hypothesis were expected for the SEA done using the SOI extremes from the Stahle *et al.* (1998) record. El Niño events bring mild wet winters to the study area (Environment Canada, 2003), resulting in better growing conditions for MH trees. In turn, the better growing conditions contribute to increased radial-growth across the transect.

The effects of El Niño / La Niña events are observed in the tree-ring record at all sites across the transect, with the exception of the ER site. Based on the results of mean differences between ring-widths between positive and negative events (Figure 6.1), there seems to be little or no pattern of sensitivity to ENSO climate effects across the transect. ENSO effects have been well documented across North America (Hare and Mantua, 2000; Trenberth *et al.*, 2002; Schoennagel *et al.*, 2005) and it follows that its strength would not dramatically change from the coast to the interior.

6.4.2 Interpreting the SEA for PDO Events

There was a strong relationship identified between the tree-ring chronologies and the reconstructed PDO index presented by Gedalof and Smith (2001b) (Table 6.3). The results of the one-tailed test showed that the annual tree-rings are statistically smaller during negative PDO phases than during positive phases (Table 6.3). During a positive phase of the PDO there is an increased cyclonic flow of warm moist air into the study area resulting in an increase in annual air temperatures. In high elevation areas, where temperature can be a limiting factor, the warmer annual air temperatures during a positive

PDO phase creates better growing conditions for MH trees by contributing to longer growing seasons and increasing rates of photosynthesis (due to increased soil and plant temperature in response to the increased air temperature).

The sensitivity of MH radial-growth to the PDO phase changes decreases from west to east along the transect. There was a pattern of greater differences in ring-width indices at the coastal sites, indicating a stronger response to PDO climate effects (Figure 6.2). By contrast, a weaker relationship between ring-width and the PDO was revealed at the eastern end of the transect. There are two possible explanations for this: (1) MH trees are increasingly sensitive to PDO phase changes towards the coast due to some sort of ecological effect; and/or, (2) the actual climatic effects of the PDO are stronger in coastal areas.

In order to answer this question a SEA of the mean annual air temperatures (derived from the monthly air temperature averages), from the Environment Canada climate stations discussed in Chapter 3, were compared during positive and negative PDO phases identified in the Gedalof and Smith (2001b) proxy. Total annual precipitation was not used because the results of Chapter 3 indicated little evidence of PDO phase changes in the total annual precipitation instrumental record (Figure 3.3). The time period of 1957 to 1998 was used because it is the only time period where all of the instrumental records from the study climate stations along the transect and the Gedalof and Smith (2001b) PDO proxy overlap. The methods and analysis used in this SEA are the same as the ones described earlier in this chapter. In this case the null H_o2 is: there is no statistically significant difference in mean annual air temperatures between

positive and negative PDO phases. The H_o1 is: the annual air temperatures during a positive PDO phase are less than during a negative PDO phase.

The results of the SEA led to the rejection of both H_o1 and H_o2, indicating that the mean annual air temperatures are greater during positive PDO phases (Table 6.4). Furthermore, based on a simple visual observation, there does not appear to be any significant trend across the transect in the mean difference between mean annual average air temperatures during positive and negative PDO phases (Figure 6.3). This leads to the conclusion that the effects of the PDO on annual average air temperature do not vary in strength along the transect. This also means that the decreasing strength of response of MH radial-growth to PDO phases from west to east along the transect can be attributed to a variability in the sensitivity of MH trees to PDO phases, and not a variability in the strength of the PDO phases on the air temperature, across the transect.

Table 6.4 t-test results for the Gedalof and Smith (2001b) reconstructed PDO index compared to mean annual air temperature from four climate stations along a longitudinal transect in northwestern BC from 1957 to 1998. At a 95% confidence, if the significance value was less than 0.05, the H_o2 was rejected; if it was less than 0.025, the H_o1 was rejected.

Site	**Mean annual air temperatures**		**t-test Sig. Value**	**95% Confidence Intervals (difference in mean annual air temperatures between +/ - PDO phases)**		**Reject (R) or Accept (A) H_o?**	
	(+) phase	*(-) phase*		*Lower*	*Upper*	*H_o1**	*H_o2**
SS	8.6524	7.9286	.000	0.3800	1.0676	R	R
PR	7.4095	6.7286	.000	0.3207	1.0412	R	R
TR	6.6190	5.9095	.002	0.2684	1.1507	R	R
SM	4.2000	3.4857	.005	0.2269	1.2017	R	R

The sample size was 21 years of + PDO phases, 21 years of – PDO phases
*H_o1 – one tailed null hypothesis
*H_o2 – two tailed null hypothesis

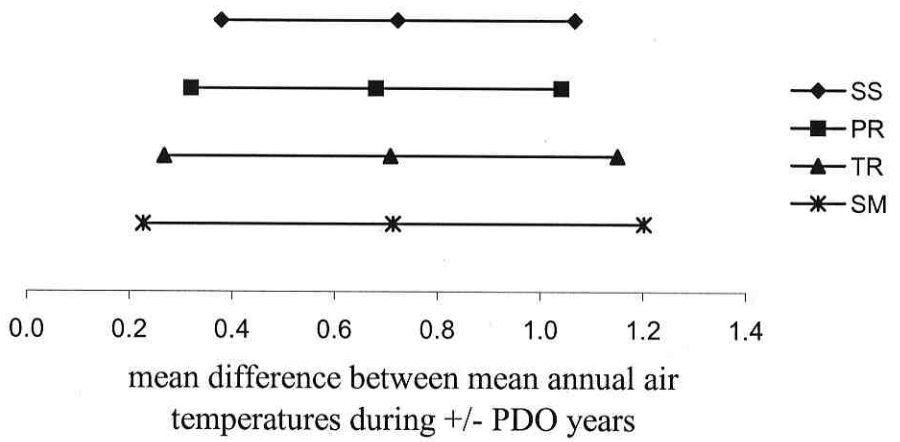

Figure 6.3 Confidence interval (95%) of the mean difference between mean annual air temperatures during positive and negative PDO phases identified in the Gedalof and Smith (2001b) record from 1957 to 1998.

6.4.3 PDO vs. SOI Response

The stronger response of MH radial-growth to PDO phase changes versus the SOI extremes could be due to the nature of the records. The PDO shifts every 20 to 30 years while the El Niño / La Niña events may only last a year or two and occur only every three to seven years. It is relatively easy to identify low frequency responses in tree-ring records because of lag effects and the methods used to standardize the chronologies. Standardization of tree-ring chronologies tends to remove singular events, while low frequency trends such as those associated with the PDO remain. Because the analysis in this thesis did not take into account any lag effects it is possible that the impact of El Niño / La Niña on radial-growth could have been stronger in the year following the actual event.

It is also important to note that the proxy PDO record (Gedalof and Smith 2001b) was constructed using data from high elevation MH trees across a latitudinal transect

stretching along the Pacific Coast of North America (from the Kenai Peninsula, Alaska to southern Oregon). Concerns have been raised that the stronger response to the PDO at coastal sites, identified in this study, is due to the similarities among chronologies prepared for this thesis and the ones used in the proxy record; however, this limitation is not a reason to dismiss the proxy as a viable PDO record. This PDO proxy was chosen because it is a good proxy of climate conditions in the area of this study and therefore best shows events affecting the trees in the study area; and it shows a long enough record to compare with the chronologies collected in this study. Also, the proxy is not simply a MH chronology, it is a climate proxy record since factor analysis was applied to MH chronologies to determine the best fit with climate indices. The highest correlation between the leading eigenvector of the MH chronologies and a number of climatic and SST indices was determined to be with the spring PDO index and a simple linear regression was used to determine the pre-instrumental proxy record. Furthermore, the actual values of the Gedalof and Smith (2001b) PDO proxy were not used in the SEA, instead the values were simply separated into three groups: positive events, negative events and undefined events (1840-1923) that correspond to PDO phases identified in other studies (Minobe and Mantua, 1999). Therefore, the use of the Gedalof and Smith (2001b) proxy PDO record in the SEA should not have a large, if any, effect on the strength of response to PDO events across the transect.

6.4.4 Limitations of a Proxy Record

The lack of a significant relationship between the SOI (Stahle *et al.*, 1998) and the ring-width indices at the MtHY, ER and CM sites has two possible explanations: (1) the trees were not sensitive to the effects of the SOI on the climate on the area; or, (2) the

SOI reconstruction was not sufficiently robust to reveal the origin of variance in ring-width growth. Stahle *et al.* (1998) acknowledge the latter and suggest there are two limitations to using proxy records to define ENSO events: (1) the trees that are used to build a chronology could be responding to dry/wet conditions caused by other circulation patterns; and, (2) there could be undocumented changes within the forest stands, such as anthropogenic interference, that could have changed the sensitivity to ENSO responses. Each of these limitations compromises the strength of the reconstruction and, therefore, the strength of the SEA.

6.5 Summary

Understanding the relationship between climate oscillations and ecosystems is important for long-term resource management. In this case, El Niño, La Niña and the PDO seem to have a relation with the radial-growth of MH trees along the study transect. El Niño events and positive PDO phases bring an increase in air temperature and perhaps available moisture, apparently resulting in better growing conditions for MH trees. The opposite effect is true for La Niña events and negative PDO phases which both appear to result in reduced growth rates and the production of narrow tree-rings. The strength of the response to ENSO events on MH radial-growth is nearly consistent across the transect. The strength of the response to PDO phases on MH radial-growth is greatest at the Queen Charlotte Islands and diminishes toward the interior. This is due to an increase in MH radial-growth sensitivity to PDO phases from east to west along the transect, and not due to variability in the strength of the climatic effects of the PDO along the transect.

Chapter 7 - Summary and Conclusions

7.1 Summary

The intent of this thesis was to examine the variability of tree growth response to climate variability along a longitudinal transect extending from the Queen Charlotte Islands to the Smithers area in northwestern BC. The expectation was that the research would lead to a better understanding of the differential growth response of one tree species to this climatically diverse landscape.

The first objective of this research was to define the magnitude, character and spatio-temporal variability of climate across the study area. As expected, there was a trend of increasing temperature ranges and decreasing moisture availability from west to east along the transect. The mean annual air temperature has increased at all sites over the instrumental record, with the lowest increase recorded at Prince Rupert. The average annual precipitation has also increased at all sites, with the largest annual increases recorded at the Sandspit station on the Queen Charlotte Islands.

The second objective of the thesis was to evaluate the radial-growth response of MH trees to air temperature and precipitation at five locations along the transect. Dendroclimatological analyses identified three regions where trees exhibited comparable growth patterns: (a) the Queen Charlotte Islands: (b) from Mount Hayes to Copper Mountain; (c) from Copper Mountain to Cable Spur, with an undistinguished area of transition surrounding Copper Mountain. Although within each zone tree growth appears to be closely correlated; at each of the study sites, local climate / radial-growth relationships were discovered. No two MH stands had the same relationship with monthly temperature and precipitation data, which suggests that the trees are responding to site-specific limiting factors.

The third objective of the thesis was to determine whether there was any evidence that regional climate forcing factors affect the radial-growth of MH trees in northwestern BC. All sites (with the exception of the ER site) showed a growth response to both ENSO events (SOI extremes) and to PDO phase changes. El Niño and positive PDO phases resulted in increased radial-growth, while La Niña and negative PDO phases resulted in decreased radial-growth. The strength of the response to ENSO events on MH radial-growth is nearly consistent across the transect. The strength of the response to PDO phases on MH radial-growth is greatest at the Queen Charlotte Islands and diminishes toward the interior. This is due to an increase in MH radial-growth sensitivity to PDO phases from east to west along the transect, and not due to variability in the strength of the climatic effects of the PDO along the transect.

7.2 Recommendations for Future Research

1. Including more study areas could have lessened uncertainties. Time and resources limited the scope of this study and only five sites were sampled. An increase in sites along the transect may have contributed to more robust results. It is difficult to base statistically significant results on such a small number of samples.
2. Further sampling is needed in the vicinity of the Exstew River tree-ring chronology since it did not correlate well to climate data. This chronology showed no response to ENSO events (SOI extremes) while every other chronology (in both coastal and continental locations) did, suggesting that the ER site was not sensitive enough to climatic parameters for the purpose of dendroclimate research.
3. Detailed microclimate, soil and tree physiology data could be used to test the supposed climate / radial-growth relationships identified in this study. Time and

resources limited the available data to tree cores and regional climate data, forcing this study to make suggestions and suppositions regarding the actual climate / radial-growth relationships. A long-term study with measurements of microclimate conditions (air temperature, precipitation, snow pack depth, wind speed, solar radiation and humidity), soil conditions (type, depth, structure, temperature, moisture), and tree conditions (temperature, rates of photosynthesis and respiration) is recommended.

7.3 Conclusions

This thesis demonstrates that climate has varied both temporally and spatially along the transect from the Queen Charlotte Islands to the Smithers area in northwestern BC. It has shown that the radial-growth of MH trees varies annually in response to climate parameters (air temperature and precipitation) and over longer intervals of time in response to climate-forcing mechanisms such as ENSO and the PDO.

The thesis has also shown that ecosystem response to changing climates is very site-specific. In light of this, resource planning initiatives being proposed to respond to future climate changes should not draw solely upon the generalized findings of regional-scale research initiatives. There continues to be a need for site-specific investigations that contribute to region specific climate modeling and ecosystem management.

Literature Cited

Allan, B.J., Lindesay, J., and Parker, D. 1996. *El Niño/Southern Oscillation and Climatic Variability*. CSIRO Publishing: Victoria, Australia.

Arno, S.F., and Hammerly, R.P. 1977. *Northwest Trees*. The Mountaineers: Seattle, Washington.

Aguado, E., and Burt, J.E. 2004. *Understanding Weather and Climate,* third edition. Pearson Education Inc.: New Jersey.

AHCCD – Adjusted Historical Canadian Climate Data. 2005. *Adjusted Precipitation and Homogenized Temperature Data Sets (*online). Climate Monitoring and Data Interpretation Division, Climate Research Branch Meteorological Service of Canada. Available from http://www.cccma.bc.ec.gc.ca/hccd/ [accessed September 20, 2005].

Barnett, T.P., Bengtsson, L., Arpe, K., Flugel, M., Graham, N., Latif, M., Ritchie, J., Roeckner, E., Schlese, U., Schulzweida, U., and Tyree, M. 1994. Forecasting global ENSO-related climate anomalies. *Tellus* 46(A): 381-397.

BC Ministry of Forests. 2001. *Biogeoclimatic Ecosystem Classification (BEC) Zones* [online]. Available from http://www.for.gov.bc.ca/HRE/becweb/index.html [accessed August 10, 2006].

BC forest information. 2006. Available from http://www.bcforestinformation.com/default.asp [online] [Accessed September 21, 2006].

Biondi, F., Gershunov, A., and Cayan, D. 2001. North Pacific Decadal Climate Variability since 1661. *Journal of Climate* 14: 5-10.

Bonsal, B., Shabbar, A., and Higuchi, K. 2001. Impacts of low frequency variability modes on Canadian winter temperature. *International Journal of Climatology* 21: 95-108.

Bostock, H.S. 1970. Geology and Economic Minerals of Canada. *Physiographic Subdivisions of Canada.* Department of Energy, Mines and Resources of Canada, Crown Copyrights: Ottawa, Ontario.

Botes, A., McGeoch, M.A., Robertson, H.G., Niekerk, A., Davids, H.P., and Chown, S.L. 2006. Ants, altitude and change in the northern Cape Floristic Region. *Journal of Biogeography* 33: 71-90.

Bowman, J., Holloway, G.L., Malcolm, J.F., Middel, K.R., and Wilson, R.J. 2005. Northern range boundary dynamics of southern flying squirrels: Evidence of an energetic bottleneck. *Canadian Journal of Zoology* 83: 1486-1494.

Briffa, K.R. 2000. Annual climate variability in the Holocene: Interpreting the message of ancient trees. *Quaternary Science Reviews* 19: 87-105.

Brown, P.M., and Wu, R. 2005. Climate and disturbance forcing of episodic tree recruitment in a southwestern ponderosa pine landscape. *Ecology* 86: 3030-3038.

Brubaker, L. 1980. Spatial patterns of tree growth anomalies in the Pacific Northwest. *Ecology* 61: 798-807.

Cayan, D.R., and Peterson, D.H. 1989. The influence of North Pacific atmospheric circulation on streamflow in the west. *Aspects of Climate Variability in the Pacific and the Western Americas.* Edited by Peterson, D.H. American Geophysical Union, Washington DC.

Chahine, M.T., and Susskind, J. 1991. Derivation of long-term climate data sets from NOAAS HIRS2 MSU. *Global and Planetary Change* 90: 121-125.

Chapin, F.S., Callaghan, T.V., Bergeron, Y., Fukuda, M., Johnstone, J.F., Juday, G., and Zimov, S.A. 2004. Global change and the boreal forest: Thresholds, shifting states or gradual change? *AMBIO* 33: 361-365.

Clague, J.J., Wohlfarth, B., Ayotte, J., Eriksson, M., Hutchingson, I., Mathewes, R.W., Walker, I.R., and Walker, L. 2004. Late Holocene environmental change at treeline in northern Coast Mountains, British Columbia, Canada. *Quaternary Science Reviews* 23: 2413-2431.

Climate Prediction Center. 2006. *Monthly Atmospheric and Sea Surface Temperature Indices* [online]. Available from http://www.cpc.ncep.noaa.gov/data/indices/ [accessed April 3, 2006]

Cook, E. 1990. A conceptual linear aggregate model for tree rings. *Methods of Dendrochronology.* Edited by Cook, E. and Kairiukstis, L. Kluwer Academic Publishers: Netherlands.

Cook, E., Briffa, K., Shiyatov, S., and Mazepa, V. 1990. Tree Ring standardization and growth-trend estimation. *Methods of Dendrochronology.* Edited by Cook, E., and Kairiukstis, L. Kluwer Academic Publishers: Netherlands.

D'Arrigo, R., Villalba, R., and Wiles, G. 2001. Tree-ring estimates of Pacific decadal climate variability. *Climate Dynamics* 18: 219-224.

D'Arrigo, R., Wilson, R., Desser, C., Wiles, G., Cook, E., Villalba, R., Tudhop, A., Cole, J., and Linsley, B. 2005. Tropical-North Pacific climate linkages over the past four centuries. *Journal of Climate* 18: 5253-5265.

Del Barrio, G., Harrison, P.A., Berry, P.M., Butt, N., Sanjuan, M.E., Pearson, R.G., and Dawson, T. 2006. Integrating multiple modelling approaches to predict the potential impacts of climate change on species' distributions in contrasting regions: comparison and implications for policy. *Environmental Science and Policy* 9: 129-147.

Driscoll, W.W., Wiles, G.C., D'Arrigo, R.D., and Wilmking, M. 2005. Divergent tree growth response to recent climatic warming, Lake Clark National Park and Preserve, Alaska. *Geophysical Research Letters* 32: L20703.

Environment Canada. 2003. *Pacific Coast Mean Climate Conditions* [online]. Available from http://www.mscsmc.ec.gc.ca/education/elnino/canadian/region/index_mean_e.cfm?region=pacific_coast [accessed January 20, 2007].

EPD – Environmental Protection Division, BC Ministry of Environment. 2002. *Indicators of Climate Change for British Columbia, 2002* [online]. Available from http://www.env.gov.bc.ca/air/climate/indicat/intro.html [accessed May 6, 2006].

Ericsson, A., Larsson, S., and Tenow, O. 1980. Effects of early and late season defoliation on growth and carbohydrate dynamics in Scots pine. *Journal of Applied Ecology* 17: 747-769.

Fagre, D.B., Peterson, D.L., and Hessl, A.E. 2003. Taking the pulse of mountains: Ecosystem responses to climatic variability. *Climatic Change* 59: 263-282.

Fritts, H.C., Blasing, T.J., Hayden, B.P., and Kutzbach, J.E. 1971. Multivariate techniques for specifying tree-growth and climate relationships and for reconstructing anomalies in paleoclimate. *Journal of Applied Meteorology* 10: 845-856.

Fritts, H.C. 1976. *Tree Rings and Climate*. Academic Press: London, England.

Fry, D.L., and Stephens, S.L. 2006. Influence of humans and climate on the fire history of a ponderosa pine-mixed conifer forest in the southeastern Klamath Mountains, California. *Forest Ecology and Management* 223: 428-438.

Gedalof, Z., and Smith, D. 2001a. Dendroclimatic response of mountain hemlock (*Tsuga mertensiana*) in Pacific North America. *Canadian Journal of Forest Research* 31: 322-332.

Gedalof, Z., and Smith, D. 2001b. Interdecadal climate variability and regime-scale shifts in Pacific North America. *Geophysical Research Letters* 28: 1515-1518.

Geertsema, M., Clague, J.J., Schwab, J.W., and Evans, S.G. 2006. An overview of recent large catastrophic landslides in northern British Columbia, Canada. *Engineering Geology* 83: 120-143.

Gershunov, A., and Barnett, T.P. 1998. Interdecadal modulations of ENSO teleconnections. *Bulletin of the American Meteorological Society* 79: 2715-2725.

Girardin, M.P., Tardif, J.C., Flannigan, M.D., and Bergeron, Y. 2006. Synoptic-scale atmospheric circulation and boreal Canada summer droughts variability of the past three centuries. *Journal of Climate* 19: 1922-1947.

GGWS – Golden Gate Weather Services. 2004. *El Nino and La Nina Years: A Consensus List* by Jan Null [online]. Available from http://ggweather.com/enso/years.htm [accessed January 7, 2007].

Gonzalez-Elizondo, M., Jurado, E., Navar, J., Gonzalez-Elizondo, M.S., Villanueva, J., Aguirre, O., and Jimenez, J. 2005. Tree-rings and climate relationships for Douglas-fir chronologies from the Sierra Madre Occidental, Mexico: A 1681-2001 rain reconstruction. *Forest Ecology and Management* 213: 39-53.

Graumlich, L.J., and Brubaker, L.B. 1986. Reconstruction of annual temperature (1590 – 1979) from Longmire, Washington, derived from tree rings. *Quaternary Research* 25: 223-234.

Guiot, J., Berger, A.L., and Munaut, A.V. 1982. Response Functions. *Climate from Tree Rings*. Edited by Hughes, M.K., Kelly, P.M., Pilcher, J.R., and LaMarche, V.C. Cambridge University Press: London, England.

Hamann, A., and Wang, T. 2006. Potential effects of climate change on ecosystem and tree species distribution in British Columbia. *Ecology* 87: 2773-2786.

Hare, S.R., and Mantua, N.J. 2000. Empirical evidence for North Pacific regime shifts in 1977 and 1989. *Progress in Oceanography* 47: 103-145.

Hartmann, B., and Wendler, G. 2005. The significance of the 1976 Pacific climate shift in the climatology of Alaska. *Journal of Climate* 18: 4824-4839.

Hartmann, D. 2006. *Compositing or Superposed Epoch Analysis* [online]. Available from http://www.atmos.washington.edu/~dennis/552_Notes_2.pdf [accessed July 7, 2006]

Hofgaard, A., Tardif, J., and Bergeron, Y. 1999. Dendroclimatic response of *Picea mariana* and *Pinus banksiana* along a latitudinal gradient in the eastern Canadian boreal forest. *Canadian Journal of Forest Research* 29: 1333-1346.

Holman, M.L., and Peterson, D.L. 2006. Spatial and temporal variability in forest growth in the Olympic Mountains, Washington: Sensitivity to climatic variability. *Canadian Journal of Forest Research* 36: 92-104.

IRI – International Research Institute for Climate and Society. 2006. *Climate Indices* [online]. Available from http://ingrid.ldeo.columbia.edu/dochelp/StatTutorial/Indices/ [accessed November 3, 2006].

Jacoby, G., Solomina, O., Frank, D., Eremenko, N., and D'Arrigo, R. 2004. Kunashir (Kuriles) Oak 400-year reconstruction of temperature and relation to the Pacific Decadal Oscillation. *Palaeogeography, Palaeoclimatology, Palaeoecology* 209: 303-311.

Kadonaga, L.K., Podlaha, O., and Whiticar, M.J. 1999. Time series analyses of tree ring chronologies from Pacific North America; evidence for sub-century climate oscillations. *Chemical Geology* 161: 339-363.

Karanka, E.A. 1986. *Trends and Fluctuations in Precipitation and Stream Runoff in the Queen Charlotte Islands*. Land Management Report No.40, British Columbia Ministry of Forests: Victoria, British Columbia.

Kendrew, W.G., and Kerr, D. 1955. *The Climate of British Columbia and the Yukon Territory*. Queen's Printer: Ottawa.

Koeppe, C.E. 1931. *The Canadian Climate*. McKnight and McKnight: Illinois.

Köppen, W.P. 1936. Das Geographische System der Klimate. *Handbuch der Klimatologie, Band* 1. Edited by Köppen, W., and Geiger, R. Gebrüder Borntraeger: Berlin.

Kramer, P.J., and Kozlowski, T.T. 1960. *Physiology of Trees*. McGraw-Hill Book Company, Inc.: New York.

Landsberg, H. 1962. *Physical Climatology*. Gary Printing Co., Inc.: DuBois, Pennsylvania.

Laroque, C.P. 1995. *The dendrochronology and dendroclimatology of yellow-cedar on Vancouver Island.* Unpublished M.Sc. Thesis, University of Victoria, Victoria.

Laroque, C.P., and Smith, D. 1999. Tree-ring analysis of yellow-cedar (*Chamaecyparis nootkatensis*) on Vancouver Island, British Columbia. *Canadian Journal of Forest Research* 29: 115-123.

Laroque, C.P., and Smith, D. 2003. Radial-growth forecasts for five high-elevation conifer species on Vancouver Island, British Columbia. *Forest Ecology and Management* 183: 313-325.

Lebourgeois, F. 2000. Climatic signals in earlywood, latewood and total ring width of Corsican pine from western France. *Annals of Forest Science* 57: 155-164.

Lindenmayer, D.B., Margules, C.R., and Botkin, D.B. 2000. Indicators of biodiversity for ecologically sustainable forest management. *Conservation Biology* 14: 941-950.

Linderholm, H.W., Sloberg, B.O., and Lindholm, M. 2003. Tree-ring records from central Fennoscandia: The relationship between tree growth and climate along a west-east transect. *The Holocene* 13: 887-895.

Lindner, M., Sohnge, B., Joyce, L.A., Price, D.T., Bernier, P.Y., and Karjalainen,T. 2002. Integrated forestry assessments for climate change impacts. *Forest Ecology and Management* 162: 117-136.

Mantua, N.J., Hare, S.R., Zhang, Y., Wallace, J.M., and Francis, R.C. 1997. A Pacific interdecadal climate oscillation with impacts on salmon production. *Bulletin of the American Meteorological Society* 78: 1069-1079.

Mantua, N.J., and Hare, S.R. 2002. The Pacific decadal oscillation. *Journal of Oceanography* 58: 35-44.

Mass, C.F., and Portman, D.A. 1989. Major volcanic eruptions and climate: A critical evaluation. *Journal of Climate* 2: 566-593.

McCain, C.M. 2005. Elevational gradients in diversity of small mammals. *Ecology* 86: 366-372.

McFarlane, G.A., King, J.R., and Beamish, R.J. 2000. Have there been recent changes in climate? Ask the fish. *Progress in Oceanography* 47: 147-169.

Means, J.E. 1990. Tsuga mertensiana / Mountain Hemlock. *Silvics of North America, Volume 1. Conifers*. Forest Service, United States Department of Agriculture: Washington, D.C.

Meehl, G.A., Teng, H., and Branstator, G. 2006. Future changes of El Niño in two global coupled climate models. *Climate Dynamics* 26: 549-566.

Minobe, S., and Mantua, N. 1999. Interdecadal modulation of interannual atmospheric and oceanic variability over the North Pacific. *Progress in Oceanography* 43: 163-192.

Moore, D.S., and McCabe, G.P. 1999. *Introduction to the Practice of Statistics*. W.H. Freedman and Co.: New York.

Moore, R.D., and McKendry, I.G. 1996. Spring snow pack anomaly patterns and winter climatic variability, British Columbia, Canada. *Water Resources Research* 32: 623-632.

Natural Resources Canada (NRC). 2006. *The Atlas of Canada – Köppen Climate Regions* [online]. Available from http://atlas.nrcan.gc.ca/site/english/maps/archives/3rdedition/environment/climate/030#download [accessed March 15, 2006].

NOAA/CPC – National Oceanic and Atmospheric Administration / Climate Prediction Center. 2004. *Climate Glossary* [online]. Available from http://www.cpc.ncep.noaa.gov/products/outreach/glossary.shtml [accessed May 6, 2006].

Owens, J. N. 1984a. Bud development in mountain hemlock (*Tsuga mertensiana)*. I Vegetative bud and shoot development. *Canadian Journal of Botany* 62: 475-483.

Owens, J. N. 1984b. Bud development in mountain hemlock (*Tsuga mertensiana)*. II Cone-bud differentiation and predormancy development. *Canadian Journal of Botany* 62: 484-494.

Owens, J.N., and Molder, M. 1975. Sexual reproduction of mountain hemlock (*Tsuga mertensiana*). *Canadian Journal of Botany* 53: 1811-1826.

Owens, J.N., and Molder, M. 1984. *The Reproductive Cycles of Western and Mountain Hemlock.* Information Services Branch, Ministry of Forests: Victoria, B.C.

Pearson, R.G., and Dawson, T.P. 2003. Predicting the impacts of climate change on the distribution of species: are bioclimate envelope models useful? *Global Ecology and Biogeography* 12: 361-371.

Peterson, D.W., and Peterson, D.L. 2001. Mountain hemlock growth responds to climatic variability at annual and decadal time scales. *Ecology* 82: 3330-3345.

Pielou, E.C. 1988. *The World of Northern Evergreens*. Comstock Publishing Associates: London, England.

Prager, M.H., and Hoenig, J.M. 1989. Superposed epoch analysis: A randomization test of environmental effects on recruitment with application to Chub Mackerel. *Transactions of the American Fisheries Society* 118: 608-618.

Ropelewski, C.F., and Jones, P.D. 1987. An extension of the Tahiti-Darwin Southern Oscillation Index. *Monthly Weather Review* 115: 2161-2165.

Rosenberg, S.M., Walker, I.R., and Mathewes, R.W. 2003. Postglacial spread of hemlock (*Tsuga*) and vegetation history in Mount Revelstoke National Park, British Columbia, Canada. *Canadian Journal of Botany* 81: 139-151.

Rutherford, S., Mann, M.E., Osborn,T.J., Bradley, R.S., Briffa, K.R., Hughes, M.K., and Jones, P.D. 2005. Proxy-based Northern Hemisphere surface temperature reconstructions: Sensitivity to method, predictor network, target season, and target domain. *Journal of Climate* 18: 2308-2329.

Salinger, M.J. 2005. Climate variability and change: Past, present and future – An overview. *Climatic Change* 70: 9-29.

Schoennagel, T., Veblen, T.T., Romme, W.H., Sibold, J.S., and Cook, E.R. 2005. ENSO and PDO variability affect drought-induced fire occurrence in Rocky Mountain subalpine forests. *Ecological Applications* 15: 2000-2014.

Schweingruber, F.H. 1989. *Tree Rings – Basics and Applications of Dendrochronology.* Kluwer Academic Publishers: Netherlands.

Schweingruber, F.H., Kairiukstis, L. and Shiyatow, S. 1989. Sample selection. *Methods of Dendrochronology*. Edited by Cook, E. and Kairiukstis, L. Kluwer Academic Publishers: Netherlands.

Shen, C., Wang, W., Gong, W., and Hao, Z. 2006. A Pacific Decadal Oscillation record since 1470 AD reconstructed from proxy data of summer rainfall over eastern China. *Geophysical Research Letters* 33: doi:10.1029/2005GL024804.

Shiogama, H., Watanabe, M., Kimoto, M., and Nozawa, T. 2005. Anthropogenic and natural forcing impacts on ENSO-like decadal variability during the second half of the 20th century. *Geophysical Research Letters* 32: doi:10.1029/2005GL023871.

Sinclair, A.J., and Smith, D.L. 1999. The Model Forest Program in Canada: Building consensus on sustainable forest management? *Society and Natural Resources* 12: 121-138.

Smith, D., and Laroque, C. 1998. Mountain hemlock growth dynamics on Vancouver Island. *Northwest Science* 72: 67-70.

Stahle, D.W., D'Arrigo, R.D., Krusic P.J., Cleaveland, M.K., Cook, E.R., Allan, R.J., Cole, J.E., Dunbar, R.B., Therrell, M.D., Gay, D.A., Moore, M.D., Stokes, M.A., Burns, B.T., Villanueva-Diaz, J., and Thompson, L.G. 1998. Experimental dendroclimatic reconstruction of the southern oscillation. *Bulletin of the American Meteorological Society* 79: 2137-2152.

Stokes, M., and Smiley, T.L. 1968. *An Introduction to Tree-Ring Dating.* The University of Chicago Press: Chicago.

Taylor, A.H., and Beaty, R.M. 2005. Climatic influences on fire regimes in the northern Sierra Nevada Mountains, Lake Tahoe Basin, Nevada, USA. *Journal of Biogeography* 32: 425-438.

Thompson, B. 1995. Stepwise regression and stepwise discriminant analysis need not apply here: A guideline editorial. *Educational and Psychological Measurement* 55: 525-534.

Thompson, D.W.J., and Wallace, J.M. 1998. The Arctic Oscillation signature in the wintertime geopotential height and temperature fields. *Geophysical Research Letters* 25: 1297-1300.

Thompson, D.W.J., and Wallace, J.M. 2000. Annual modes in the extratropical circulation. Part I: Month-to-month variability. *Journal of Climate* 13: 1000-1016.

Trenberth, K.E. 1997a. Short-term climate variations: Recent accomplishments and issues for future progress. *Bulletin of the American Meteorological Society* 78: 1081-1096.

Trenberth, K.E. 1997b. The definition of El Niño. *Bulletin of the American Meteorological Society* 78: 2771-2777.

Trenberth, K.E., and Hurrell, J.W. 1994. Decadal atmosphere-ocean variations in the Pacific. *Climate Dynamics* 9: 303-319.

Trenberth, K.E., Caron, J.M., Stepaniak, D.P., and Worley, S. 2002. Evolution of El Niño-Southern Oscillation and global atmospheric surface temperatures. *Journal of Geophysical Research-Atmospheres* 107: doi:10.1029/2000JD000298

Tuller, S. 2001. Climate. In *British Columbia, The Pacific Province: Geographical Essays.* Edited by Wood, C.. Canadian Western Geographical Series 36, Western Geographical Press: Victoria, B.C: 45-63.

Verdon, D.C., and Franks, S.W. 2006. Long-term behaviours of ENSO: Interactions with the PDO over the past 400 years inferred from paleoclimate records. *Geophysical Research Letters* 33: doi:10.1029/2005GL025052.

Vincent, L.A. 1998. A technique for the identification of inhomogeneities in Canadian temperature series. *Journal of Climate* 11: 1094-1104.

Vincent, L., and Gullett, D. 1999. Canadian historical and homogeneous temperature datasets for climate change analyses. *International Journal of Climatology* 19: 1375-1388.

Watson, E., and Luckman, B.H. 2005. Spatial patterns of preinstrumental moisture variability in the southern Canadian Cordillera. *Journal of Climate* 18: 2847-2863.

Weather Network. 2006. *Prince Rupert Statistics* [online]. Available from http://www.theweathernetwork.com/weather/stats/pages/C02100.htm [cited October 11 2006]

Wiles, G.C., D'Arrigo, R.D., and Jocoby, G. 1998. Gulf of Alaska atmosphere-ocean variability over recent centuries inferred from coastal tree-ring records. *Climatic Change* 38: 289-306.

Wilmking, M., and Juday, G.P. 2005. Longitudinal variation of radial growth at Alaska's northern treeline - Recent changes and possible scenarios for the 21st century. *Global and Planetary Change* 47 : 282-300.

Woodward, A. 1998. Relationship among environmental variables and the distribution of tree species at high elevation in the Olympic Mountains. *Northwest Science* 72: 10-22.

Woodward, A., Silsbee, D.G., Schreiner, E.G., and Means, J.E. 1994. Influence of climate on radial growth and cone production in subalpine fir (*Abies lasiocarpa*) and mountain hemlock (*Tsuga mertensiana*). *Canadian Journal of Forest Research* 24: 1133-1143.

Yarnal, B., and Diaz, H.F. 1986. Relationships between extremes of the Southern Oscillation and the winter climate of the Anglo-American Pacific coast. *Journal of Climatology* 6: 197-219.

Zhang, Q.B., and Hebda, R.J. 2005. Abrupt climate change and variability in the past four millennia of the southern Vancouver Island, Canada. *Geophysical Research Letters* 32: doi:10.1029/2005GL022913

Appendix A - Köppen Climatic Regions of Canada

(Adopted from Natural Resources Canada "The Atlas of Canada" http://atlas.nrcan.gc.ca/site/english/maps/archives/3rdedition/environment/climate/030?w=3&h=3&l=2&r=0&c=0 - accessed on August 10, 2006).

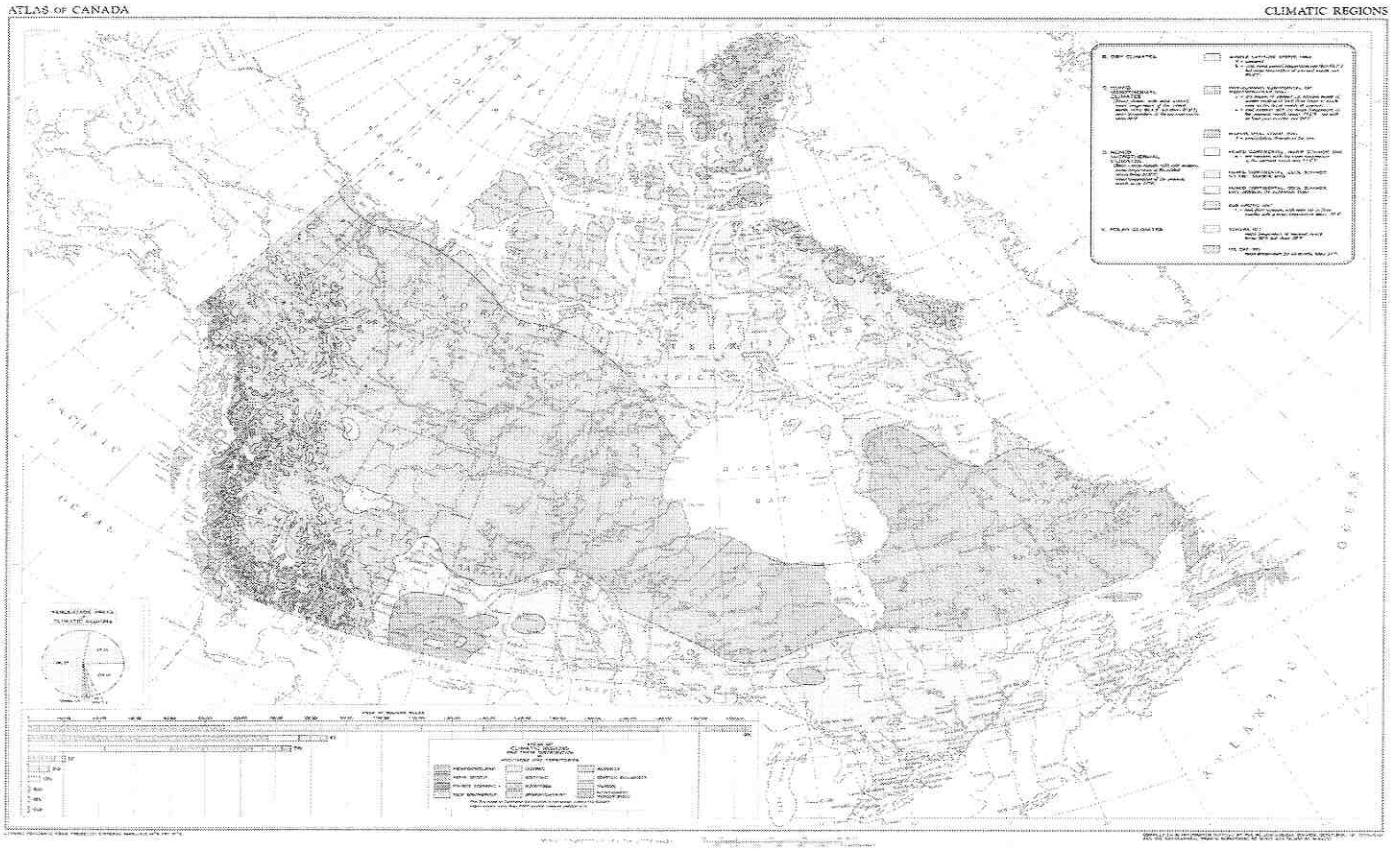

Appendix B - Biogeoclimatic Ecosystem Classification (BEC) Zones Along the Study Transect

(Adopted from the Ministry of Forests BEC web program http://www.for.gov.bc.ca/HRE/becweb/index.html - accessed on August 10, 2006)

Zones	Range	Soils	Common Vegetation
Coastal Western Hemlock (CWH)	South - Sea level to 1000m North – Sea level to 300m	Podzolic soils derived from coarse textured morainal, colluvial, glaciofluvial and marine parent materials	**Hypermaritime**: western hemlock, western redcedar, Sitka spruce, yellow cedar, salal (*Gaultheria shallon*), lanky moss (*Rhytidialdelphus loreus*)
			Maritime: western hemlock, western redcedar, Sitka spruce, yellow cedar, Douglas-fir and amabilis fir, flat moss (*Plagiothecium undulatum*), pipecleaner moss (*Rhytidiopsis robusta*), oval-leaved blueberry (*Vaccinium ovalifolium*), and Oregon beaked moss (*Kindbergia oregana*)
			Submaritime: western hemlock, western redcedar, Douglas-fir and amabilis fir, electrified cat's tail moss (*Rhytiadelphus triquetrus*), Step moss (*Hylocomium splendens*), and five-leaved bramble (*Rubus pedatus*)
Mountain Hemlock (MH)	South - 900-1600m North – 300 – 900m	Podzols and Folisols	Mountain hemlock, amabilis fir, yellow cedar dominate. **Lower elevations** - western redcedar, western hemlock, Sitka spruce, Douglas-fir and western white pine. **Leeward part of the range** - subalpine fir occupies high elevation sites indicating the transition to a more continental climate.
Alpine Tundra (AT)	+1650m	Regosolic (undeveloped). Subject to frost heaving, solifluction and permafrost	Usually treeless with occasional groups in krummholtz form. Mountain heathers *(Phyllodoce spp and Cassiope spp.)*, numerous species of sedge (*Carex spp*), arrow-leaved groundsel (*Senecio triangularis*), arctic lupine (*Lupinus arcticus*), arnica (*Arnica spp.*), indian hellebore (*Viratrum viride*), western pasqueflower (*Anenome occidentalis*), white marsh marigold (*Caltha leptosepala*), paintbrush (*Castilleja spp*) and subalpine buttercup *(Ranunculus eshscholtzii*).

Zones	Range	Soils	Common Vegetation
Engelmann Spruce – Subalpine Fir (ESSF)	North - 900-1700m	Podzolic soils and thick Mor humus forms	Subalpine fir, Engelmann spruce and lodgepole pine, black huckleberry, white-flowered rhododendron, false azalea (*Menziesia ferruginnea*), oak fern (*Gymnocarpium dryopteris*) and Sitka valerian (*Valeriana sitchensis*).

Appendix C - Annual and Seasonal Temperature and Precipitation Trends

Data is from the Environment Canada's Adjusted Historical Canadian Climate Data Set. The straight line in each of the records is the trendline.

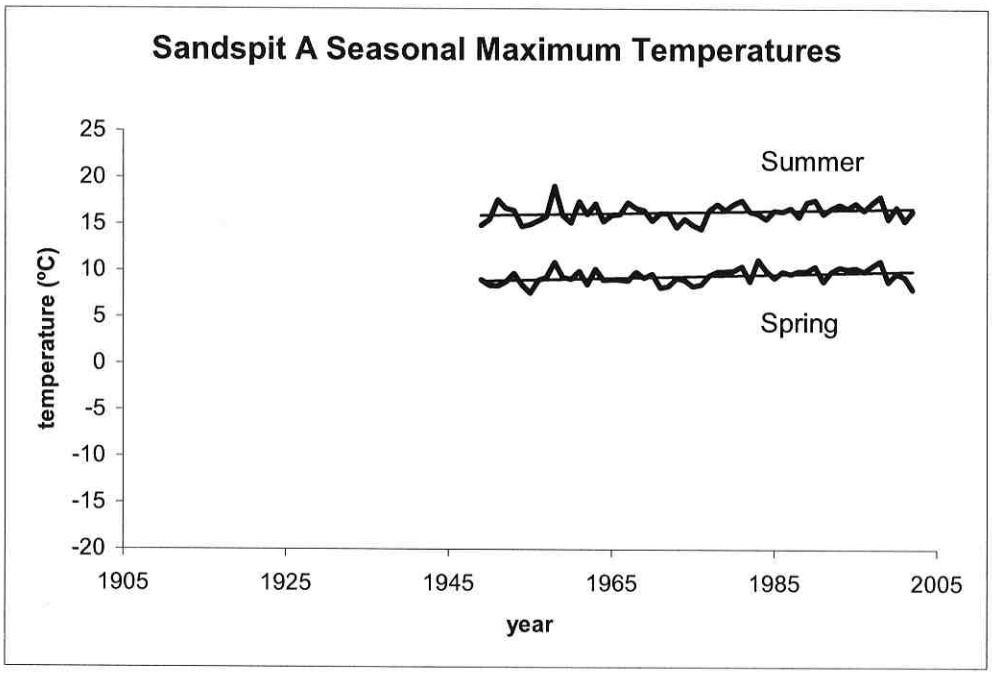

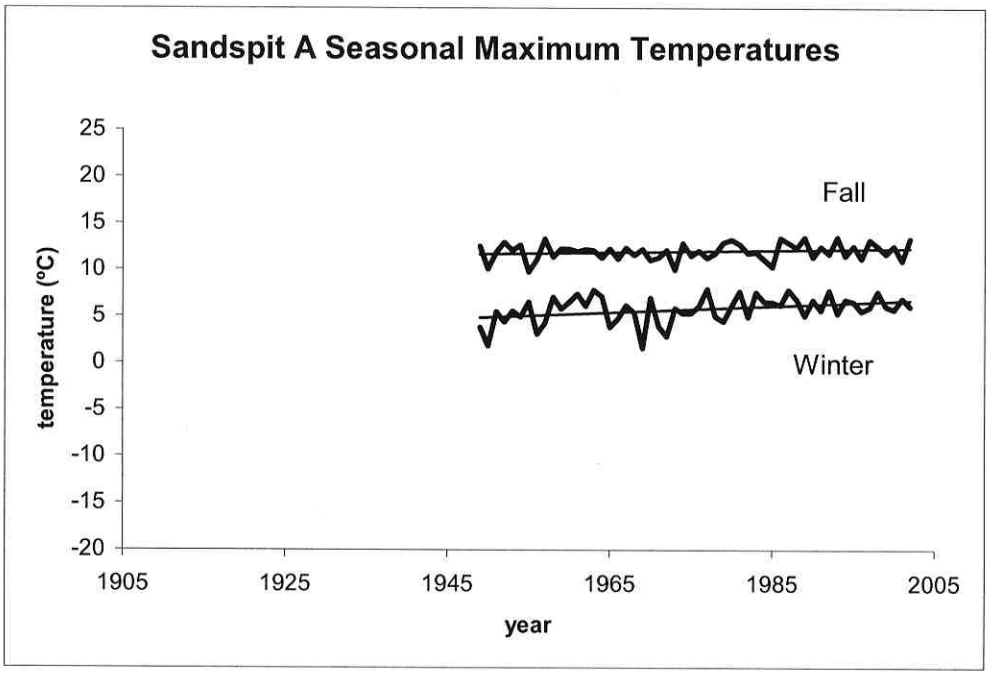

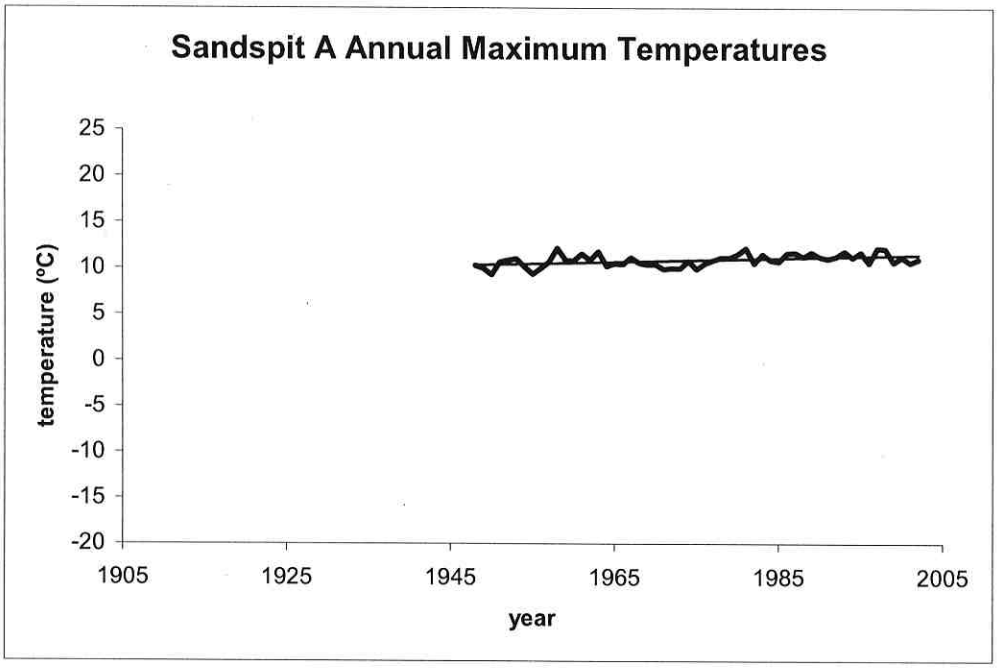
Sandspit A Annual Maximum Temperatures
temperature (°C)
25
20
15
10
5
0
-5
-10
-15
-20
1905
1925
1945
1965
1985
2005
year

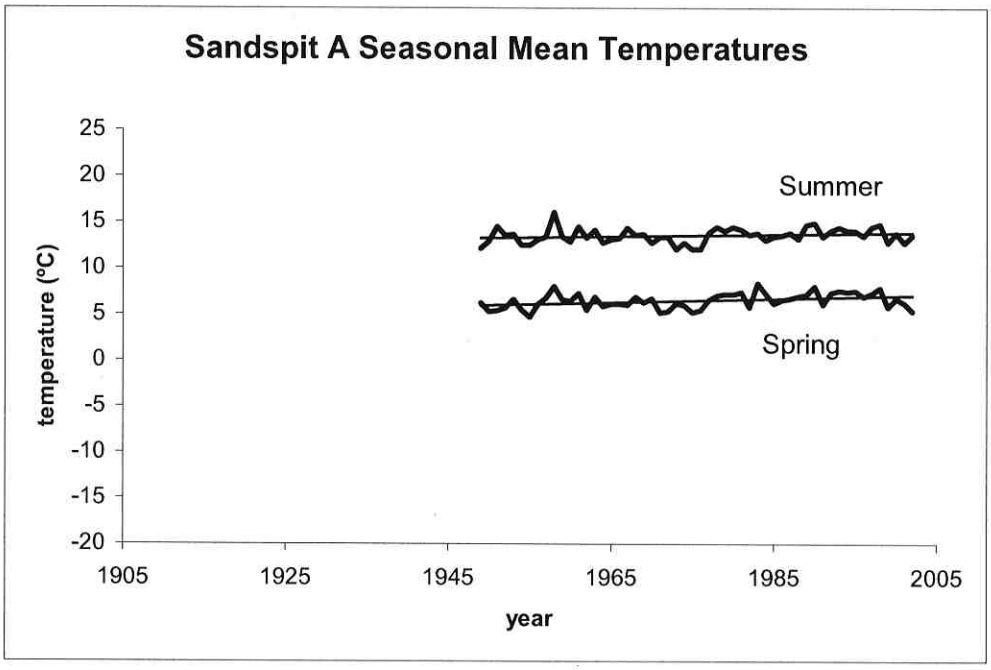
Sandspit A Seasonal Mean Temperatures
temperature (°C)
25
20
15
10
5
0
-5
-10
-15
-20
1905
1925
1945
1965
1985
2005
year
Summer
Spring

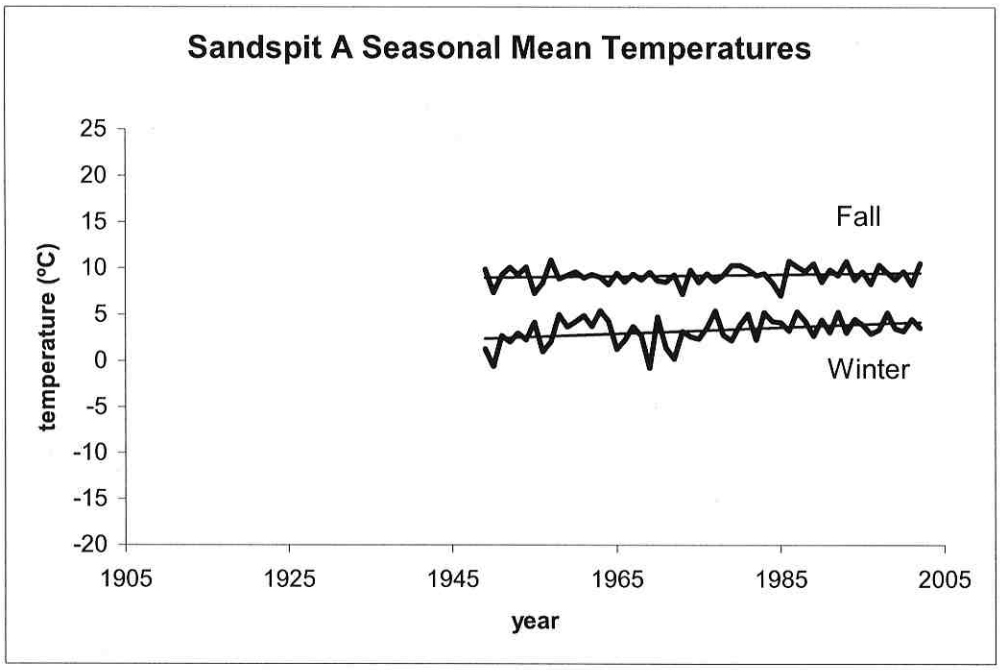
Sandspit A Seasonal Mean Temperatures
temperature (°C)
25
20
15
10
5
0
-5
-10
-15
-20
1905
1925
1945
1965
1985
2005
year
Fall
Winter

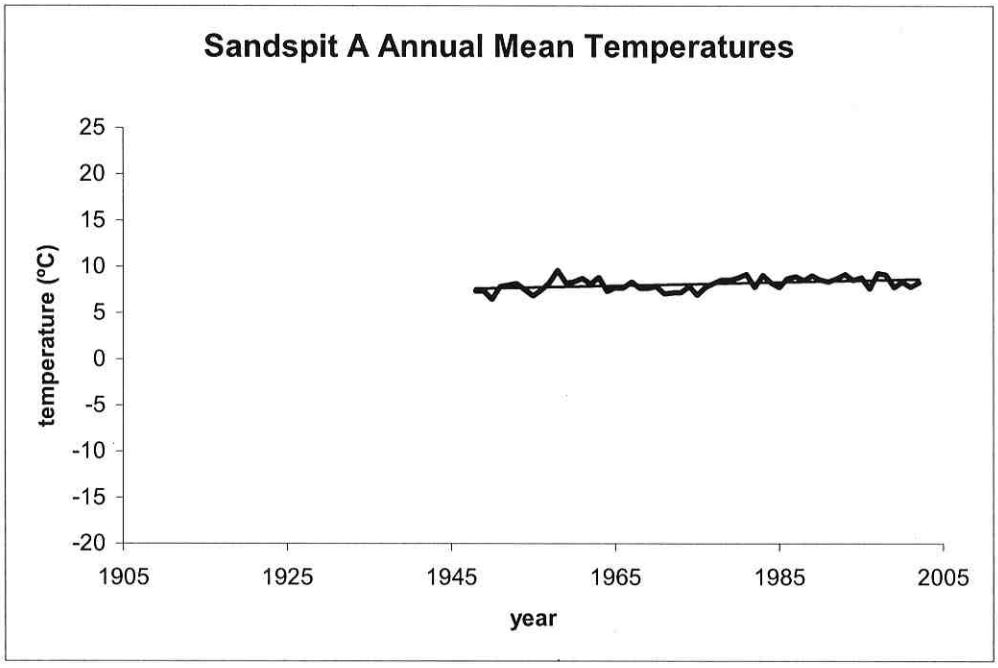
Sandspit A Annual Mean Temperatures
temperature (°C)
25
20
15
10
5
0
-5
-10
-15
-20
1905
1925
1945
1965
1985
2005
year

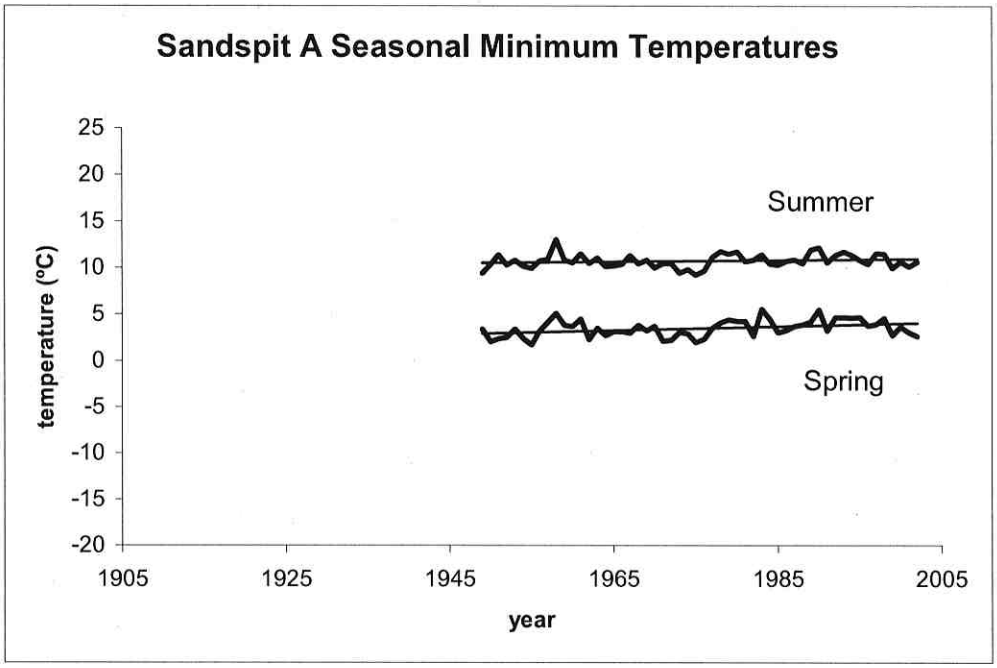
Sandspit A Seasonal Minimum Temperatures
25
20
15
10
5
0
-5
-10
-15
-20
temperature (°C)
Summer
Spring
1905
1925
1945
1965
1985
2005
year

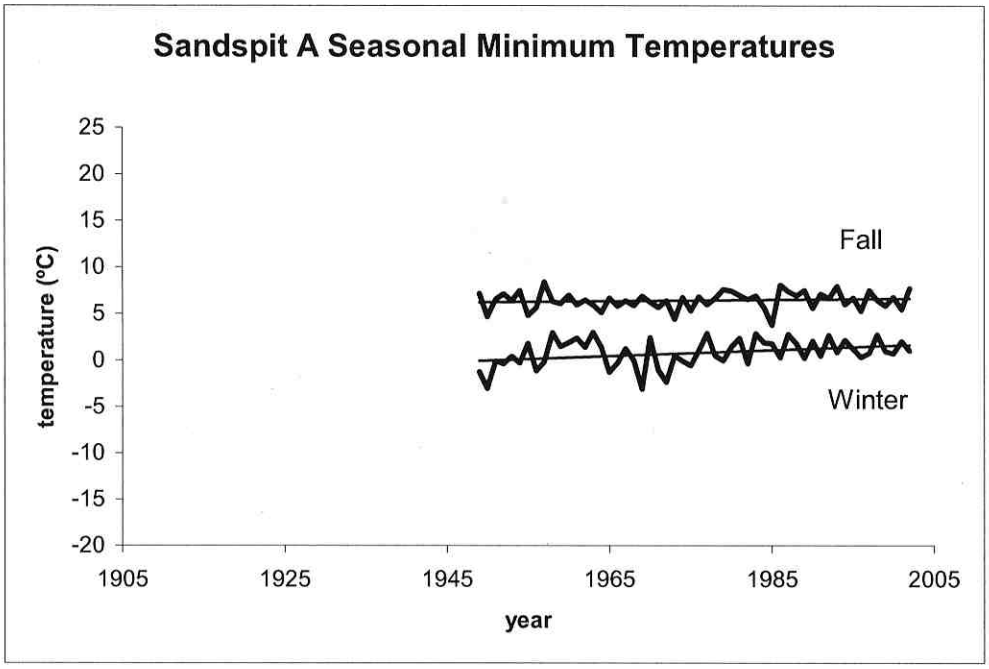
Sandspit A Seasonal Minimum Temperatures
25
20
15
10
5
0
-5
-10
-15
-20
temperature (°C)
Fall
Winter
1905
1925
1945
1965
1985
2005
year

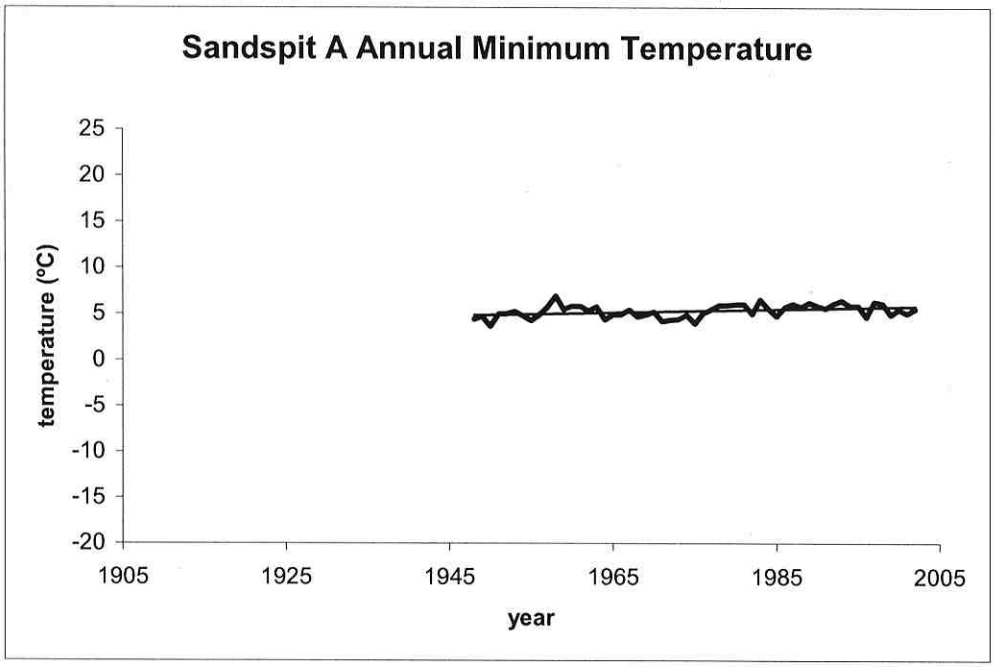
Sandspit A Annual Minimum Temperature
temperature (°C)
25
20
15
10
5
0
-5
-10
-15
-20
1905
1925
1945
1965
1985
2005
year

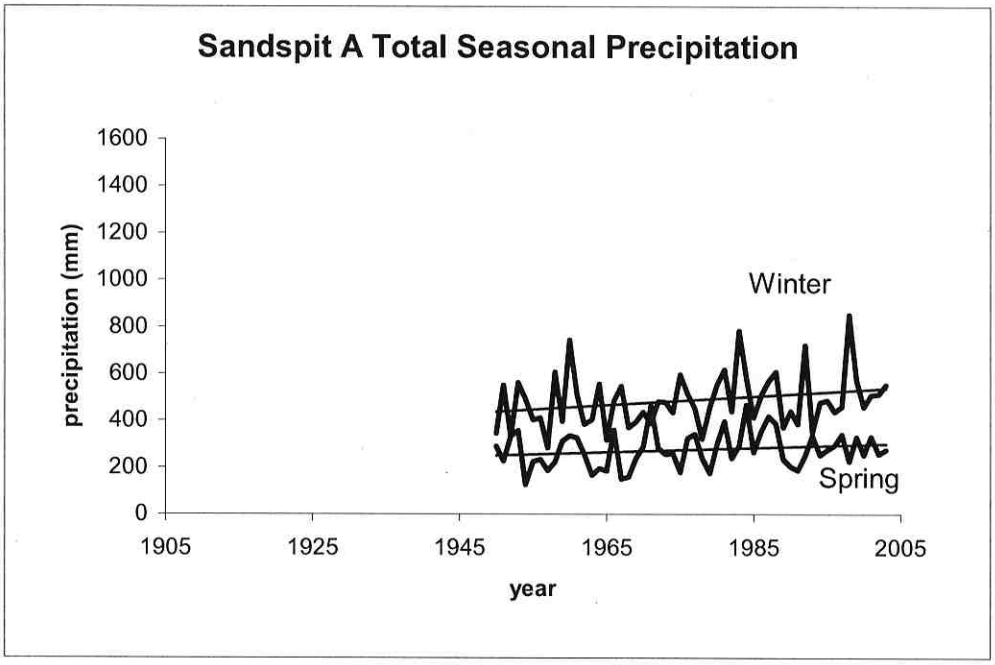
Sandspit A Total Seasonal Precipitation
precipitation (mm)
1600
1400
1200
1000
800
600
400
200
0
Winter
Spring
1905
1925
1945
1965
1985
2005
year

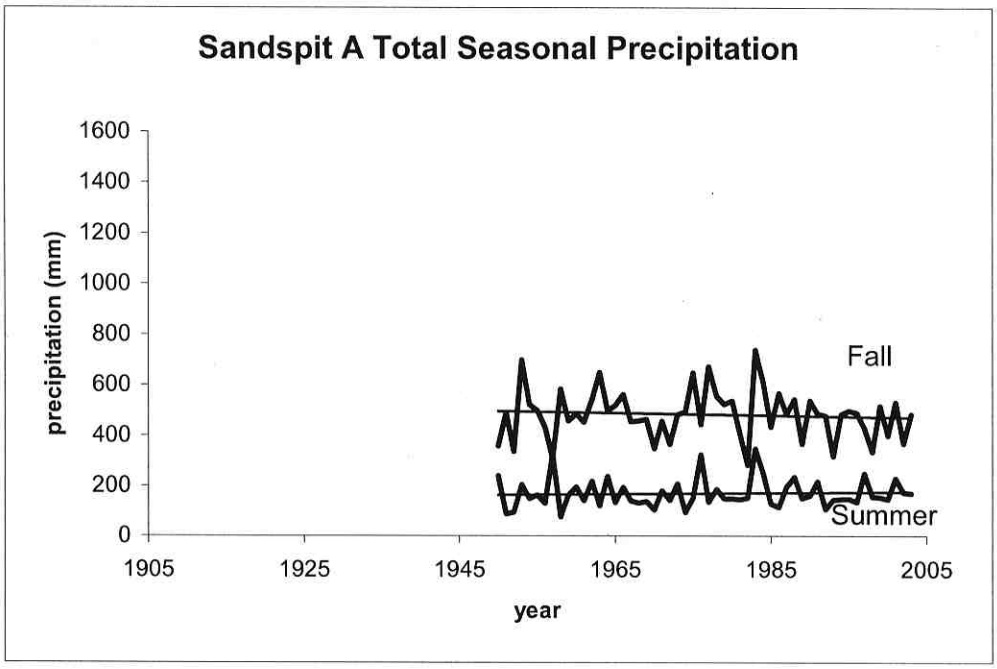
Sandspit A Total Seasonal Precipitation
precipitation (mm)
1600
1400
1200
1000
800
600
400
200
0
1905
1925
1945
1965
1985
2005
year
Fall
Summer

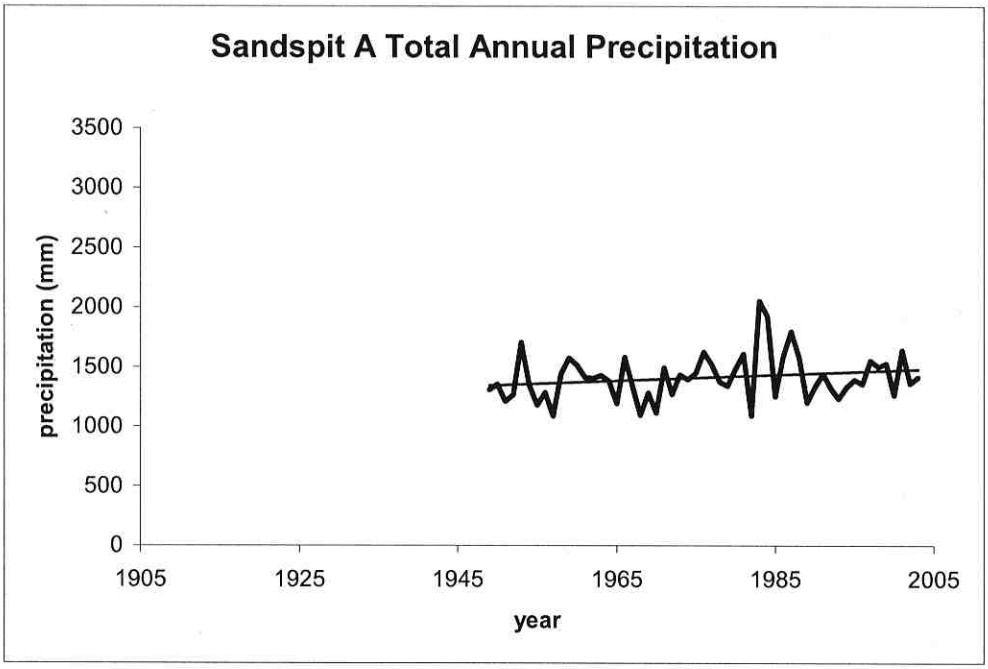
Sandspit A Total Annual Precipitation
precipitation (mm)
3500
3000
2500
2000
1500
1000
500
0
1905
1925
1945
1965
1985
2005
year

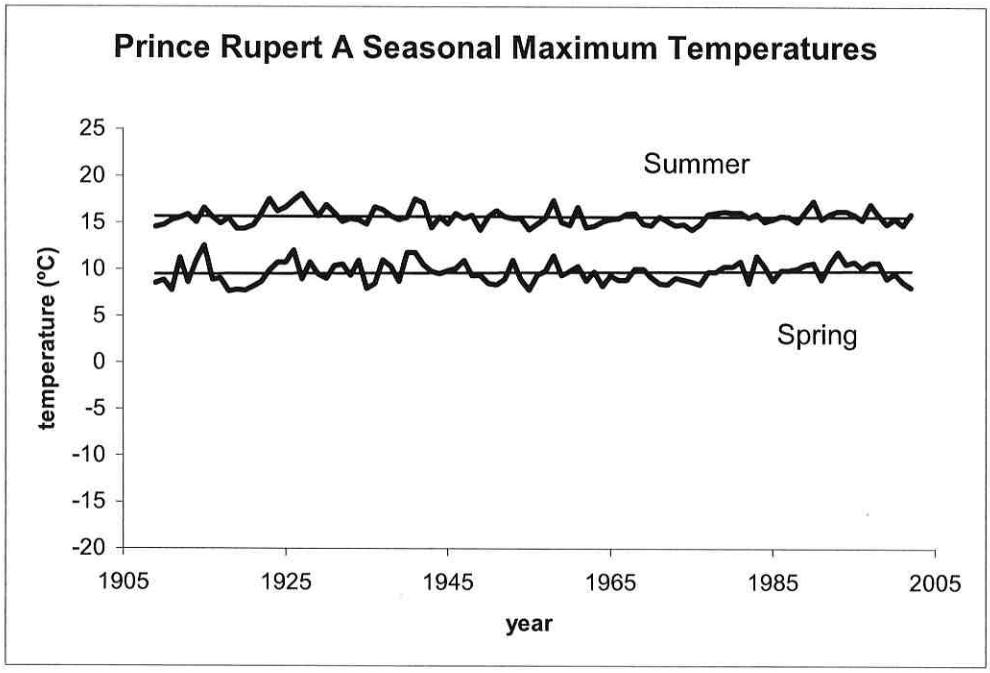
Prince Rupert A Seasonal Maximum Temperatures
Summer
Spring
temperature (°C)
25
20
15
10
5
0
-5
-10
-15
-20
1905
1925
1945
1965
1985
2005
year

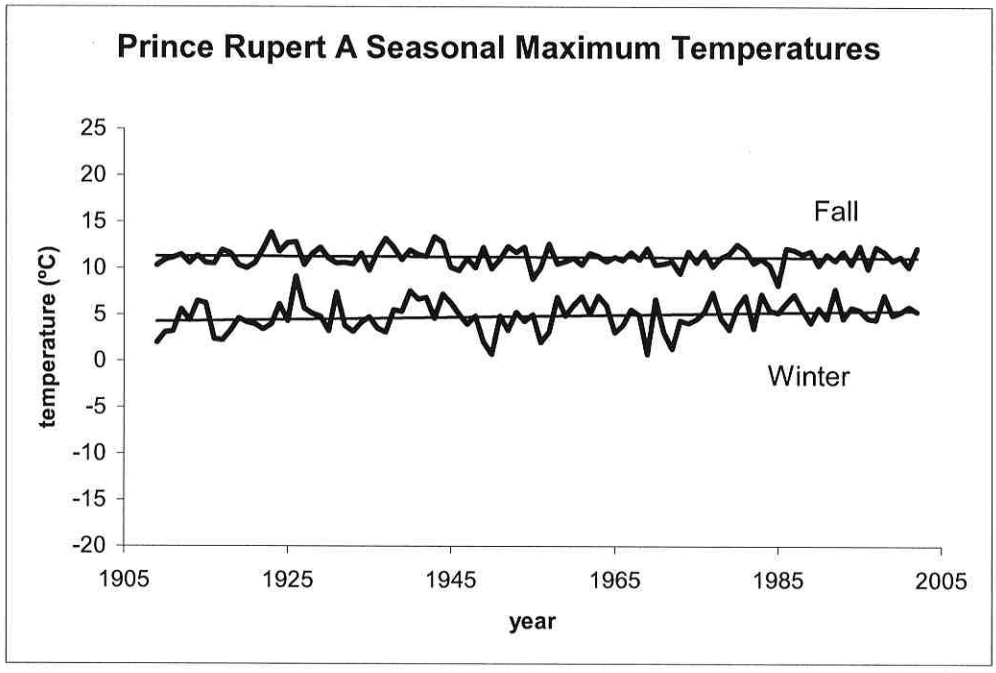
Prince Rupert A Seasonal Maximum Temperatures
Fall
Winter
temperature (°C)
25
20
15
10
5
0
-5
-10
-15
-20
1905
1925
1945
1965
1985
2005
year

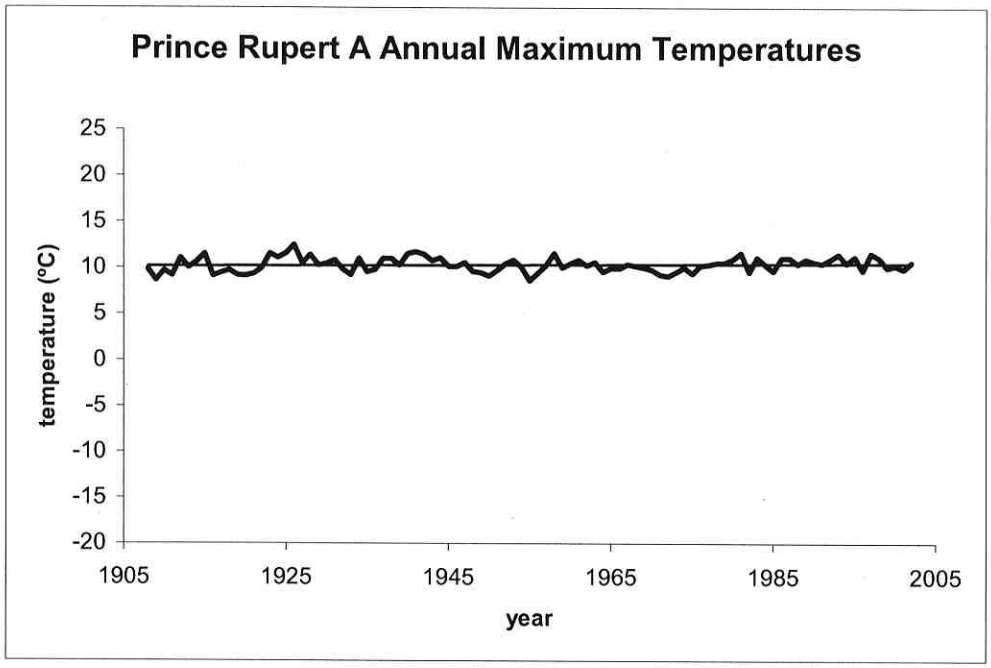
Prince Rupert A Annual Maximum Temperatures
temperature (°C)
25
20
15
10
5
0
-5
-10
-15
-20
1905
1925
1945
1965
1985
2005
year

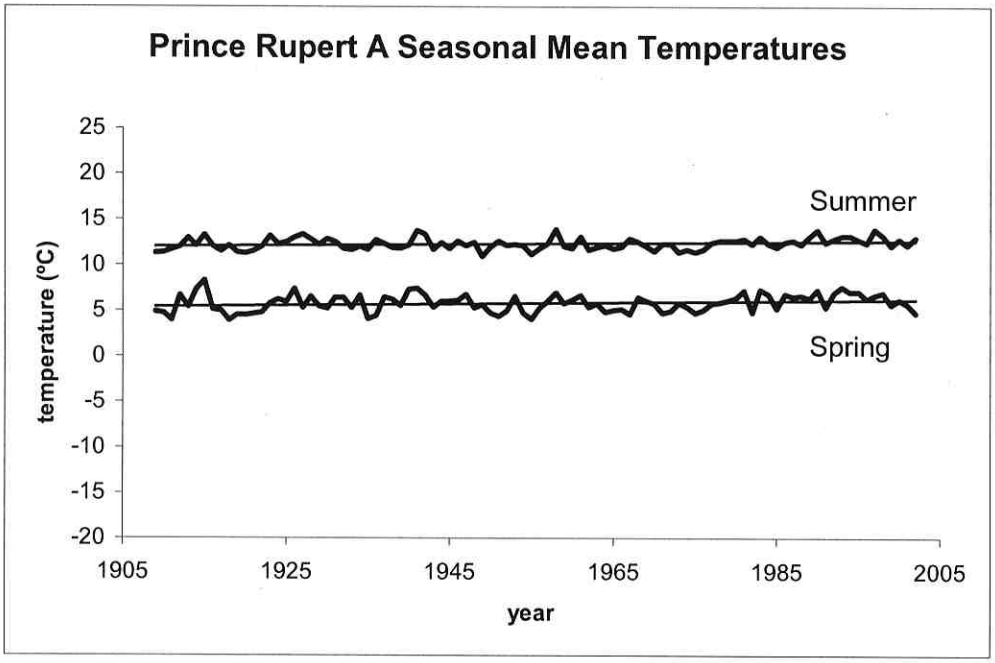
Prince Rupert A Seasonal Mean Temperatures
temperature (°C)
25
20
15
10
5
0
-5
-10
-15
-20
Summer
Spring
1905
1925
1945
1965
1985
2005
year

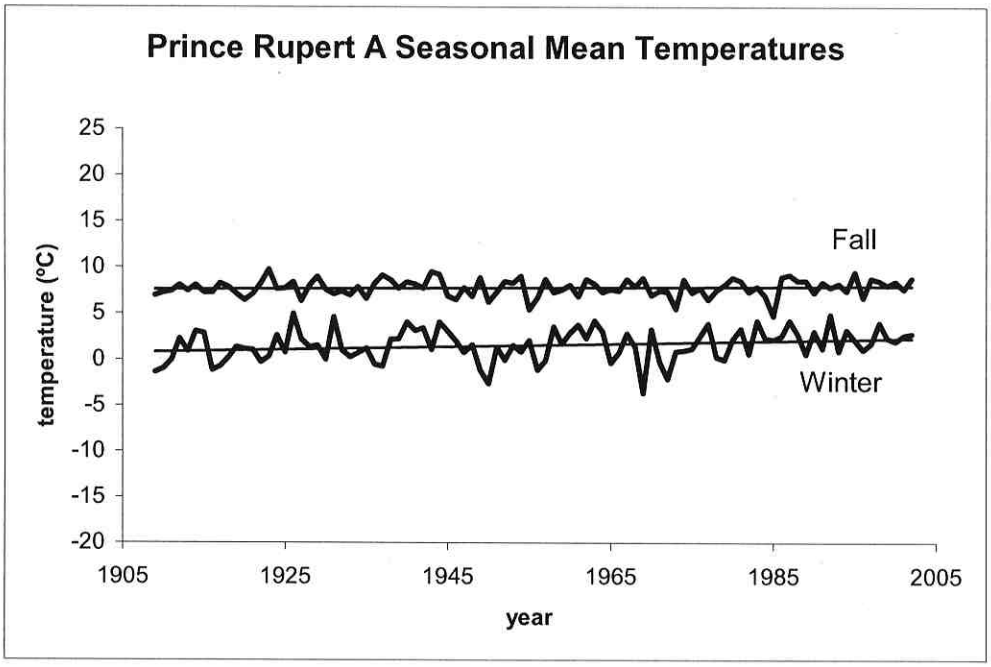
Prince Rupert A Seasonal Mean Temperatures
temperature (°C)
25
20
15
10
5
0
-5
-10
-15
-20
1905
1925
1945
1965
1985
2005
year
Fall
Winter

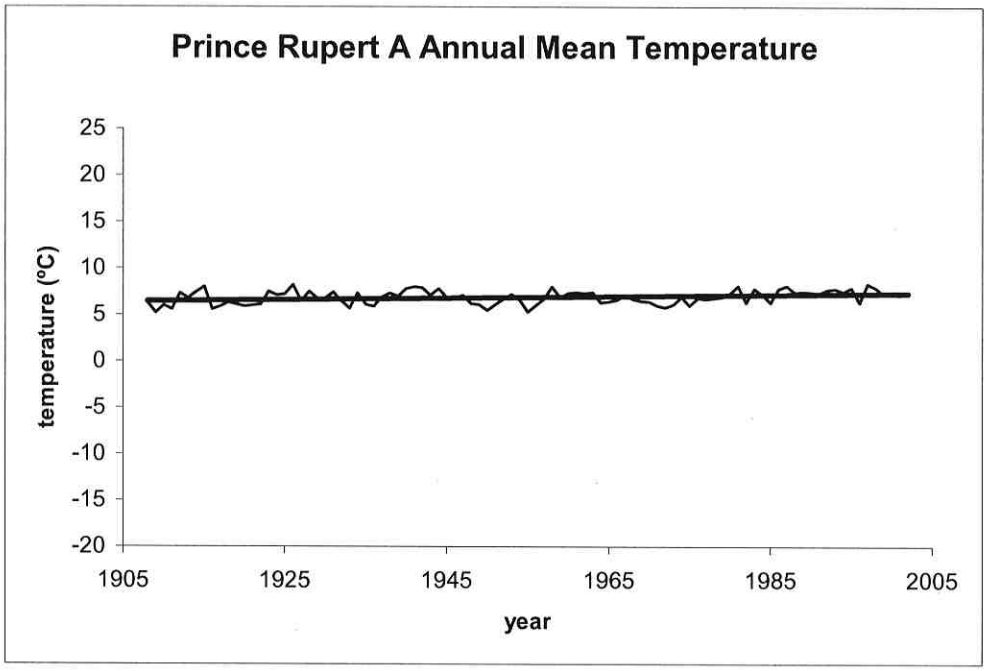
Prince Rupert A Annual Mean Temperature
temperature (°C)
25
20
15
10
5
0
-5
-10
-15
-20
1905
1925
1945
1965
1985
2005
year

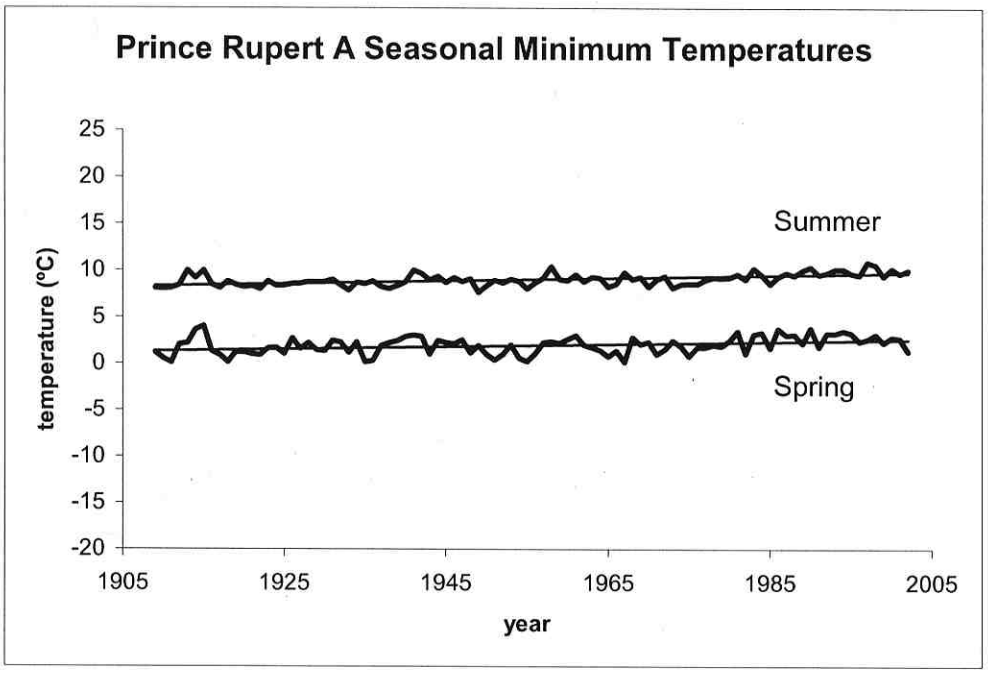
Prince Rupert A Seasonal Minimum Temperatures
temperature (°C)
25
20
15
10
5
0
-5
-10
-15
-20
1905
1925
1945
1965
1985
2005
year
Summer
Spring

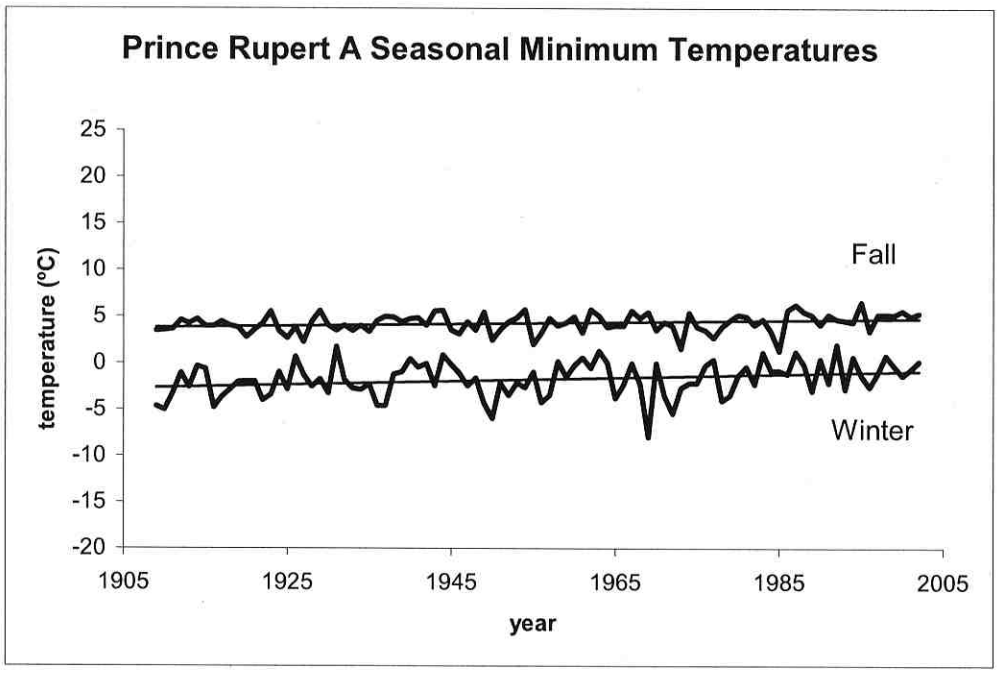
Prince Rupert A Seasonal Minimum Temperatures
temperature (°C)
25
20
15
10
5
0
-5
-10
-15
-20
1905
1925
1945
1965
1985
2005
year
Fall
Winter

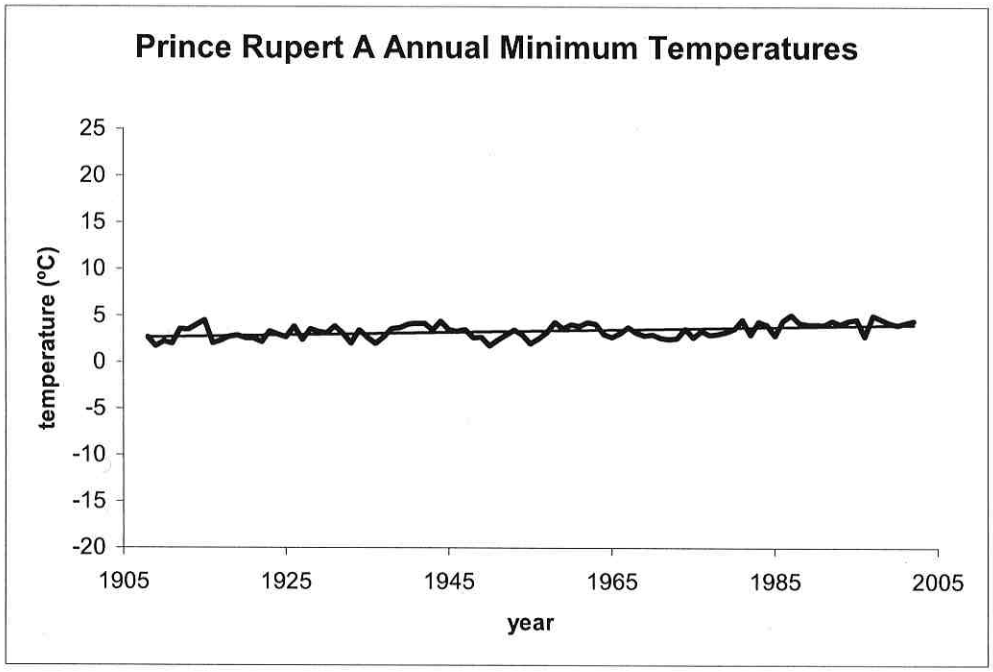
Prince Rupert A Annual Minimum Temperatures
temperature (°C)
25
20
15
10
5
0
-5
-10
-15
-20
1905
1925
1945
1965
1985
2005
year

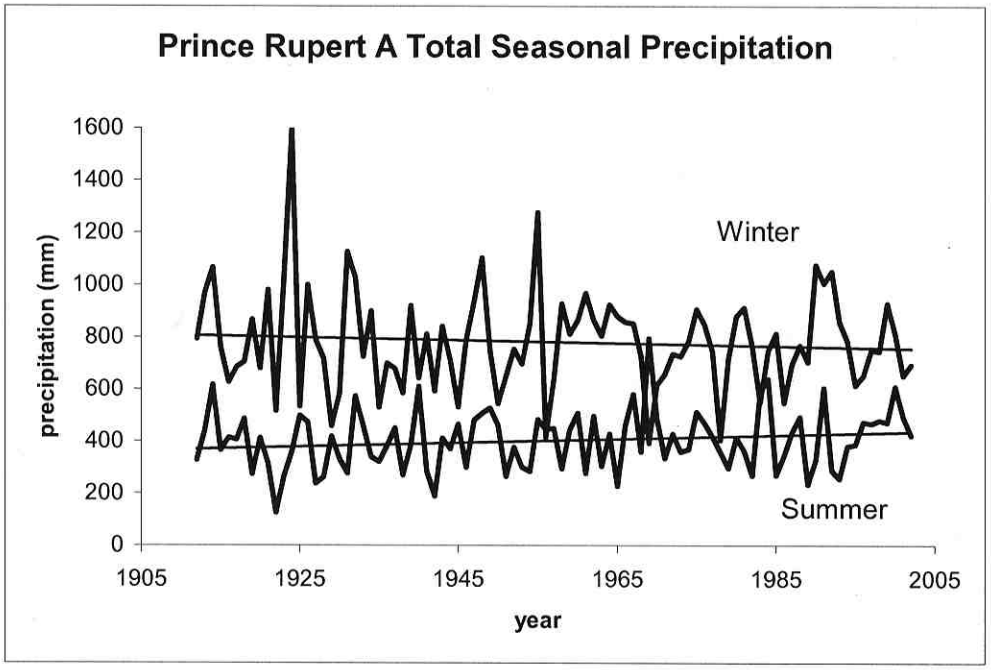
Prince Rupert A Total Seasonal Precipitation
precipitation (mm)
1600
1400
1200
1000
800
600
400
200
0
Winter
Summer
1905
1925
1945
1965
1985
2005
year

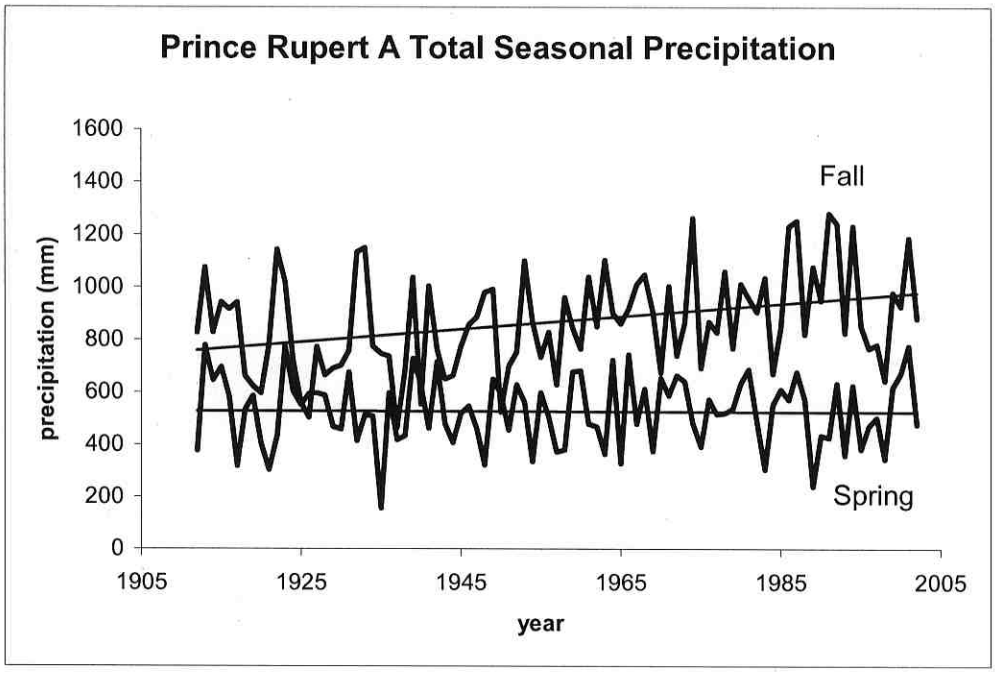
Prince Rupert A Total Seasonal Precipitation
precipitation (mm)
1600
1400
1200
1000
800
600
400
200
0
1905
1925
1945
1965
1985
2005
year
Fall
Spring

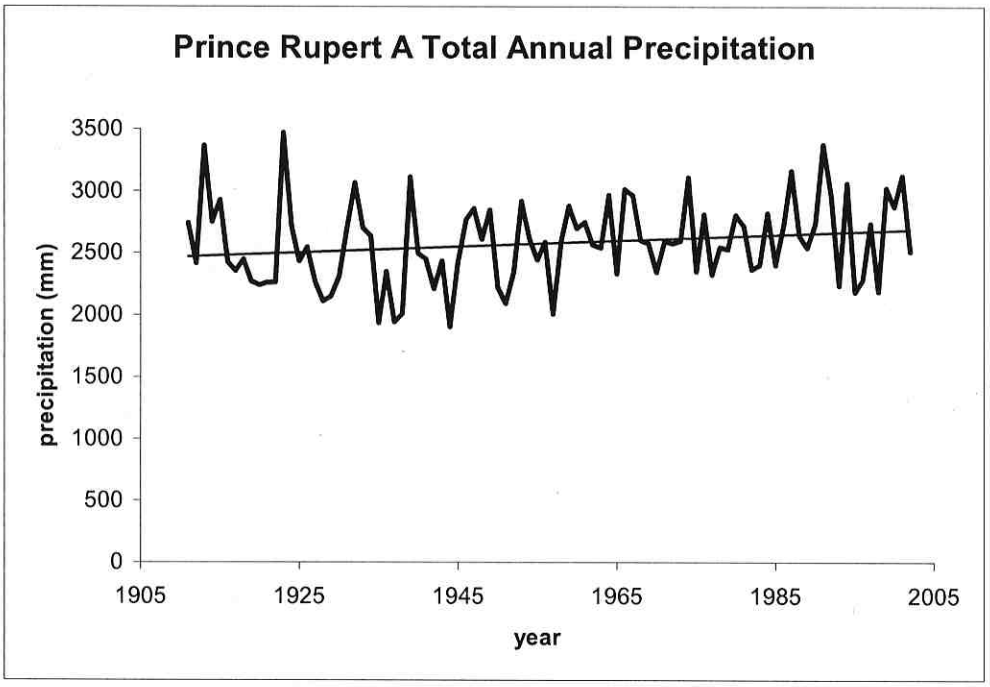
Prince Rupert A Total Annual Precipitation
precipitation (mm)
3500
3000
2500
2000
1500
1000
500
0
1905
1925
1945
1965
1985
2005
year

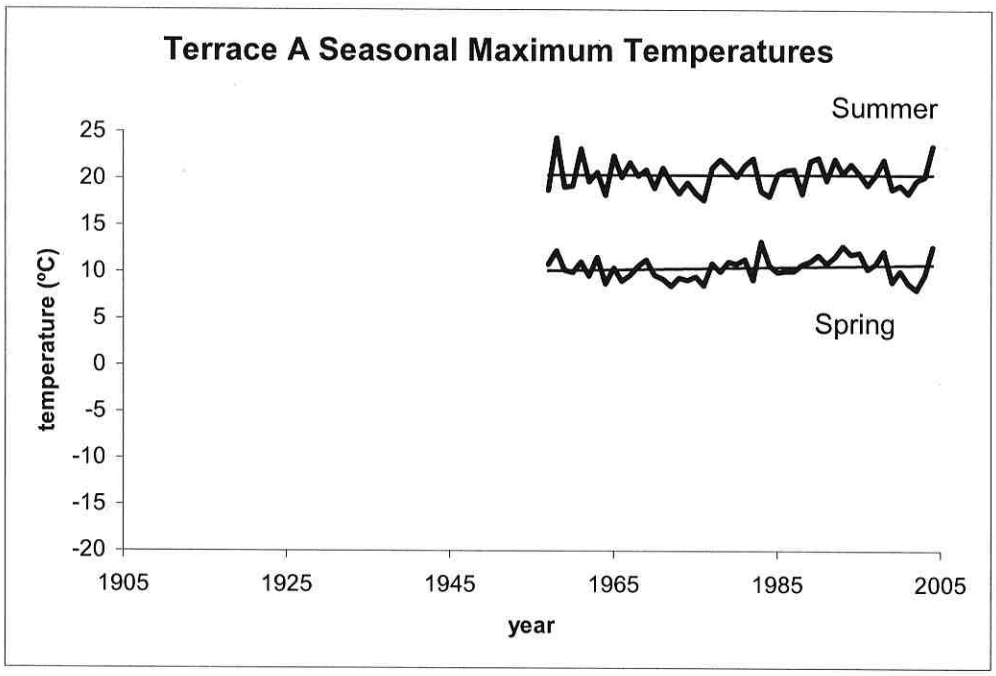
Terrace A Seasonal Maximum Temperatures
Summer
Spring
temperature (°C)
25
20
15
10
5
0
-5
-10
-15
-20
1905
1925
1945
1965
1985
2005
year

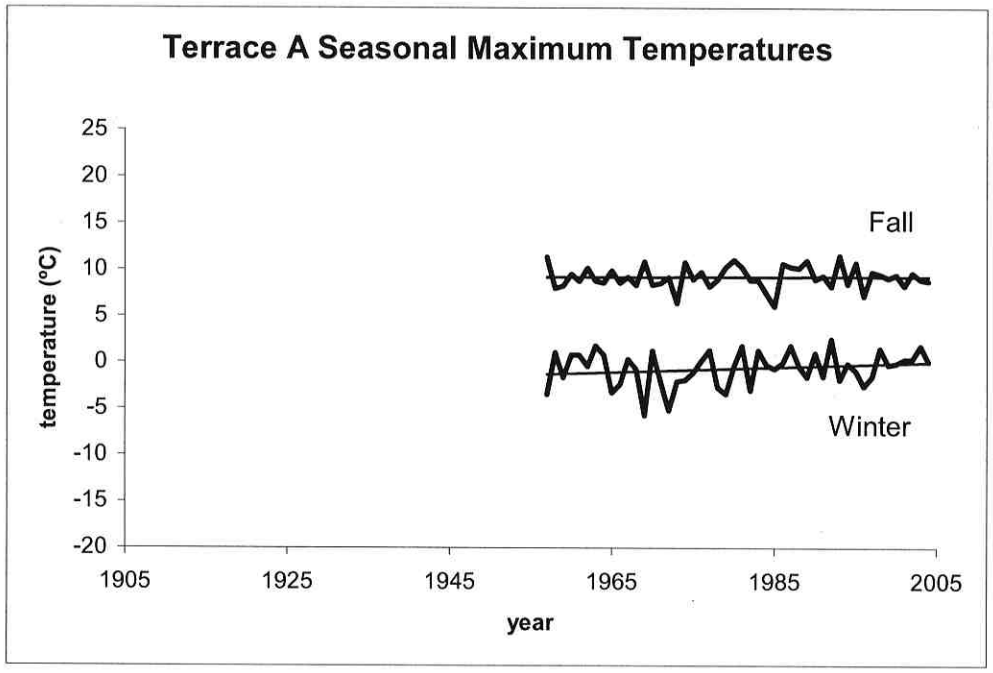
Terrace A Seasonal Maximum Temperatures
Fall
Winter
temperature (°C)
25
20
15
10
5
0
-5
-10
-15
-20
1905
1925
1945
1965
1985
2005
year

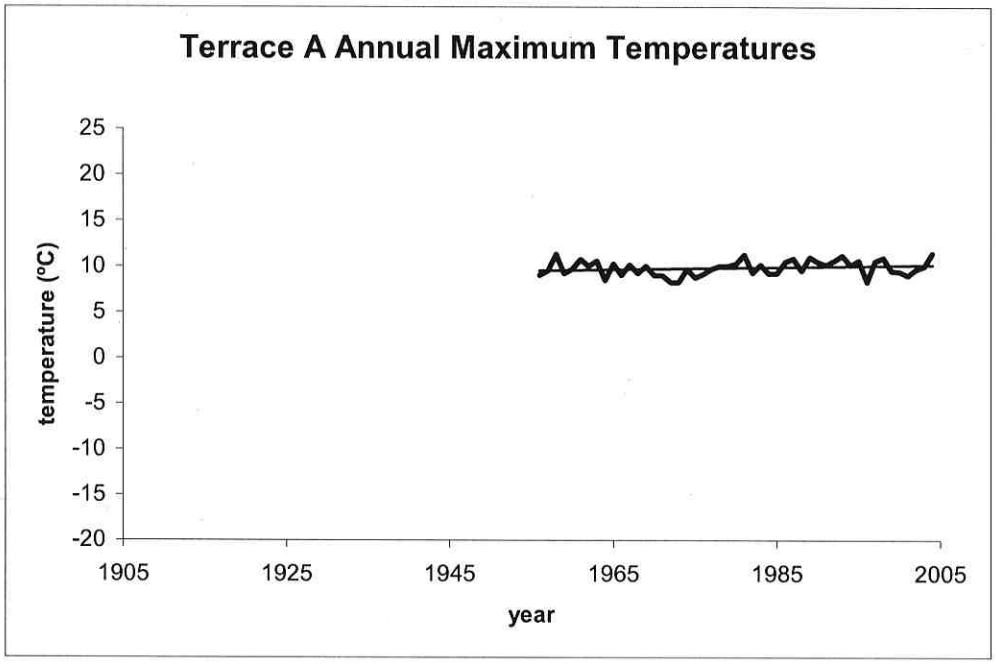
Terrace A Annual Maximum Temperatures
temperature (°C)
25
20
15
10
5
0
-5
-10
-15
-20
1905
1925
1945
1965
1985
2005
year

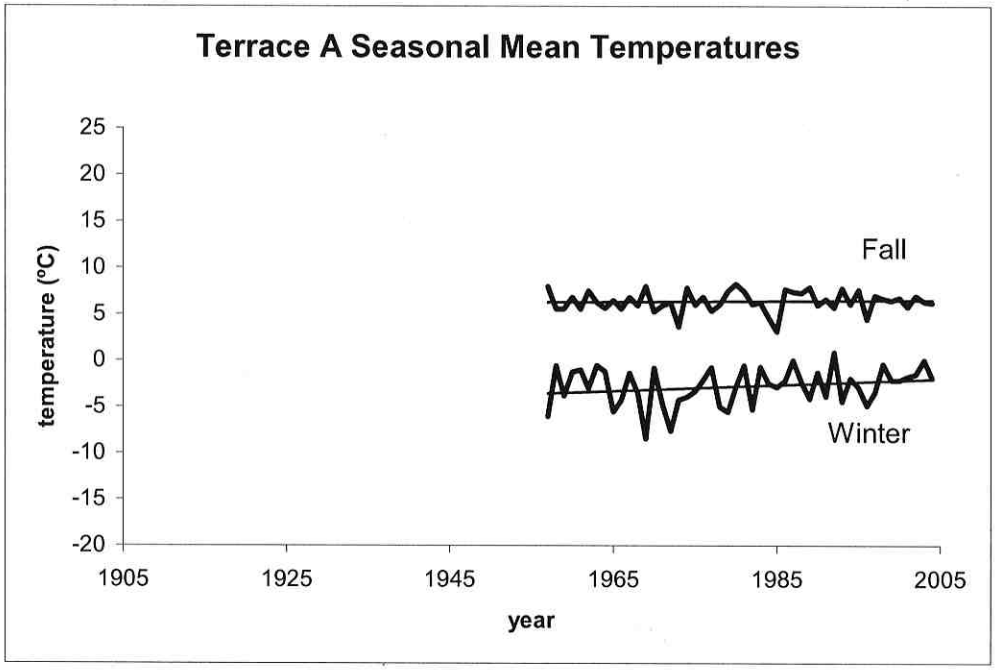
Terrace A Seasonal Mean Temperatures
temperature (°C)
25
20
15
10
5
0
-5
-10
-15
-20
1905
1925
1945
1965
1985
2005
year
Fall
Winter

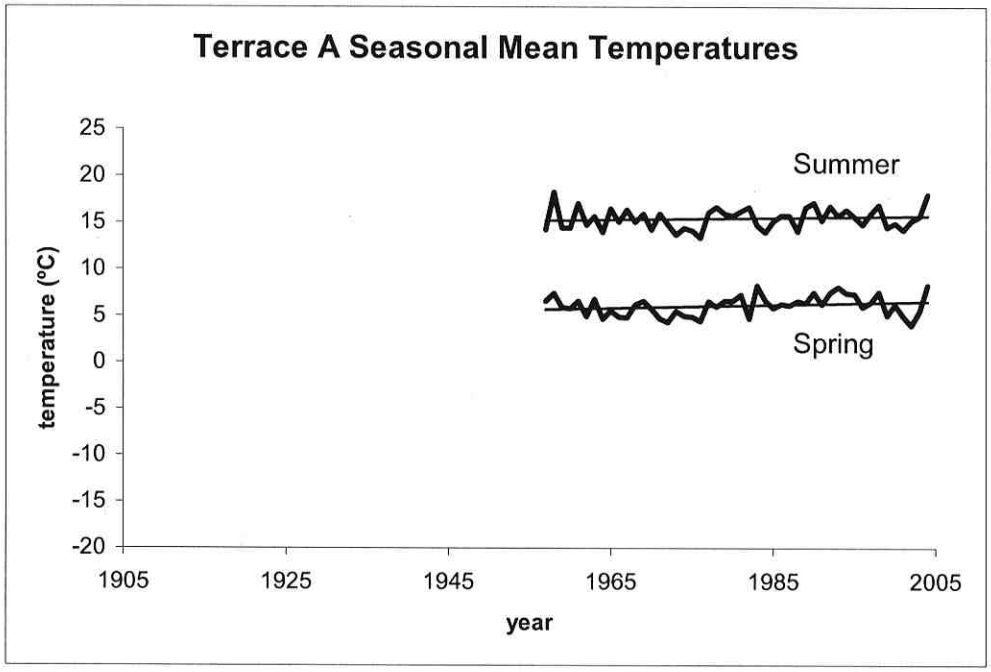
Terrace A Seasonal Mean Temperatures
25
20
15
10
5
0
-5
-10
-15
-20
temperature (°C)
Summer
Spring
1905
1925
1945
1965
1985
2005
year

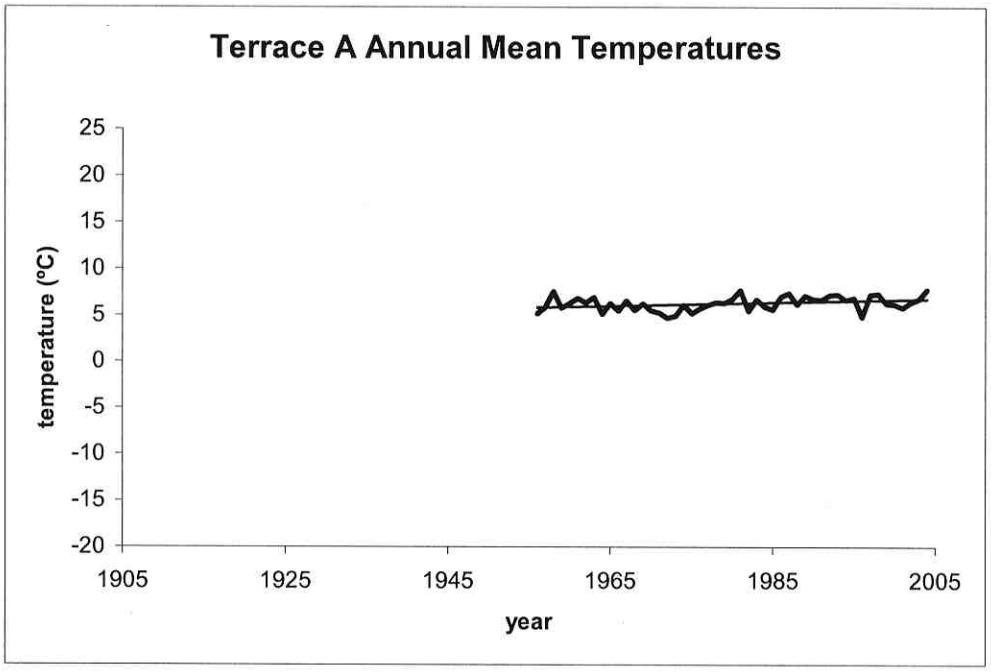
Terrace A Annual Mean Temperatures
25
20
15
10
5
0
-5
-10
-15
-20
temperature (°C)
1905
1925
1945
1965
1985
2005
year

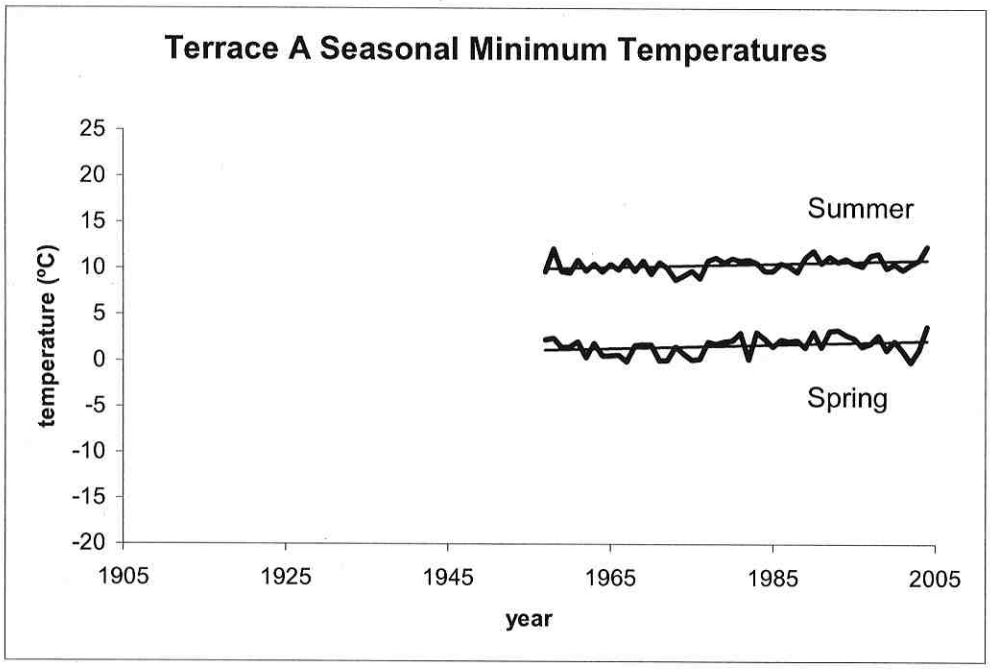
Terrace A Seasonal Minimum Temperatures
temperature (°C)
25
20
15
10
5
0
-5
-10
-15
-20
1905
1925
1945
1965
1985
2005
year
Summer
Spring

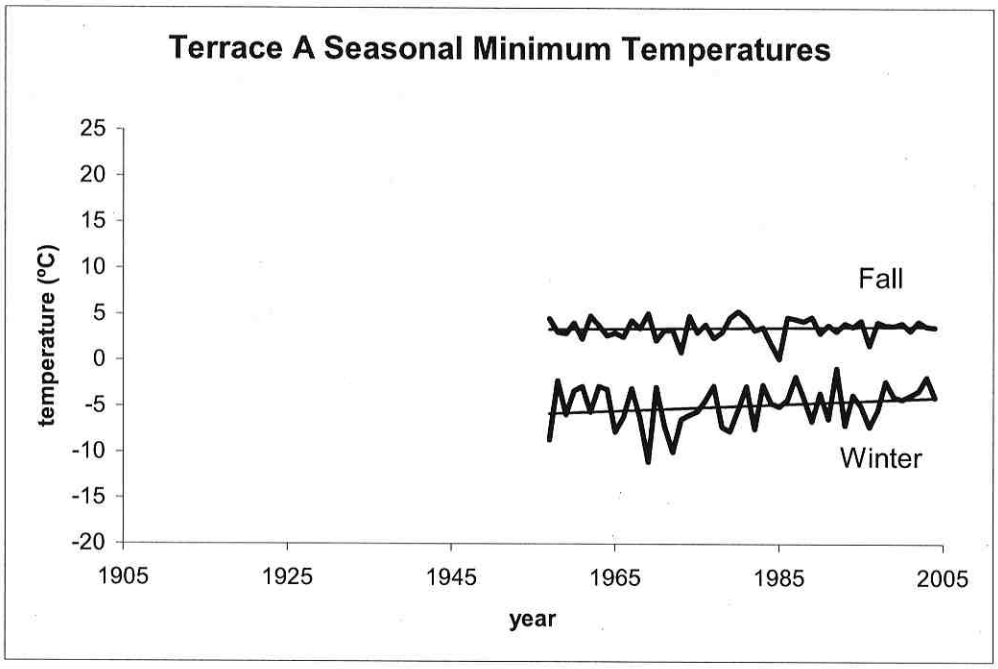
Terrace A Seasonal Minimum Temperatures
temperature (°C)
25
20
15
10
5
0
-5
-10
-15
-20
1905
1925
1945
1965
1985
2005
year
Fall
Winter

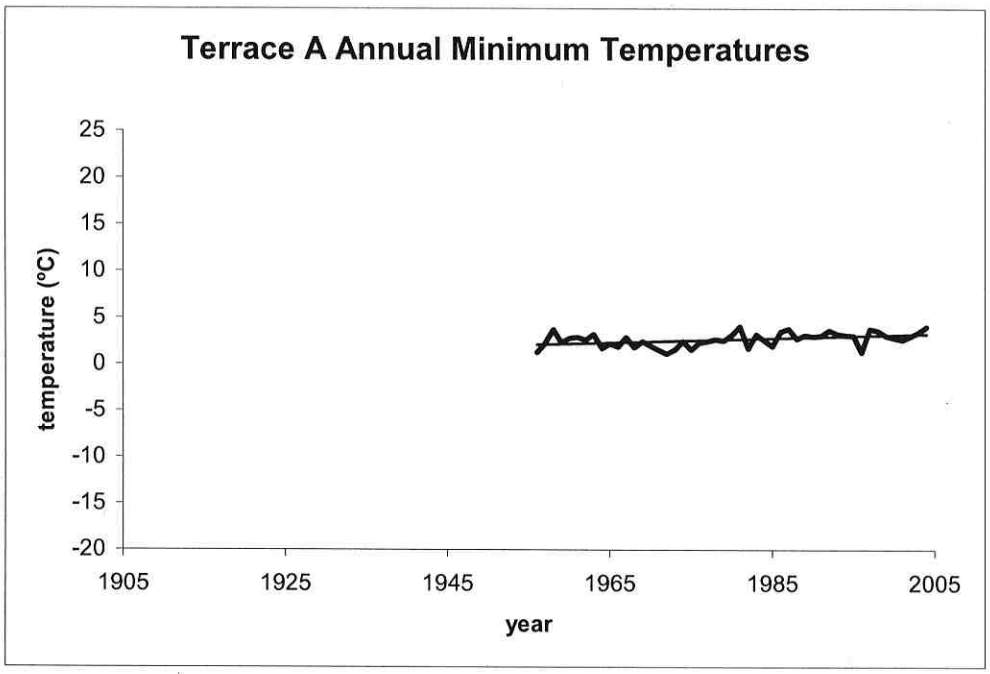
Terrace A Annual Minimum Temperatures
temperature (°C)
25
20
15
10
5
0
-5
-10
-15
-20
1905
1925
1945
1965
1985
2005
year

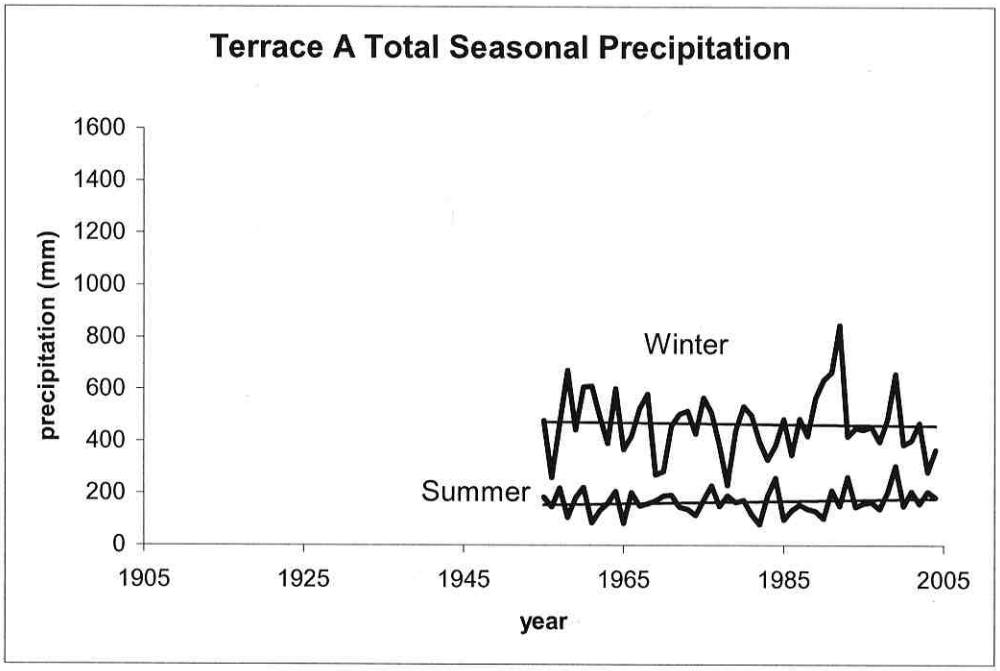
Terrace A Total Seasonal Precipitation
precipitation (mm)
1600
1400
1200
1000
800
600
400
200
0
Winter
Summer
1905
1925
1945
1965
1985
2005
year

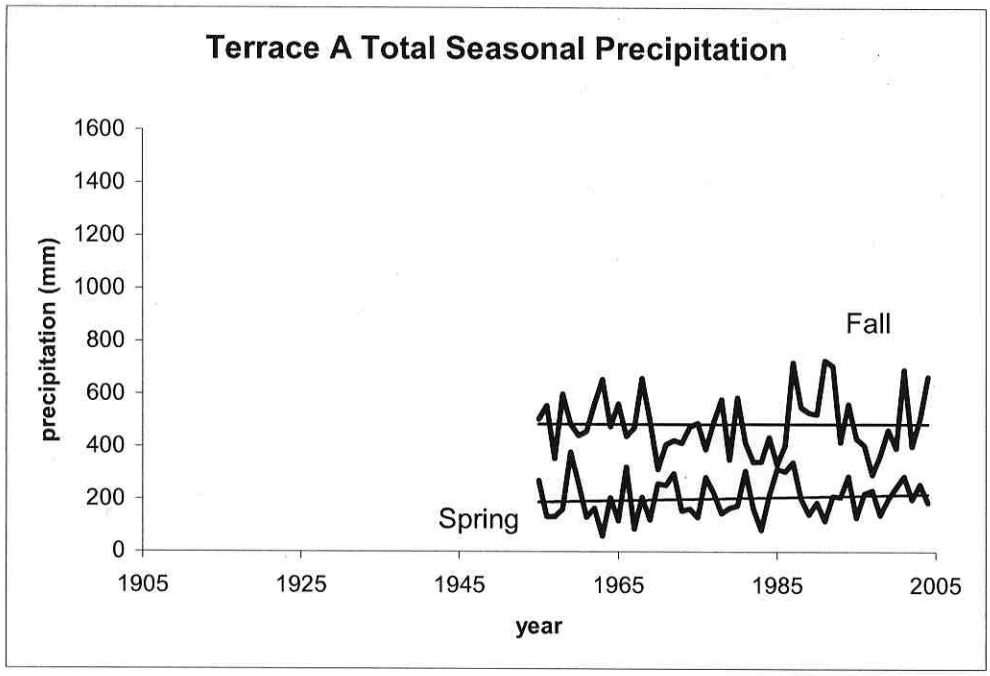
Terrace A Total Seasonal Precipitation
precipitation (mm)
1600
1400
1200
1000
800
600
400
200
0
Fall
Spring
1905
1925
1945
1965
1985
2005
year

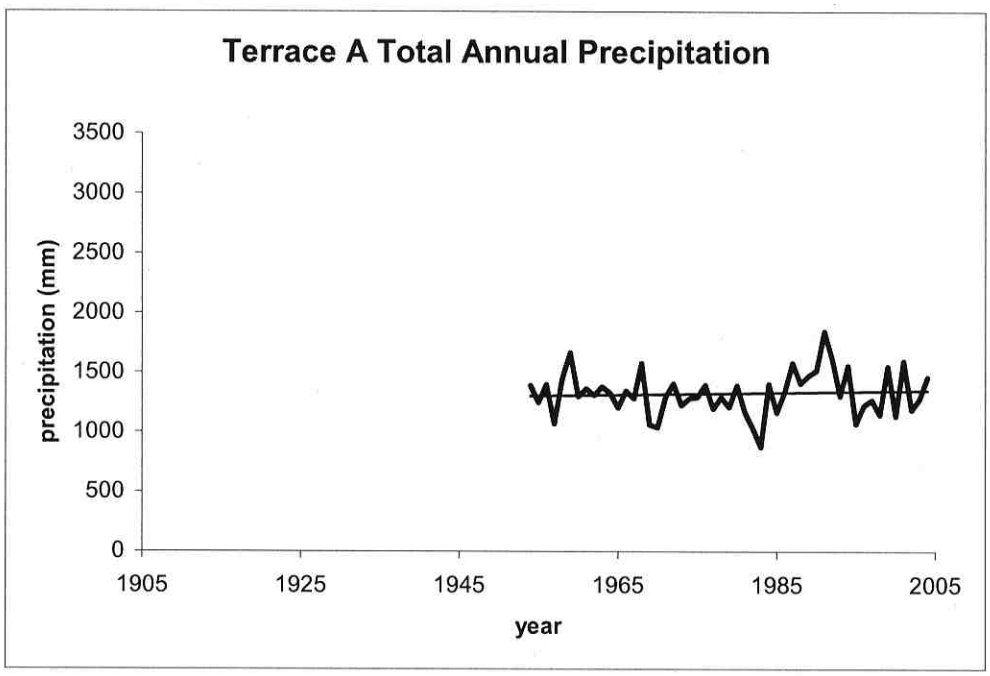
Terrace A Total Annual Precipitation
precipitation (mm)
3500
3000
2500
2000
1500
1000
500
0
1905
1925
1945
1965
1985
2005
year

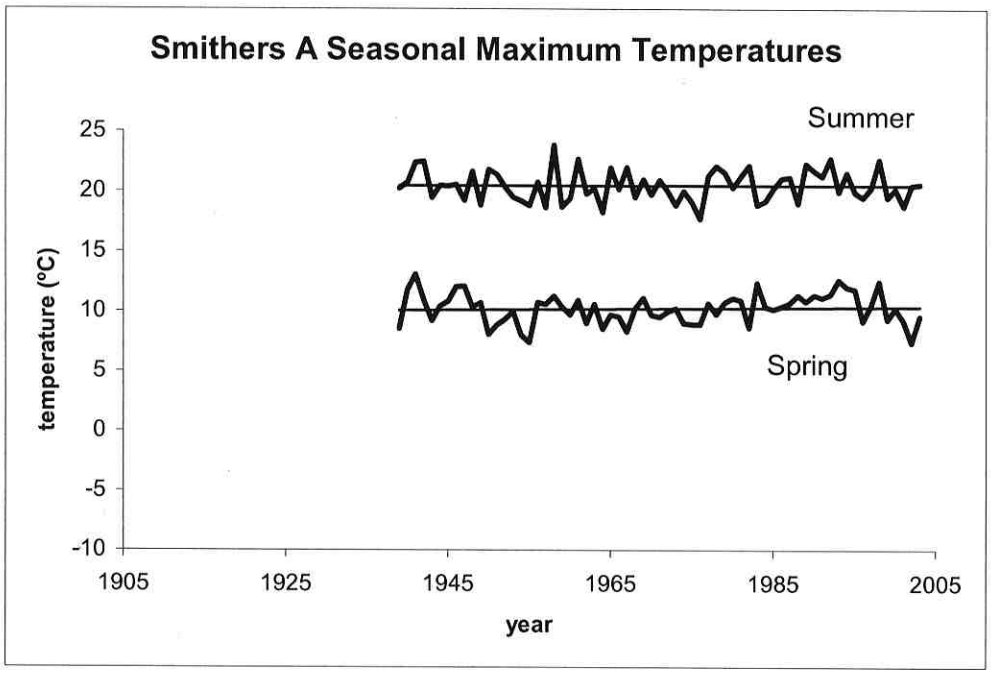
Smithers A Seasonal Maximum Temperatures
Summer
Spring
temperature (°C)
25
20
15
10
5
0
-5
-10
1905
1925
1945
1965
1985
2005
year

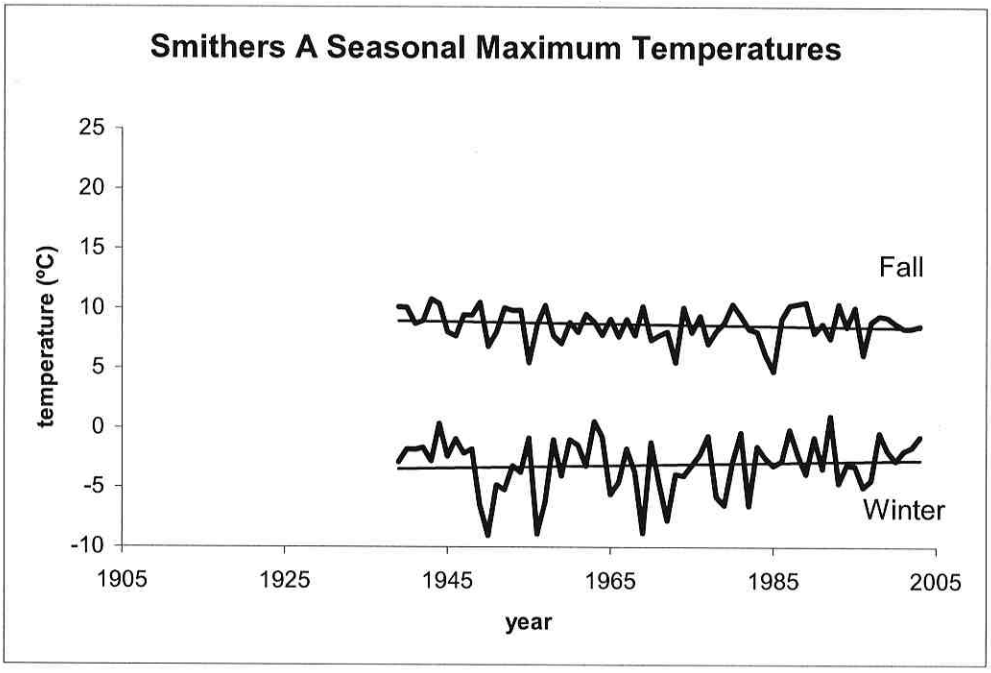
Smithers A Seasonal Maximum Temperatures
Fall
Winter
temperature (°C)
25
20
15
10
5
0
-5
-10
1905
1925
1945
1965
1985
2005
year

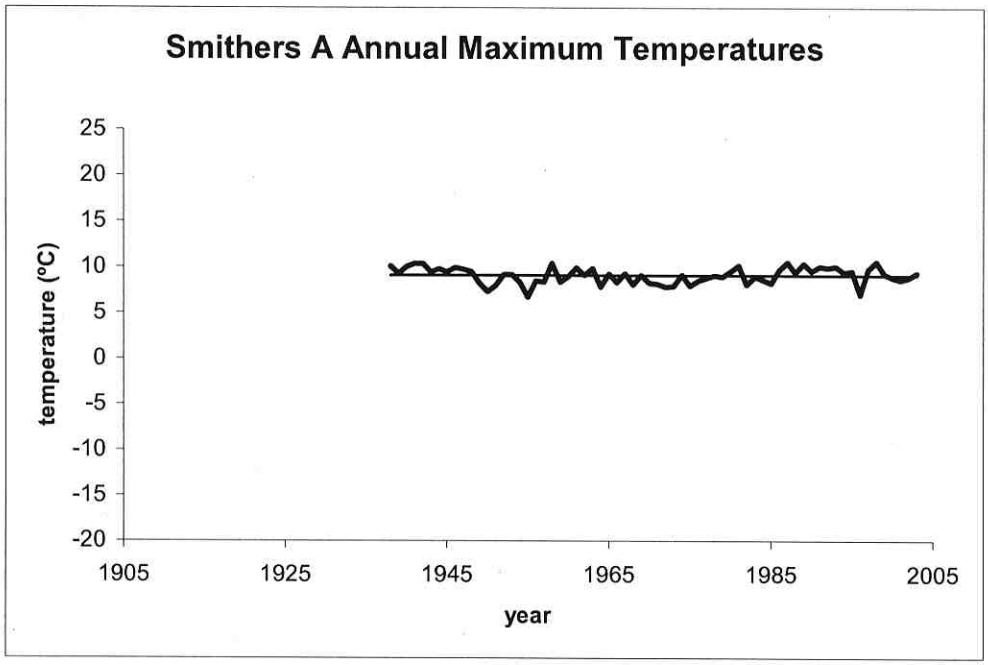
Smithers A Annual Maximum Temperatures
temperature (°C)
25
20
15
10
5
0
-5
-10
-15
-20
1905
1925
1945
1965
1985
2005
year

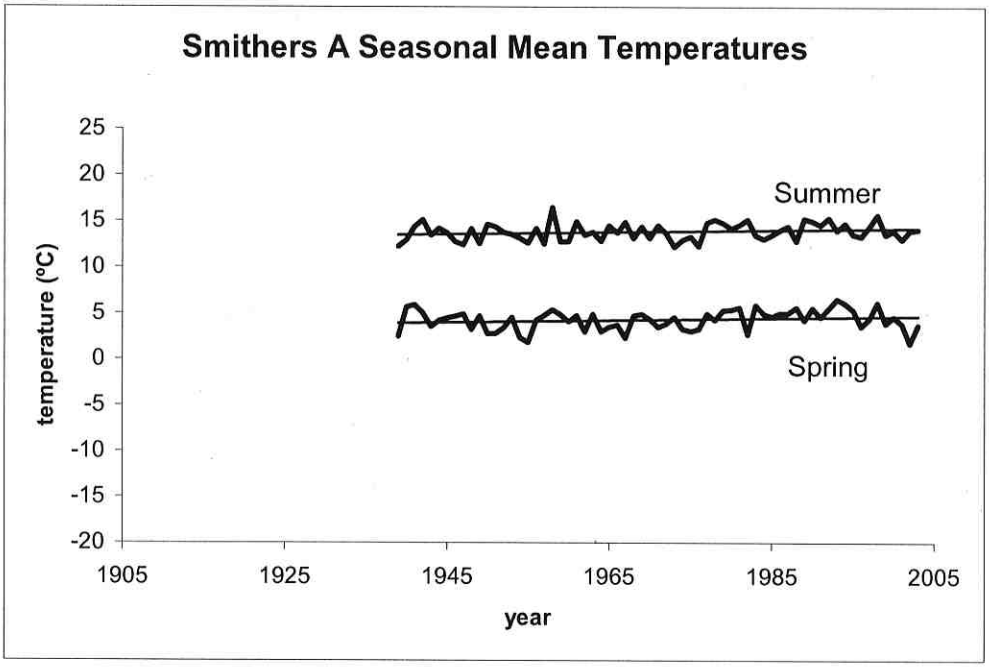
Smithers A Seasonal Mean Temperatures
temperature (°C)
25
20
15
10
5
0
-5
-10
-15
-20
Summer
Spring
1905
1925
1945
1965
1985
2005
year

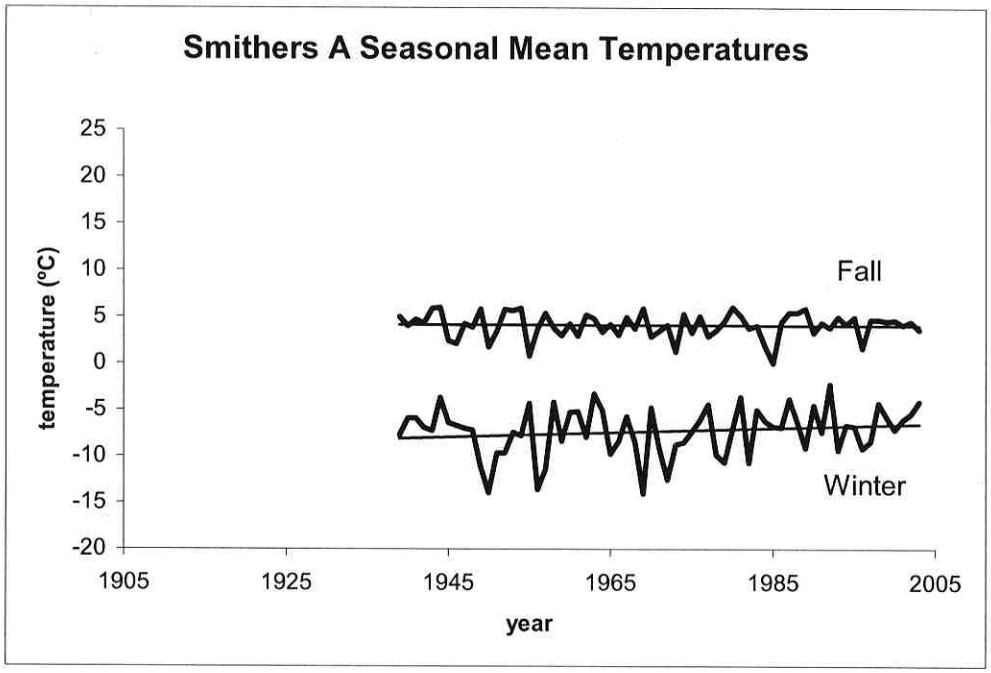
Smithers A Seasonal Mean Temperatures
temperature (°C)
25
20
15
10
5
0
-5
-10
-15
-20
1905
1925
1945
1965
1985
2005
year
Fall
Winter

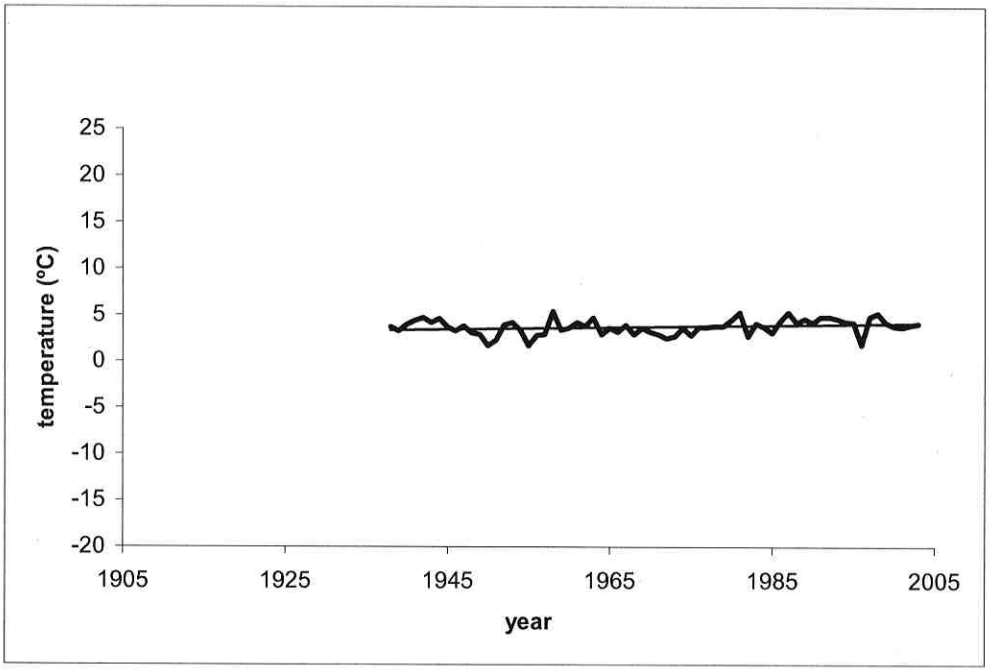
temperature (°C)
25
20
15
10
5
0
-5
-10
-15
-20
1905
1925
1945
1965
1985
2005
year

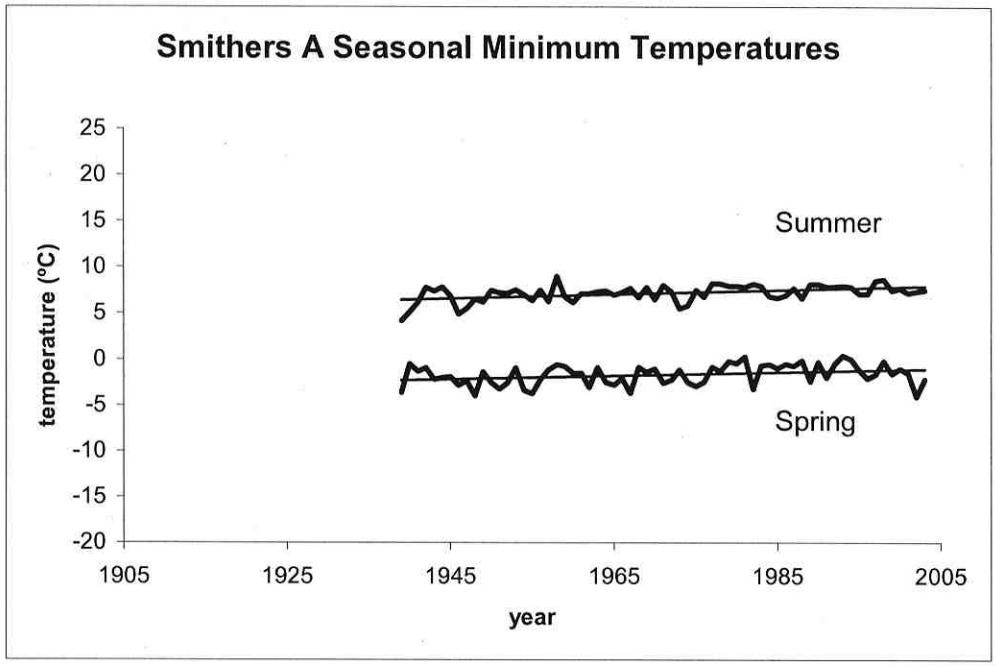
Smithers A Seasonal Minimum Temperatures
temperature (°C)
25
20
15
10
5
0
-5
-10
-15
-20
1905
1925
1945
1965
1985
2005
year
Summer
Spring

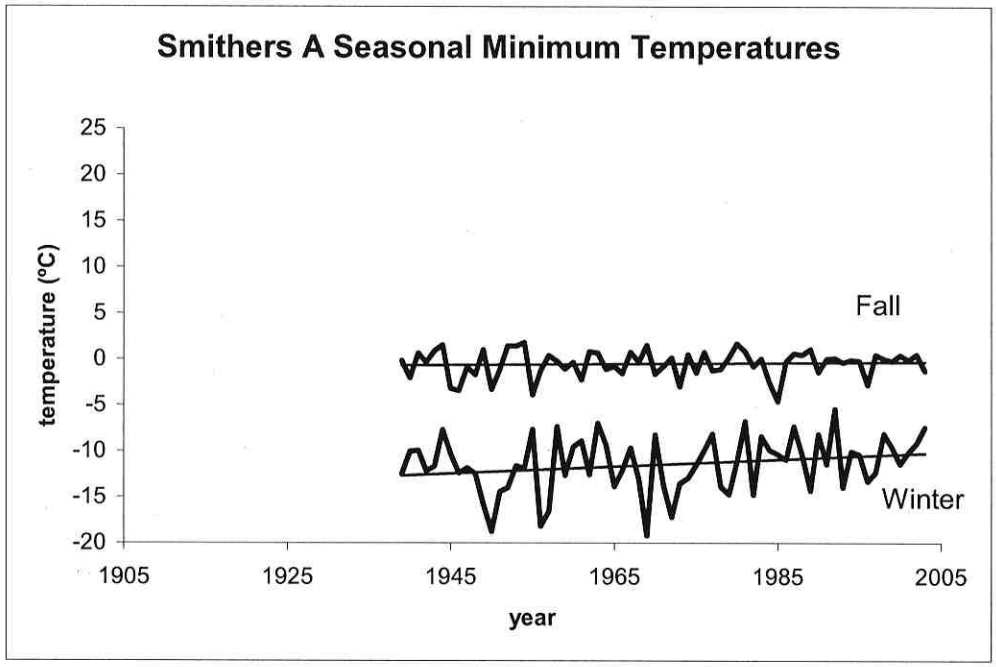
Smithers A Seasonal Minimum Temperatures
temperature (°C)
25
20
15
10
5
0
-5
-10
-15
-20
1905
1925
1945
1965
1985
2005
year
Fall
Winter

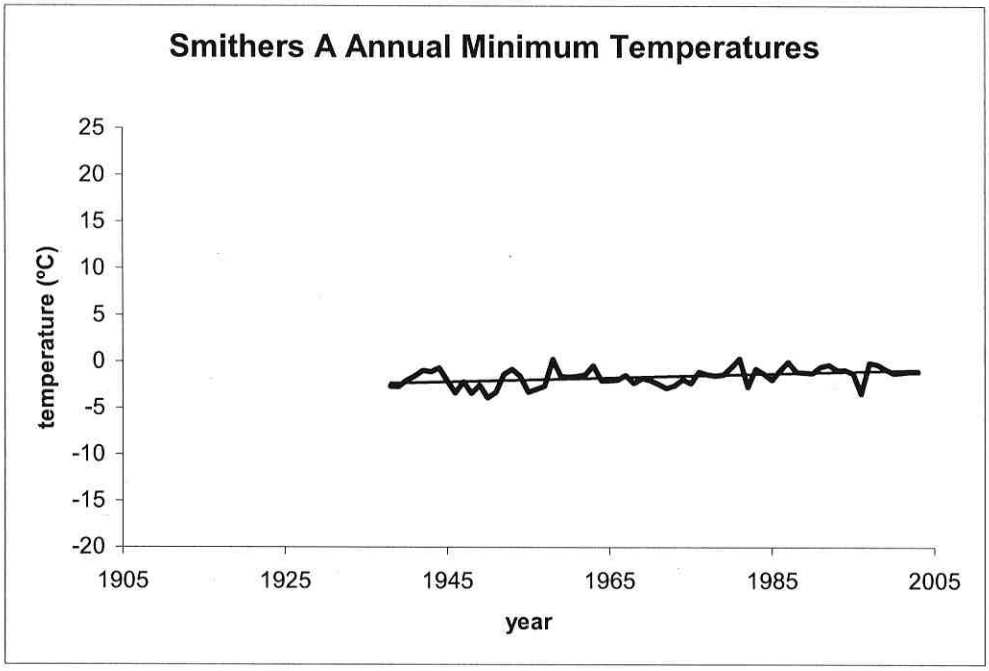
Smithers A Annual Minimum Temperatures
temperature (°C)
25
20
15
10
5
0
-5
-10
-15
-20
1905
1925
1945
1965
1985
2005
year

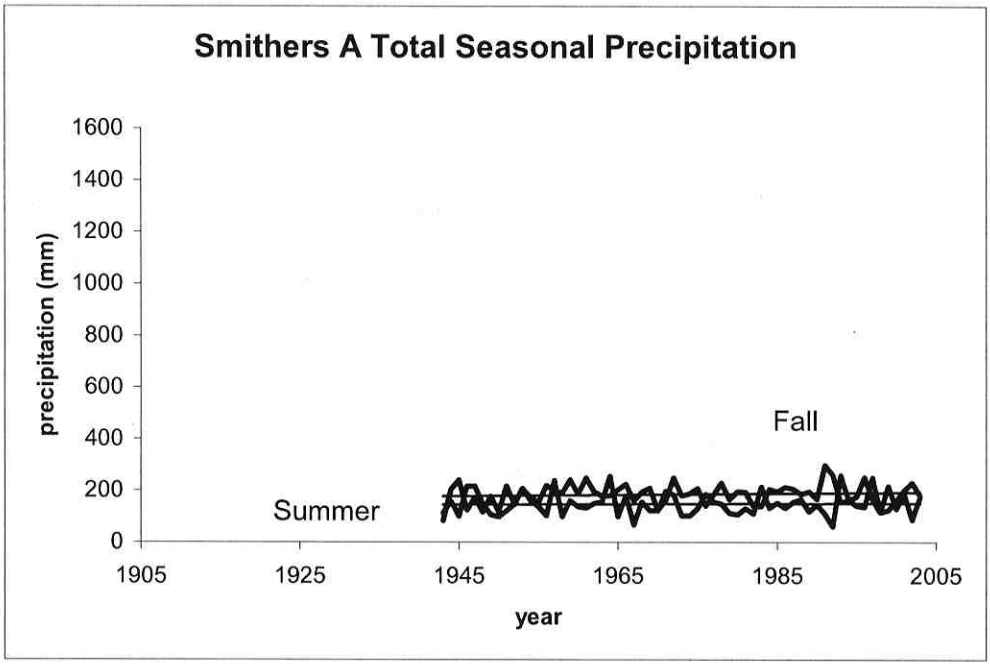
Smithers A Total Seasonal Precipitation
precipitation (mm)
1600
1400
1200
1000
800
600
400
200
0
Fall
Summer
1905
1925
1945
1965
1985
2005
year

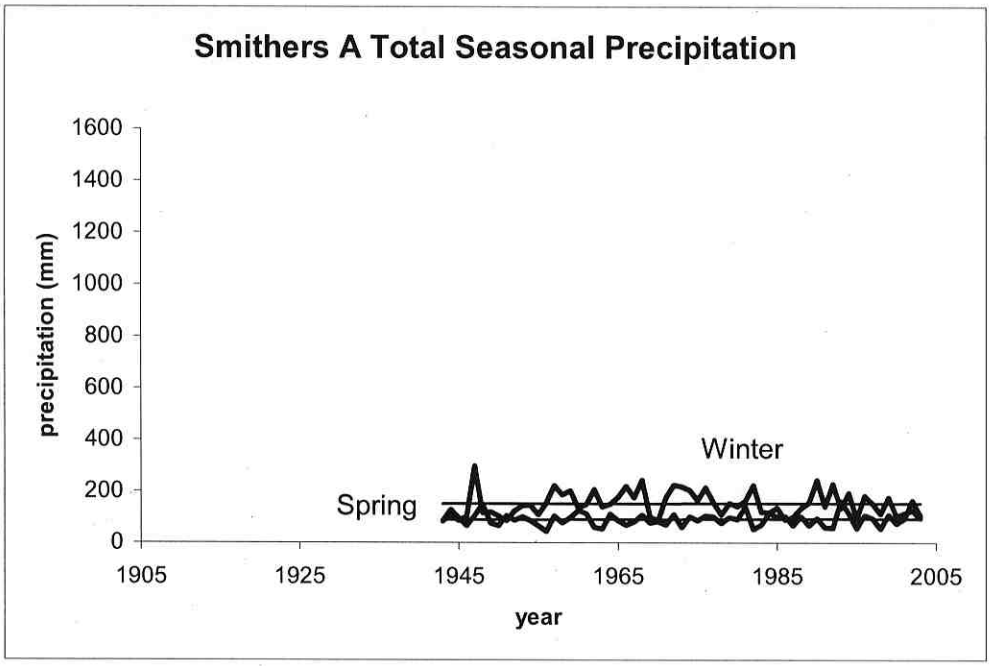
Smithers A Total Seasonal Precipitation
precipitation (mm)
1600
1400
1200
1000
800
600
400
200
0
Winter
Spring
1905
1925
1945
1965
1985
2005
year

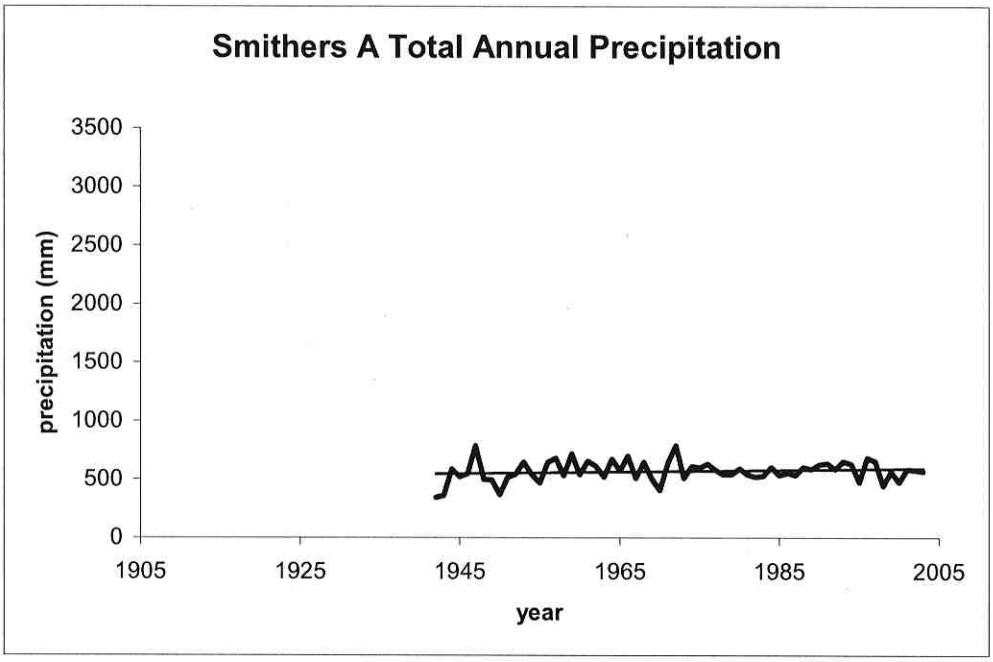
Smithers A Total Annual Precipitation
precipitation (mm)
3500
3000
2500
2000
1500
1000
500
0
1905
1925
1945
1965
1985
2005
year

Appendix D - Stahle *et al.* (1998) / Allan *et al.* (1996) SOI index with phases and extremes

(-1) negative phase, (+1) positive phase, (0) neither

Year	SOI	Phase	Extremes
1706	-2.737	-1	0
1707	2.022	1	0
1708	-2.449	-1	0
1709	4.547	1	0
1710	-4.538	-1	0
1711	-1.837	-1	0
1712	-2.562	-1	0
1713	-5.815	-1	-1
1714	-2.749	-1	0
1715	0.04	1	0
1716	1.459	1	0
1717	5.445	1	1
1718	-4.631	-1	0
1719	-5.906	-1	-1
1720	-1.639	-1	0
1721	-4.417	-1	0
1722	0.81	1	0
1723	-8.015	-1	-1
1724	-1.085	-1	0
1725	6.29	1	1
1726	-7.089	-1	-1
1727	-6.683	-1	-1
1728	-0.628	-1	0
1729	2.543	1	0
1730	0.649	1	0
1731	-1.728	-1	0
1732	-1.531	-1	0
1733	3.908	1	0
1734	-1.372	-1	0
1735	-1.053	-1	0
1736	2.708	1	0
1737	-4.434	-1	0
1738	-1.712	-1	0
1739	6.189	1	1
1740	-3.938	-1	0
1741	-5.903	-1	-1
1742	4.888	1	0
1743	0.954	1	0
1744	-3.698	-1	0
1745	-6.38	-1	-1
1746	-10.926	-1	-1
1747	-9.919	-1	-1
1748	5.997	1	1
1749	-7.922	-1	-1
1750	-3.797	-1	0
1751	-1.083	-1	0
1752	7.308	1	1
1753	0.904	1	0
1754	-0.652	-1	0
1755	6.548	1	1
1756	-0.799	-1	0
1757	-0.033	-1	0
1758	-0.312	-1	0
1759	-4.421	-1	0
1760	-2.414	-1	0
1761	3.131	1	0
1762	-4.499	-1	0
1763	-3.421	-1	0
1764	0.333	1	0
1765	2.621	1	0
1766	-0.945	-1	0
1767	1.405	1	0
1768	2.306	1	0
1769	-5.073	-1	-1
1770	-9.214	-1	-1
1771	-4.915	-1	0
1772	4.017	1	0
1773	4.846	1	0
1774	-4.093	-1	0
1775	-2.808	-1	0
1776	0.979	1	0
1777	-0.896	-1	0
1778	2.418	1	0
1779	-0.406	-1	0
1780	-3.327	-1	0
1781	1.907	1	0
1782	-0.386	-1	0
1783	-7.076	-1	-1
1784	-7.256	-1	-1
1785	3.774	1	0
1786	6.341	1	1
1787	-1.971	-1	0
1788	-6.663	-1	-1
1789	0.141	1	0
1790	6.355	1	1
1791	-1.274	-1	0
1792	-7.333	-1	-1
1793	-6.516	-1	-1
1794	1.004	1	0
1795	-2.532	-1	0
1796	-1.851	-1	0
1797	3.033	1	0
1798	3.545	1	0
1799	-4.088	-1	0

Year	SOI	Phase	Extremes
1800	-5.286	-1	-1
1801	5.961	1	1
1802	2.289	1	0
1803	-4.691	-1	0
1804	-9.672	-1	-1
1805	5.599	1	1
1806	6.619	1	1
1807	-3.008	-1	0
1808	3.356	1	0
1809	2.306	1	0
1810	-3.357	-1	0
1811	-1.428	-1	0
1812	2.108	1	0
1813	2.419	1	0
1814	-2.876	-1	0
1815	-5.836	-1	-1
1816	-11.171	-1	-1
1817	0.299	1	0
1818	1.564	1	0
1819	0.247	1	0
1820	3.96	1	0
1821	-3.784	-1	0
1822	-3.57	-1	0
1823	1.667	1	0
1824	-3.947	-1	0
1825	-12.29	-1	-1
1826	3.017	1	0
1827	-2.454	-1	0
1828	-7.342	-1	-1
1829	-2.807	-1	0
1830	1.985	1	0
1831	2.464	1	0
1832	0.566	1	0
1833	-6.17	-1	-1
1834	-5.607	-1	-1
1835	-3.33	-1	0
1836	1.04	1	0
1837	-2.772	-1	0
1838	-1.593	-1	0
1839	-7.744	-1	-1
1840	-3.033	-1	0
1841	0.201	1	0
1842	1.282	1	0
1843	-1.535	-1	0
1844	-2.473	-1	0
1845	-1.237	-1	0
1846	-2.841	-1	0
1847	3.587	1	0
1848	-4.266	-1	0
1849	-3.522	-1	0
1850	-2.07	-1	0
1851	4.075	1	0

Year	SOI	Phase	Extremes
1852	-7.528	-1	-1
1853	-5.482	-1	-1
1854	4.458	1	0
1855	3.131	1	0
1856	-8.866	-1	-1
1857	0.292	1	0
1858	-1.198	-1	0
1859	1.424	1	0
1860	1.947	1	0
1861	3.436	1	0
1862	2.35	1	0
1863	2.311	1	0
1864	6.702	1	1
1865	-4.463	-1	0
1866	-0.319	-1	0
1867	0.078	1	0
1868	-3.515	-1	0
1869	-10.665	-1	-1
1870	2.312	1	0
1871	4.425	1	0
1872	0.181	1	0
1873	-1.511	-1	0
1874	-1.496	-1	0
1875	-3.256	-1	0
1876	0.45	1	0
1877	-9.607	-1	-1
1878	-0.879	-1	0
1879	4.667	1	0
1880	6.055	1	1
1881	-2.012	-1	0
1882	-2.501	-1	0
1883	5.364	1	1
1884	-2.042	-1	0
1885	-8.077	-1	-1
1886	-2.056	-1	0
1887	7.372	1	1
1888	-2.982	-1	0
1889	-8.922	-1	-1
1890	2.086	1	0
1891	-2.003	-1	0
1892	0.354	1	0
1893	4.611	1	0
1894	7.666	1	1
1895	-1.368	-1	0
1896	-2.229	-1	0
1897	-6.24	-1	-1
1898	-0.665	-1	0
1899	8.701	1	1
1900	-0.492	-1	0
1901	-4.743	-1	0
1902	8.637	1	1
1903	-5.858	-1	-1

Year	SOI	Phase	Extremes
1904	8.794	1	1
1905	-7.502	-1	-1
1906	-11.506	-1	-1
1907	-3.296	-1	0
1908	-5.618	-1	-1
1909	1.15	1	0
1910	8.354	1	1
1911	-0.181	-1	0
1912	-4.821	-1	0
1913	-1.521	-1	0
1914	-7.762	-1	-1
1915	-12.314	-1	-1
1916	1.423	1	0
1917	3.738	1	0
1918	7.959	1	1
1919	-9.767	-1	-1
1920	-9.455	-1	-1
1921	2.881	1	0
1922	7.221	1	1
1923	5.521	1	1
1924	-7.6	-1	-1
1925	6.977	1	1
1926	-7.502	-1	-1
1927	-6.53	-1	-1
1928	-1.32	-1	0
1929	5.968	1	1
1930	-5.255	-1	-1
1931	-9.425	-1	-1
1932	-3.778	-1	0
1933	-1.186	-1	0
1934	4.864	1	0
1935	0.228	1	0
1936	-5.487	-1	-1
1937	-4.556	-1	0
1938	-0.513	-1	0
1939	8.325	1	1
1940	-5.664	-1	-1
1941	-15.426	-1	-1
1942	-13.713	-1	-1
1943	5.97	1	1
1944	-6.961	-1	-1
1945	-0.297	-1	0
1946	7.425	1	1
1947	-3.435	-1	0
1948	-6.869	-1	-1
1949	-6.385	-1	-1
1950	1.882	1	0
1951	6.376	1	1
1952	-2.924	-1	0
1953	1.229	1	0
1954	3.325	1	0

Year	SOI	Phase	Extremes
1955	1.732	1	0
1956	3.574	1	0
1957	2.373	1	0
1958	-4.788	-1	0
1959	-1.259	-1	0
1960	-1.753	-1	0
1961	-0.643	-1	0
1962	-1.238	-1	0
1963	3.741	1	0
1964	0.094	1	0
1965	-1.445	-1	0
1966	-7.397	-1	-1
1967	6.418	1	1
1968	-4.904	-1	0
1969	-3.709	-1	0
1970	-4.863	-1	0
1971	9.215	1	1
1972	2.595	1	0
1973	-12.499	-1	-1
1974	4.807	1	0
1975	-0.137	-1	0
1976	1.159	1	0
1977	-1.385	-1	0
1978	-15.12	-1	-1
1979	-0.92	-1	0
1980	-2.72	-1	0
1981	-2.32	-1	0
1982	3.28	1	0
1983	-31.12	-1	-1
1984	0.78	1	0
1985	-1.12	-1	0
1986	-2.12	-1	0
1987	-13.02	-1	-1
1988	-3.32	-1	0
1989	9.68	1	1
1990	-10.12	-1	-1
1991	-0.62	-1	0
1992	-19.32	-1	-1
1993	-9.12	-1	-1
1994	-1.42	-1	0
1995	-8.12	-1	-1
1996	-0.42	-1	0

Appendix E - PDI from Gedalof and Smith (2001b)

(-1) negative phase, (+1) positive phase, (0) unidentified

Year	Phase
1662	-1
1663	-1
1664	-1
1665	-1
1666	-1
1667	-1
1668	-1
1669	-1
1670	-1
1671	-1
1672	-1
1673	-1
1674	-1
1675	-1
1676	-1
1677	-1
1678	-1
1679	-1
1680	-1
1681	1
1682	1
1683	1
1684	1
1685	1
1686	1
1687	1
1688	1
1689	1
1690	1
1691	1
1692	1
1693	1
1694	1
1695	1
1696	1
1697	-1
1698	-1
1699	-1
1700	-1
1701	-1
1702	-1
1703	-1
1704	-1
1705	-1

Year	Phase
1706	-1
1707	-1
1708	-1
1709	-1
1710	-1
1711	-1
1712	-1
1713	1
1714	1
1715	1
1716	1
1717	1
1718	1
1719	1
1720	1
1721	1
1722	1
1723	1
1724	1
1725	1
1726	1
1727	1
1728	1
1729	1
1730	1
1731	1
1732	1
1733	1
1734	1
1735	-1
1736	-1
1737	-1
1738	-1
1739	-1
1740	-1
1741	-1
1742	-1
1743	-1
1744	-1
1745	-1
1746	-1
1747	-1
1748	-1
1749	-1

Year	Phase
1750	-1
1751	-1
1752	-1
1753	-1
1754	-1
1755	-1
1757	-1
1758	-1
1759	1
1760	1
1761	1
1762	1
1763	1
1764	1
1765	1
1766	1
1767	1
1768	1
1769	1
1770	1
1771	1
1772	1
1773	1
1774	1
1775	1
1776	1
1777	1
1778	1
1779	1
1780	1
1781	1
1782	1
1783	1
1784	1
1785	1
1786	1
1787	1
1788	1
1789	1
1790	1
1791	1
1792	1
1793	1
1794	1

Year	Phase
1795	1
1796	1
1797	1
1798	1
1799	-1
1800	-1
1801	-1
1802	-1
1803	-1
1804	-1
1805	-1
1806	-1
1807	-1
1808	-1
1809	-1
1810	-1
1811	-1
1812	-1
1813	-1
1814	-1
1815	-1
1816	-1
1817	1
1818	1
1819	1
1820	1
1821	1
1822	1
1823	1
1824	1
1825	1
1826	1
1827	1
1828	1
1829	1
1830	1
1831	1
1832	1
1833	1
1834	1
1835	1
1836	1
1837	1
1838	1

Year	Phase
1839	1
1840	1
1841	0
1842	0
1843	0
1844	0
1845	0
1846	0
1847	0
1848	0
1849	0
1850	0
1851	0
1852	0
1853	0
1854	0
1855	0
1856	0
1857	0
1858	0
1859	0
1860	0
1861	0
1862	0
1863	0
1864	0
1865	0
1866	0
1867	0
1868	0
1869	0
1870	0
1871	0
1872	0
1873	0
1874	0
1875	0
1876	0
1877	0
1878	0
1879	0
1880	0
1881	0
1882	0

Year	Phase
1883	0
1884	0
1885	0
1886	0
1887	0
1888	0
1889	0
1890	0
1891	0
1892	0
1893	0
1894	0
1895	0
1896	0
1897	0
1898	0
1899	0
1900	0
1901	0
1902	0
1903	0
1904	0
1905	0
1906	0
1907	0
1908	0
1909	0
1910	0
1911	0
1912	0
1913	0
1914	0
1915	0
1916	0
1917	0
1918	0
1919	0
1920	0
1921	0
1922	0
1923	0
1924	1
1925	1
1926	1

Year	Phase
1927	1
1928	1
1929	1
1930	1
1931	1
1932	1
1933	1
1934	1
1935	1
1936	1
1937	1
1938	1
1939	1
1940	1
1941	1
1942	1
1943	1
1944	1
1945	1
1946	1
1947	-1
1948	-1
1949	-1
1950	-1
1951	-1
1952	-1
1953	-1
1954	-1
1955	-1
1956	-1
1957	-1
1958	-1
1959	-1
1960	-1
1961	-1
1962	-1
1963	-1
1964	-1
1965	-1
1966	-1
1967	-1
1968	-1
1969	-1

Year	Phase
1970	-1
1971	-1
1972	-1
1973	-1
1974	-1
1975	-1
1976	-1
1977	-1
1978	1
1979	1
1980	1
1981	1
1982	1
1983	1
1984	1
1985	1
1986	1
1987	1
1988	1
1989	1
1990	1
1991	1
1992	1
1993	1
1994	1
1995	1
1996	1
1997	1
1998	1